The Pennsylvania State University

The Graduate School

Department of Mechanical and Nuclear Engineering

IMPROVED NEUTRON KINETICS FOR COUPLED THREE-DIMENSIONAL BOILING WATER REACTOR ANALYSIS

A Thesis in

Nuclear Engineering

by

Bedirhan Akdeniz

Submitted in Partial Fulfillment
of the Requirements
for the Degree of

Doctor of Philosophy

December 2007

The thesis of Bedirhan Akdeniz was reviewed and approved* by the following:

Kostadin N. Ivanov
Professor of Nuclear Engineering
Thesis Advisor
Chair of Committee

Lawrence E. Hochreiter
Professor of Nuclear Engineering

Yousry Y. Azmy
Professor of Nuclear Engineering

Cengiz Camcı
Professor of Aerospace Engineering

Erwin Müller
Fellow Engineer
Westinghouse Electric, Sweden
Special Member

Dobromir Panayotov
Principal Engineer
Westinghouse Electric, Sweden
Special Member

Jack S. Brenizer, Jr.
Professor of Nuclear Engineering
Chair of Nuclear Engineering Program

*Signatures are on file in the Graduate School

ABSTRACT

The need for a more accurate method of modelling cross section variations for off-nominal core conditions is becoming an important issue with the increased use of coupled three-dimensional (3-D) thermal-hydraulics/neutronics simulations. In traditional reactor core analysis, thermal reactor core calculations are customarily performed with 3-D two-group nodal diffusion methods. Steady-state multi-group transport theory calculations on heterogeneous single assembly domains subject to reflective boundary conditions are normally used to prepare the equivalent two-group spatially homogenized nodal parameters. For steady-state applications, the equivalent nodal parameters are theoretically well-defined; but, for transient applications, the definition of the nodal kinetics parameters, in particular, delayed neutron precursor data is somewhat unclear. The fact that delayed neutrons are emitted at considerably lower energies than prompt neutrons and that this difference cannot be accounted for in a two-group representation is of particular concern. To compensate for this inherent deficiency of the two-group model a correction is applied to the nodal values of the delayed neutron fractions; however, the adequacy of this correction has never been tested thoroughly for Boiling Water Reactor (BWR) applications, especially where the instantaneous thermal-hydraulic conditions play an important role on the core neutron kinetics calculations. This thesis proposes a systematic approach to improve the 3-D neutron kinetics modelling in coupled BWR transient calculations by developing, implementing and validating methods for consistent generation of neutron kinetics and delayed neutron data for such coupled thermal-hydraulics/neutronics simulations.

TABLE OF CONTENTS

LIST OF FIGURES

LIST OF TABLES

NOMENCLATURE

ACRONYMS AND ABBREVIATIONS:

1-D	One-Dimensional
2-D	Two-Dimensional
3-D	Three-Dimensional
ADF	Assembly Discontinuity Factor
AEBUXY	Lattice Physics Code Developed by Atomenergi AB
APRM	Average Range Power Monitor
AW	Adjoint Weighted
Beta	Delayed Neutron Fraction
BP	Burnable Poison
BPV	By-pass Valve
BWR	Boiling Water Reactor
CASMO	Lattice Physics Code Developed by Studsvik Scandpower
CO	Coupled Calculation
CPM-3	Lattice Physics Code Developed by EPRI
CR	Control Rod
DF	Discontinuity Factor
DN	Delayed Neutron
ENDF	Evaluated Nuclear Data Files
EPRI	Electric Power Research Institute
Gd	Gadolinium

ACRONYMS AND ABBREVIATIONS:

GE	General Electric
HELIOS	Lattice Physics Code Developed by Studsvik Scandpower
HZP	Hot Zero Power
JEFF	Joint European Fission and Fusion File
JENDL	Japanese Evaluated Nuclear Data Library
Lambda	Decay Constant
LMW	Langenbuch, Maurer, and Werner
LPRM	Local Power Range Monitor
LWR	Light Water Reactor
MOX	Mixed Oxide
MSIV	Main Steam Isolation Valve
NEA	Nuclear Energy Agency
NEM	Nodal Expansion Method
NSSS	Nuclear Steam Supply System
OD	Outer Diameter
OECD	Organisation for Economic Co-Operation and Development
PARCS	Purdue Advanced Reactor Simulator
PBTT	Peach Bottom Turbine Trip
PHOENIX	Lattice Physics Code Developed by Westinghouse Electric Co.
PRMTRZ	Importance Factor Parameterization Technique
PWR	Pressurized Water Reactor

ACRONYMS AND ABBREVIATIONS:

RPS	Reactor Protection System
SA	Stand-Alone Calculation
SG6	Subgroup 6
SRV	Safety Relief Valve
T-H	Thermal-Hydraulics
TRACE	TRAC RELAP5 Advanced Computational Engine
TRACE/PARCS	Coupled T-H (TRACE) and Neutronics (PARCS) Code
TransLAT	Lattice Physics Code Developed by Transware Enterprises Inc.

SYMBOLS:

A_0 , A_1 , A_2	Fuel type and control rod dependent constants in the delayed neutron importance factor parameterization technique
$a_{i,d}$	Fraction of delayed neutrons from nuclide *i* related to delayed neutron precursor family, *d*
α	Void fraction
β	Total delayed Neutron Fraction
β^{eff}	Total Effective Delayed Neutron Fraction
β_d^{eff}	Effective delayed neutron fraction for each precursor family
β_d	Delayed neutron fraction for each precursor family
β_i	Total fraction of delayed neutrons from nuclide *i*
$\beta_{i,d}$	Delayed neutron fraction from nuclide *i* for each precursor family

SYMBOLS:

B^2	Buckling
C_d	Concentration of the delayed neutron precursor family
D_g	Diffusion coefficient at energy group *g*
d	Index for delayed neutron precursor family group
E_D	Upper energy boundary of the delayed neutron emission spectrum.
G	Total number of energy groups in multi-group energy form
g	Multi-group energy index
h	Macro-energy group index for few-group calculations
h^{node}	Height of the node
h^{unrod}	Height the unrodded part of the node
I	Total importance factor
I_d	Importance factor for delayed neutron precursor family *d*
I_{AW}	Adjoint weighted total importance factor
$I_{k-ratio}$	Total importance factor for simplified k-ratio method
i	Fissionable nuclide index
j	Cell region index in the lattice
k	Multiplication factor
k_D	Delayed neutron multiplication factor
k_{eff}	Effective multiplication factor
L_g	Leakage rate at energy group *g*
λ_d	Decay constant for delayed neutron precursor family *d*
$\lambda_{i,d}$	Decay constant for delayed neutron precursor family *d* after fissions in nuclide *i*

SYMBOLS:

$N_{i,j}$	Number density of nuclide *i* at region *j*
$\nu\sigma_{f,i,j}$	Microscopic nu-fission cross section of nuclide *i* at region *j*
$\nu_g \sum_{fg}$	Macroscopic nu-fission cross section at energy group *g*
R^2	Least squares fitting
$\sum_{ag}$	Macroscopic absorption cross section at energy group *g*
$\sum_{rg}$	Macroscopic removal cross section at energy group *g*
$\sum_{sg}$	Macroscopic scattering cross section at energy group *g*
S	Total fission source
$S^{i,j}$	Fission source from nuclide *i* at region *j*
S_g^{ext}	External source at energy group *g*
SI	Spectral index in delayed neutron importance factor parameterization technique
SI^*	Dimensionless spectral index in delayed neutron importance factor parameterization technique
T_f	Fuel temperature
Φ_g	Lattice average neutron flux at energy group *g*
Φ_g^*	Lattice average adjoint neutron flux at energy group *g*
Φ_j	Average neutron flux for each region in the lattice
Φ	Lattice average neutron flux
Φ^{node}	Node average neutron flux
Φ^{unrod}	Average heterogeneous neutron flux in unrodded part of the node
$\chi_{d,g}^D$	Delayed neutron fission spectra for each precursor family in multi-group energy form. Superscript "*D*" donates the term "*delayed*"

SYMBOLS:

χ_g^D	Delayed neutron fission spectra in multi-group energy form. Superscript "*D*" donates the term "*delayed*"
χ^D	Total delayed neutron fission spectra
χ_g^P	Prompt neutron fission spectra in multi-group energy form. Superscript "*P*" donates the term "*prompt*"
χ^P	Prompt neutron fission spectra
χ_g	Total fission spectra in multi-group energy form.
χ	Total neutron fission spectra
V_j	Volume of each region in the lattice
υ_g	Neutron speed at energy group *g*

ACKNOWLEDGEMENTS

First of all, I have to mention that this thesis is not a result of a long and lonely work but rather a product of collaboration and interactions among many people. My task was to elaborate ideas, develop suggestions, implement recommendations presented by these people and, of course, formulate all this in a scientific way in order to communicate with other researchers in the field. Unfortunately, I am not able to thank everybody personally in this connection but I must refer to the ones who had a major contribution to realization of my thesis.

I would first and foremost like to express my sincere gratitude to my academic advisor, Dr. Kostadin N. Ivanov, without whose patience and guidance none of this work would have been possible. Dr. Ivanov has always gone out of his way to provide me with academic and professional opportunities; he consistently portrays me in the best possible light to colleagues; and he has taught me not only the essential practices for performing good research, but also the necessary steps for getting it accepted in the scientific community. Definitively, his enthusiasm and commitment to his work provide me a terrific model for how to manage a productive scholarly career.

I owe also many thanks to the members of my dissertation committee, Dr. Lawrence E. Hochreiter, Dr. Yousry Y. Azmy, and Dr. Cengiz Camcı, for reading drafts and providing valuable references, insight, and constructive suggestions.

I would like to reveal that, in my dissertation committee, I have had the privilege to work with two great special members; Dr. Erwin Müller, and Dr. Dobromir Panayotov from Westinghouse Electric Co., Sweden. I think very few people make contributions to

a protégé's research in the way they did. I would like to acknowledge that, together with families, their warm friendship and hospitality made me feel home in Västerås, Sweden during my three internships.

In particular, I am indebted to Dr. Erwin Müller not only for his dedication to my thesis but also his prodigious knowledge and ideas which made this research work outstanding. His enthusiasm, his inspiration, his sense of humor, and his efforts to explain things clearly and simply, helped to make this thesis fun for me. Needless to say, his contributions to my technical writing and programming skills are priceless.

I am also very grateful to Dr. Dobromir Panayotov for his valuable encouragements and discussions on my thesis, for sharing his ideas with me, and helping me in all ways. He always had time for me, and he has spent a lot of hours discussing my ideas and examining my work.

I would like to acknowledge generous financial support from Nuclear Engineering Program of the Pennsylvania State University, and Westinghouse Electric Co. Without their founding this thesis would not be possible.

Fortunately, I was truly honored to be a member of Reactor Dynamics and Fuel Management Group (RDFMG) at Penn State. My peers at RDFMG served not only as exceptional colleagues but also as amazing friends. Their intellectual contributions to this thesis are significant.

I also want special thanks to Kürşat B. Bekar, Şule Ergün, and A. Özgür Erdemli for their invaluable support, time, comment, and feedback during this study. I am grateful to their assistance that helped me to get through the difficult times.

Of particular note are the efforts of Dr. Thomas Downar and Dr. Yunlin Xu from Purdue University. Their support made computer code modifications which were inevitable for this thesis possible.

My parents, Müjgan and Osman Akdeniz deserve my highest respect and deepest gratitude for their constant support and encouragement in all the steps that I have taken over the years. They had done all the things that perfect parents do, and more. It was they who made personal sacrifices to provide me to think freely and a good education that gave me the abilities necessary to complete this work. My gratitudes also go to my sister, Müge for her sincere love and support over the years. I would like to also express my deep appreciation to my in-law family for their support and encouragement during this study.

Last but by no means least it gives me immense pleasure to thank my lovely wife, Ece, who has supported me unconditionally throughout the long process of this thesis, and my wonderful son, Atahan who is a motivational source for me. Thank you for being there for me whenever I needed you.

To my family

Chapter 1

INTRODUCTION

The need for a more accurate method of modelling cross section variations for off-nominal core conditions is becoming an important issue with the increased use of coupled three-dimensional (3-D) thermal-hydraulics/neutronics simulations. In traditional reactor core analysis for both steady state and transient calculations of conventional light water nuclear power plants, condensed few-group and two-dimensional (2-D) cross section sets are used as input data. These cross sections are generated by separate database calculations using characteristic weighting spectra and parameterized in terms of burnup and thermal-hydraulic feedback parameters. Under the real reactor conditions, especially in transient calculations, these spectra change and the 2-D cross sections modelling based on a parameterization model only approximately describe the effects of neutron flux distributions, which change in space, time and energy. This so called 2-D off-line cross section generation and modelling on one hand is well established and computationally efficient. However, on the other hand it constitutes a basic input data uncertainty affecting the results of coupled 3-D thermal-hydraulics/neutronics calculations.

The above-mentioned two-step process, which is applied in the traditional reactor core analysis for both steady state and transient applications, is described in more detail as follows. The first step is to calculate few-group cross sections with different dependencies (i.e. as a function of burnup and local feedback parameters) for various

regions of a reactor core in 2-D geometry, employing lattice physics codes such as CASMO [**1**], HELIOS [**2**], TransLAT [**3**] and PHOENIX [**4**]. The second step is to use this cross section data in a 3-D nodal diffusion code for determination of different parameters throughout the reactor core. The amount of few-group cross section data, which is necessary for steady state, depletion and transient analysis, is significant. The standard cross section modelling for coupled 3-D steady state and transient simulations are based on the data generated in the so-called base depletion (or history) and instantaneous branch calculations using a lattice physics code. In this standard cross section generation technique, cross section history and instantaneous dependence models are based on burnup and local feedback parameters (i.e. fuel temperature, moderator temperature, void fraction, and control rod insertion for BWRs).

In addition to the cross section values, especially for transient analysis, the current lattice physics codes provide neutron kinetics and delayed neutron data for each material composition/assembly in 2-D geometry. The provided information contains total delayed neutron fraction and delayed neutron fractions in six precursor family groups; decay constants for delayed neutron groups; neutron lifetime, and inverse neutron velocities. Then the generated data are further utilized in coupled 3-D transient diffusion calculations in different way: either one set of core averaged kinetics parameters is utilized or separate set of local kinetics parameters is utilized for each spatial node. In both cases, the assumption is often made for the kinetics parameters to be dependent only on burnup. This assumption implies that the kinetics parameters only depend on the isotopic content in a given node but not on the instantaneous thermal-hydraulic variations since the burnup dependence is a function of exposure, spectral history and control

history conditions in the node. The basis of such assumption is mostly based on a Pressurized Water Reactor (PWR) studies and its approximate validity has not been investigated thoroughly for BWR applications.

Another issue that has to be considered in two-group transient calculations is the fact that the difference between prompt and delayed neutron emission spectra cannot be directly accounted for. Steady-state multi-group transport theory calculations on heterogeneous single assembly domains subject to reflective boundary conditions are normally used to prepare the equivalent two-group spatially homogenized nodal parameters. For steady-state applications the equivalent nodal parameters are theoretically well-defined but for transient applications the definition of the nodal delayed neutron precursor data is somewhat unclear. The fact that delayed neutrons are emitted at considerably lower energies than prompt neutrons and that this difference cannot be accounted for in a two-group representation (since all fission neutrons are born in the fast group) is of particular concern. To compensate for this inherent deficiency of the two-group model a correction is customarily applied to the nodal values of the delayed neutron fractions; however, the adequacy of this correction has never been tested thoroughly for BWR applications, especially where the instantaneous thermal-hydraulic conditions play an important role on the core neutron kinetics calculations.

In the light of the deficiencies briefly described above, this thesis proposes a systematic approach to improve the 3-D neutron kinetics modelling in coupled BWR transient calculations by developing, implementing and validating methods for consistent generation of neutron kinetics and delayed neutron data for such coupled thermal-hydraulics/neutronics simulations.

Brief background information and the ideas behind the thesis were presented in this chapter so far. More detailed background analysis related to the philosophy of this thesis is given in the Chapter 2 as a summary of the comprehensive literature review which was performed with a focus on two issues: evaluation of basic delayed neutron data at nuclear data level, and evaluation of delayed neutron fraction techniques at the application level. In addition to the literature review, descriptions of the computer codes utilized in this study, and preliminary sensitivity studies using established BWR benchmark problems are presented in this chapter. Briefly, the Chapter 2 emphasizes the necessity of the developments and improvements accomplished in the further chapters.

The methodology, developments and improvements are mainly discussed in the Chapter 3 that provides sophisticated contributions and approaches to the current techniques. In particular, the methods of calculation schemes of nodal (homogenized and collapsed) kinetics data, currently used in the lattice physics codes are given in the first section. The studies on enhancing the accuracy of the simplified k-ratio method are presented in the second section while a comprehensive analysis of state parameter effects on the delayed neutron fractions is analyzed by using the delayed neutron fraction methodologies in the third section of the Chapter 3. Particular attention is paid to understanding of leakage effects on the kinetics parameters in this section. Conclusions from the state parameter studies lead to the last section of Chapter 3, which focuses on developing an appropriate functionalization (parameterization) of the state dependencies of the delayed neutron importance factor, which is a correction applied to the nodal values of the delayed neutron fractions.

Chapter 4 summarizes the computer code developments and implementations of the parameterization technique developed in the third chapter. The studies in this chapter establish a proper computational platform which makes an investigation of the accuracy and efficiency of the parameterization method possible.

Chapter 5 focuses on investigating the accuracy of the mentioned two-group approach and evaluating the potential improvement that might be gained by adopting a few-group approach in coupled 3-D transient calculations. The basic idea is to perform 3-D transient calculations using a range of carefully selected energy group structures in order to find a reference group structure that can be used as basis for evaluating the accuracy of the two-group structure approach (which utilizes the importance factors). A linkage code is also developed in the course of this work to enable nodal data transfer between lattice physics code and the neutron kinetics code in an efficient and consistent way. A final and very important analysis is performed in this chapter by employing 3-D coupled TRACE/PARCS transient calculations. This analysis emphasize the significance of the delayed neutron importance factor parameterization method in the case of thermal-hydraulic feedbacks are accounted in the nodal kinetics calculations. Briefly, the Chapter 5 questions the accuracy and efficiency of the delayed neutron importance factor method by performing consistent comparative analyses for current techniques and the methods developed in this thesis.

The final chapter, Chapter 6, presents conclusions and a general summary of the studies performed in the first five chapters. At the end of this chapter, a number of recommendations are given for future work to take the new techniques proposed in this doctoral study to forward.

For the convenience of the reader, the following figure (Figure 1-1) summarizes and visualizes the work performed in this thesis as a flow diagram.

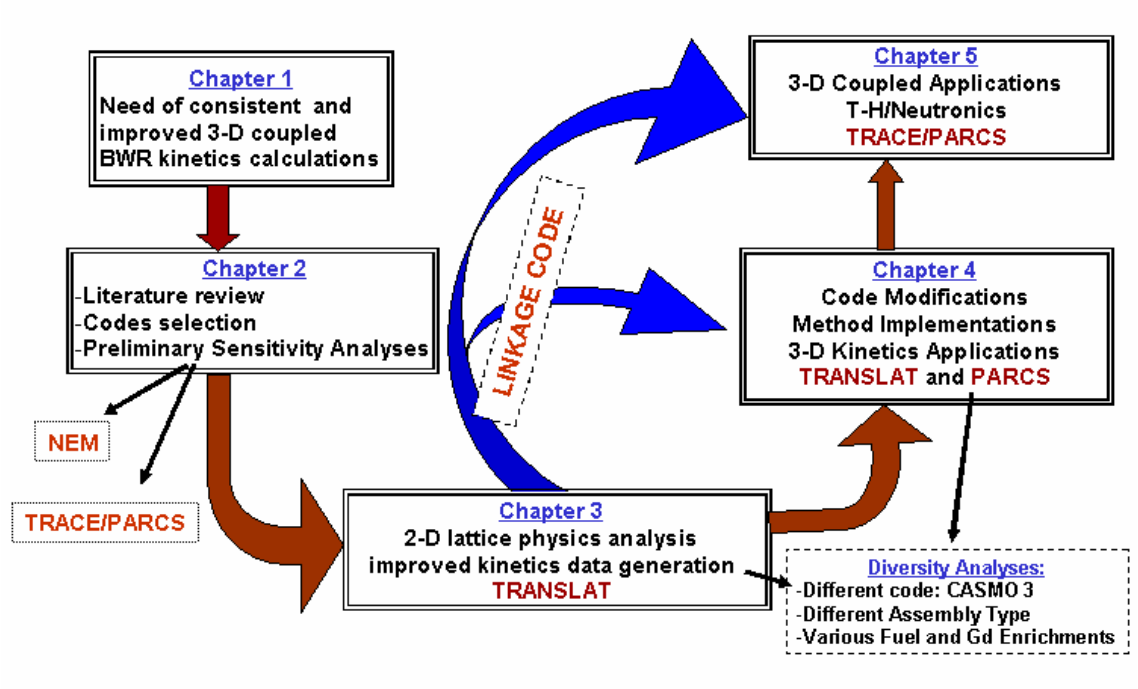

Figure 1-1: General Overview of the Thesis Organization

Chapter 2

BACKGROUND AND SENSITIVITY ANALYSES

Modern nuclear reactor designs depend heavily on the simulation of the reactor core behavior and plant dynamics as well their mutual interactions. This simulation is possible by utilizing digital computer programs or so-called "codes" in which various mathematical models are included. However, a number of approximated methods simplifying the complex problems in reactor core modeling need to be employed for the computationally expensive reactor analysis applications. For example, the current reactor analysis methods extensively use few-group nodal diffusion approximations to calculate core eigenvalues and power distributions. Such approaches (the so-called nodal methods), simply decompose the reactor core into nodes (cells) and calculate only the average flux (or power) in these nodes.

As it is briefly mentioned in the previous chapter, lattice physics codes are utilized to generate few-group 2-D nodal group constants (cross sections, diffusion coefficients, and discontinuity factors) and kinetics parameters (delayed neutron fractions, decay constants, neutron lifetime, and inverse neutron velocities). In lattice calculations, the basic source of these data is the nuclear data libraries (i.e. ENDF/B) which contain data compiled and evaluated from all possible known nuclear information. The data generated by the lattice code is further employed in a 3-D nodal diffusion code for determination of different parameters throughout the reactor core. It should be noted

that the amount of few-group nodal data is significant since typical LWRs have about 30,000 nodes.

Over the last few decades, studies have mostly focused on the proper and efficient generation of the group constants, in particular mainly on the cross sections and their applications in diffusion codes. Although, many studies have been performed for the kinetics parameters on the nuclear data level, there are some deficiencies and inconsistencies for the equivalent nodal kinetics parameters on the current transient reactor kinetics application level. These deficiencies summarized in this chapter emphasize the necessity of the developments and improvements accomplished in this thesis.

In general, the scope of this chapter is not only to summarize the literature review related to this study but also to provide a comprehensive background which will be a basis for the work performed in the further chapters. In particular, nuclear data libraries utilized in the lattice codes along with current kinetics data generation techniques are analyzed thoroughly in the first section while the descriptions of the computer codes used in this study are given along with the thermal-hydraulics and neutronics coupling information in the second section. Last section of this chapter focuses on some preliminary sensitivity studies performed by employing two well known benchmark problems to understand significance and importance of kinetics parameters in such reactor kinetics applications: the first is the *Langenbuch, Maurer, and Werner* (LMW) [**5**] which is simply a numerical transient problem; and the second is an advanced coupled 3-D thermal-hydraulics/neutronics problem – the so called *Peach Bottom Turbine Trip* (PBTT) Benchmark [**6**][**7**][**8**][**9**].

2.1 LITERATURE REVIEW

There has been a significant progress in developing nuclear data libraries (evaluated nuclear data files) for the last fifteen years. Different updates and versions of the United States (US) Evaluated Nuclear Data Files (ENDF/B), the Joint European Files (JEFF) and the Japanese Evaluated Nuclear Data Libraries (JENDL) have been issued and subsequently validated and utilized. There have been also attempts to improve the basic delayed neutron data as part of these libraries to be consistent with the rest of cross-section data in the libraries. This is important since later in the process of evaluating delayed neutron parameters with a lattice physics code this cross-section data is utilized in the homogenization and collapsing process. In addition, at this stage different correction techniques can be utilized in the evaluation process of delayed neutron fraction to account for the delayed neutron data, in order to obtain on accurate estimate of the effective delayed neutron fractions. Therefore, the literature review of the basic delayed neutron data and evaluation of delayed neutron fractions is the first step of this research such that the conclusions and recommendations of this step are utilized in performing the rest of the investigations.

This section mainly reviews the status of delayed neutron data and evaluation of delayed neutron fractions into two distinct parts. In the first part, the performed studies on the evaluation of basic delayed neutron data are discussed and summarized with the current status of the nuclear data libraries. The first part concludes with recommendation and proposal for the library to be utilized in this research. In the second part, the current methods for the evaluation of delayed neutron fractions are discussed and summarized

with the study of the choice of the best correction methods to be utilized in this work and future applications.

2.1.1 Evaluation of Basic Delayed Neutron Data

Delayed neutron data uncertainties may result in undesirable conservatism in the design and operation of nuclear power plants. Interest in improving the accuracy of the delayed neutron (DN) data began to grow in early 1990s. As a result an international working group was formed at the Nuclear Energy Agency (NEA), Organisation for Economic Co-Operation and Development (OECD) - NEA (Working Party on International Nuclear Data Evaluation Co-operation) WPEC (Subgroup 6) SG6 - to review, improve and validate DN data [**10**]. The SG6 has reviewed the DN data at three different levels: individual precursor (**microscopic**) level; aggregate precursors (**macroscopic**) level, in-pile (**integral**) measurement level. This group completed its work at 1999 with the following major results:

- Recommending a new set of DN yields for the major fissile isotopes
- Developing a new 8-group model that has a better physical basis than the presently used 6-group model
- Investigating the need that the DN group parameters be made an explicit function of the incident neutron energy

As a result of the NEA WPEC SG6 work conclusions concerning the DN data for major actinides were summarized and published in a special issue of *Progress of Nuclear*

Energy on DN data of 2002 [**11**]. The recommended data is compared with the DN data currently in use. The Tuttle's 1975 and 1979 evaluations of total yields, together with Keepin's 6 group parameters representing time dependence, are still widely used and comparison between these, the data in the current nuclear data libraries (ENDF/B, JEFF and JENDL), and the recommended one by SG6 are very important.

In summary, the studies performed for the delayed neutron data have addressed the following issues:

- the programs of effective delayed neutron fraction (β^{eff}) measurements
- the energy dependence of delayed neutron yields
- evaluations of total delayed neutron yields
- time-dependent data
- the energy spectra of delayed neutrons

At the microscopic level, the measurements and associated evaluations have significantly improved the database. These measurements and evaluations are being incorporated in the fission product yield and radioactive decay data files in the major nuclear data libraries such as ENDF/B, JEFF, and JENDL. Although the accuracy of the data on microscopic level has improved, for β^{eff} (effective delayed neutron fraction) calculations, the reliance must be still placed on the macroscopic measurements of the delayed neutron emission data for major isotopes and validation of the data using integral reactor measurements of β^{eff} and time-dependent effects.

There is a tendency for the measurements made in the different experimental programs to yield different values of β^{eff}. The uncertainties associated with measurements

are estimated and the adoption of an average of the adjusted values based on the different studies is suggested. It is considered that using these averaged values an accuracy of ± 3% (1 s.d.) will be achieved in β^{eff} calculations for conventional thermal reactors and ± 2% to ± 3% for fast reactors fuelled with the major actinide isotopes. The significance of these deviations is discussed in the papers presented by Okajima et al (2002) [**12**], and Fort et al (2002) [**13**]. These papers show that the agreement between the measured and calculated β^{eff} values is good, within ± 3% for the data in the current nuclear data libraries, ENDF/B-VI, JEFF-2.2, and JENDL-3.2. However, ENDF/B-VI yield data underestimate β^{eff} values measured in the (Mixed Oxide) MOX fueled cores, which have a high dependence on ^{238}U. Further inter-comparisons of techniques, and measurements made on cores, would be helpful in understanding the differences and give confidence in the measured values.

The incident neutron energy dependence of total delayed neutron yields is believed to be small - the difference between thermal reactor and fast reactor spectrum averaged values is at most few percents. Fission product precursor summation calculations give much larger differences and the reason for these differences needs to be understood. The uncertainty about the possible variations through resonances also prevents a clear conclusion being reached about the relationship between thermal and fast spectrum yields. More work is needed to define the energy dependence of total yields. However, very accurate relative measurements (+1%) will be required for the major actinide isotopes. For the secondary isotopes, the uncertainties are larger and more measurements having a lower precision would be useful. Accurate relative measurements of the energy dependence of total yields, and of the fractional yields used to represent

time dependence, would enable the systematic of the interrelationships to be explored in more detail. The dependence on incident neutron energy may be further studied but a capability to treat it can be incorporated in advance.

Improved representations of the time dependence of the delayed neutron emission was proposed by Spriggs, Campbell, and Piksaikin (1999) based on a new 8-group precursor structure for delayed neutron group constants and spectra. The new structure is defined based on current knowledge of the half-lives of the dominant precursor isotopes. In particular, the half-lives of the first three groups have been fixed at the half-lives of the three longest-lived dominant precursors. The new 8-group structure is characterized by the same set of half-lives for all fissioning isotopes and for fission induced by neutrons of different energies. Therefore, the data in the new structure can be correctly used in point reactor kinetics calculations by solving only nine differential equations (eight for the precursors in different groups and one for the neutron density). On the contrary, the Keepin's 6-group structure (characterized by different sets of half-lives for different isotopes and for different incident neutron energies) in principle requires the solution of six differential equations for each fissioning isotope and for each different incident neutron energy.

The use of the 8 group representation of time dependence proposed by Spriggs, Campbell and Piksaikin [**15**], with the half-lives of the three predominant long-lived precursors being explicitly treated, is recommended as having a better physical basis than the traditional 6 group representation of Keepin. The relative yields and energy spectra derived by them are also recommended. The NEA WPEC SG6 conclusion paper summarizes the recommended total delayed neutron yield values in [**11**] as:

U-235 thermal	U-235 fast	U-238 fast	Pu-239 thermal	Pu-239 fast
0.0162	0.0163	0.0465	0.00650	0.00651

Based on these spectrum-averaged values energy dependent values have been derived, suitable for inclusion in nuclear data library files. The data is given in the Appendix of the Reference [**11**]. The statuses of ENDF/B-VI and JEFF-3.0 libraries are summarized as follow.

Delayed neutron parameters using the ENDF/B-VI basic nuclear data:

- The initial DN data prepared on the basis of the first release of ENDF/B-VI (1989) suffered somewhat from the "parallel" way of data evaluation typical for the environment of ENDF/B versions' development
- The initial set of ENDF/B-VI 6-group DN parameters have been found inadequate in many applications
- In 1993 – an improved set of DN data based on ENDF/B-VI was released
- In 2002 – the latest update of the DN parameters based on ENDF/B-VI was published (W. Wilson and T. England, "Delayed Neutron Study Using ENDF/B-VI Basic Nuclear Data", Progress in Nuclear Energy, Vol. 41, No. 1-4, pp. 71-107, 2002) [**16**]
- The above study has confirmed that there is no compelling reason for reactor design codes to depart from using six DN groups especially if they are used with variable decay constants (lambdas). [**17**][**18**]

- The use of 8 groups with variable lambdas is better than 6 groups, but the difference is not significant in terms of the uncertainty in DN fraction. However, there is a penalty for using 8 groups with variable lambdas [**19**].

In JEFF-3.0 for some important fissile nuclides the DN data is presented in 8 groups with energy spectra depending on incident neutron energy [**15**]. The code developers of core dynamics models should adopt a new scheme to utilize such data:

- Using a mixture of 8 and 6 group data
- Modeling the energy spectra dependence on incident neutron energy i.e. using different delayed neutron groups for the each energy group

The question is under what circumstances would code developers adopt such scheme and would the industry be willing to go that way. Although the choice of nuclear data library is not so easy because of the questionable accuracy of the information in the nuclear data libraries, the recommendation here, in the light of the summarized review so far, is to use 6 delayed neutron groups with variable lambdas based on the latest update of the delayed neutron parameters in the well-known nuclear data library ENDF/B-VI (Progress in Nuclear Energy, Vol. 41, No. 1-4, pp. 71-107, 2002) [**16**].

2.1.2 Evaluation of Delayed Neutron Fractions (β)

As it was stated in the introduction chapter, in a two-group model of the core no explicit distinction is made between prompt fission neutrons and delayed neutrons. Both

types of fission source neutrons are born in the fast group, even though they have different energy spectra. Their mutual importance to the chain reaction must be weighted separately (the delayed neutrons have smaller chance to leak the system) and an effective fraction must be determined for the delayed neutrons born in each node. The formally correct importance weighting for neutrons of different energy is given by the spectrum of the adjoint flux in each node. However, this spectrum is not precisely known in advance. In CASMO series codes as CASMO-3 [**1**] and CASMO-4 [**20**], the adjoint spectrum is determined by assuming zero buckling i.e. no leakage. This is an approximation for large cores especially for spatial kinetics applications [**20**]. The beta-effective for each fuel assembly should, in principle, be computed using the adjoint spectrum consistent with the local leakage fraction.

Current approaches for generation of kinetics data can be illustrated on the example of the methods used in modern lattice physics codes such as TransLAT or CASMO codes, which utilize delayed-neutron data stored in a database for six precursor groups. The delayed neutron fractions – the so-called betas (β) for a given material composition for a given energy group are generated using this database by summation and averaging with the fission neutron production rate as given in the Eq. 2.1. Since beta in the Eq. 2.1 is computed by using the direct information from nuclear data libraries, it is called as “direct beta” or “physical beta”. Further these betas are flux averaged over all the energy groups and corrected for the fact that the fission spectrum of delayed neutrons is softer than that of the prompt neutrons. These corrected betas are usually called as “effective betas” (β^{eff}).

The CASMO-3 formulas for direct beta (Eq. 2.1), corresponding decay constants (Eq. 2.2), and effective beta (Eq. 2.3), and inverse neutron velocities (Eq. 2.4) are as follows:

$$\beta_d = \sum_i \beta_{i,d} \sum_g \left(\frac{\sum_j \nu\sigma_{f,i,j,g} \upsilon_i \Phi_{j,g} N_{i,j}}{\sum_i \sum_g \sum_j \nu_{f,j,i,g} \upsilon_j \Phi_{j,g} N_{i,j}} \right) \qquad \textbf{(2.1)}$$

$$\lambda_d = \frac{\sum_i \lambda_{i,d} \beta_{i,d} \sum_g \sum_j \nu\sigma_{f,i,j,g} \upsilon_j \Phi_{j,g} N_{j,i}}{\overline{\beta_d}} \qquad \textbf{(2.2)}$$

where

d = delayed neutron precursor family group

g = multi-group energy index

i = fissionable nuclide index and j= cell region index

β_i = total fraction of delayed neutrons from nuclide i

$a_{i,d}$ = the fraction of delayed neutrons from nuclide i related to delayed neutron group d and $\beta_{i,d} = \beta_i \, a_{i,d}$

$\lambda_{i,d}$ = the decay constant for delayed neutron group d after fissions in nuclide i

Values of β_i, $a_{i,d}$, and $\lambda_{i,d}$ are taken from ENDF/B-VI.

$$\beta_d^{eff} = \frac{\sum_i \left(\sum_h \Phi_h^* \chi_{d,h}^P \right) \beta_{i,d} \sum_j \nu\sigma_{f,i,j} V_j \Phi_j N_{i,j}}{\sum_i \left[\left(1 - \sum_d \beta_{i,d} \right) \left(\sum_h \Phi_h^* \chi_h^P \right) + \sum_d \beta_{i,d} \left(\sum_h \Phi_h^* \chi_{d,h}^D \right) \right] \sum_j \nu\sigma_{f,i,j} V_j \Phi_j N_{i,j}} \qquad \textbf{(2.3)}$$

where;

h = macro-energy group index,

i = fissionable nuclide index, and j= cell region index

Φ_h^* = adjoint cell average flux for macro group *h*

$\beta_{i,d}$ = neutron fraction for delayed group *d*

$\chi_{d,h}^D$ = delayed neutron fission spectra where *D* donates term "delayed"

χ_h^P = prompt neutron fission spectra where *P* donates term "prompt"

$\beta^{eff} = \sum_d \beta_d^{eff}$ (Total effective delayed neutron fraction)

Φ = Lattice average flux

Three different evaluation methods for inverse neutron velocities are given in the following equation.

$$(1/\upsilon)_h = \frac{\sum_{g\in h} \frac{1}{\upsilon_h} \Phi_g}{\sum_{g\in h} \Phi_g} \quad \text{(s/cm)}$$

$$(1/\upsilon)_h^* = \frac{\sum_h \frac{1}{\upsilon_h} \Phi_h^*}{\sum_h \Phi_h^*} \quad \text{(s/cm)} \qquad \textbf{(2.4)}$$

$$(1/\upsilon)_h' = \frac{\sum_h \Phi_h^* \frac{1}{\upsilon_h} \Phi_h}{\sum_h \Phi_h^*} \quad \text{(s/cm)}$$

Since the energy of the delayed fission spectrum is lower than that of the prompt fission spectrum, delayed neutrons have a smaller chance to leak out of the system. As discussed above and shown in Eq. 2.3, this is taken into consideration by weighting the

physical beta with the energy dependent adjoint spectra, which quantifies the energy importance of neutrons in the system. Alternatively, the effective delayed neutron fraction in CPM-3 [**21**] is defined by introducing the delayed neutron multiplication factor k_D:

$$\beta_d^{eff} = \frac{k_D}{k}\beta_d \qquad (\mathbf{2.5})$$

where k_D is computed in a separable real spectrum calculations with a delayed neutron source. As it can be seen from Eq. 2.5 in this alternative method β^{eff} is calculated by simple k-eigenvalue solutions and can be referred as k-ratio (k_D / k) method in which some codes (i.e. CASMO, PHOENIX) do not have this option while others have (i.e. TransLAT). Theoretical justification of this method was provided in the Reference [**22**]. Comparisons between the adjoint-weighted method [**21**] and k-ratio method [**23**] were performed for different fuel assembly cases indicating minor differences except for the cases with significant neutron leakage where larger differences are observed [**24**]. This is important for the neutron spatial kinetics where the local leakages are explicitly taken into account during generation of homogenized group constants and kinetics data.

In some lattice physics codes such as PHOENIX [**4**] and HELIOS [**2**] the simplified k-ratio method is used such that all the quantities in Eq. 2.5 are leakage dependent (i.e. obtained from B_1 calculations) quantities of a finite system. It was mentioned in the above paragraph that k_D should be calculated by a separate spectrum calculation since the slowing down of the delayed neutrons relates to a specific spectrum; however, this is complicated and expensive for computation. Instead of real spectrum calculation, the spectrum is calculated with the ordinary fission source but the reaction

rates above the selected energy group are neglected. In other words the formula for the k_D is the same as for k except that the summation over energy are over the groups below about 0.45 MeV which is roughly the average emission energy for delayed neutrons. It seems that the common source for this energy choice (i.e., 0.45 MeV) as well as the description of the simplified k-ratio method can be tracked to an old technical note related to the AEBUXY code [**25**]. It should be noted that, each assembly needs a B_1 calculation to obtain quantities used in Eq. 2.5 to produce effective delayed neutron data for fuel assemblies.

Choice of the Best Correction:

There are outstanding issues, connected with developing a consistent practical scheme for generation of kinetics data for multi-dimensional two group core transient calculations, which need to be addressed. The 3-D two-group kinetics codes used for coupled transient calculations require as input data - besides the two-group cross-sections – also kinetics parameters as group velocities, delayed neutron precursor decay constants, and delayed neutron yields. The discussions are based on the example of delayed neutron yields (or effective delayed neutron fractions). The value of these parameters is affected by the difference between prompt and delayed neutron spectra. This effect, which can be clearly seen in multi-group formulation, is lost in two-group diffusion equations with linearly collapsed cross-sections used for the calculations of delayed neutron parameters [**23**][**24**][**26**][**27**][**28**]. The disappearance of the difference between prompt and delayed spectra leads also to differences in the calculated flux changes (as compared to reference

multi-group results) during transient calculations. The described above adjoint-weighted method – see Eq. 2.3 – is called also a bilinear weighting procedure (with real flux and adjoint flux as weighting functions), which is completely applicable only with bilinear weighted cross-sections. However, so far in practical reactor physics applications, the linear-collapsing procedure is used as a standard approach for cross-section generation based only on real flux weighting, which does not give the exact kinetics parameters in two-group approximation.

This situation can be improved, when for the two group equations corrected values for delayed neutron parameters can be used for each material composition [**23**][**26**]. The correction factors can be generated using multi-group spectral cell/assembly calculations, performed with lattice physics codes. However, these correction factors do not reproduce the multi-group delayed neutron parameters for a general 3-D case especially with strong flux spatial variations in the reactor core. Thus the use of correction factors of the delayed neutron parameters in two-group diffusion equations is only a practical approximation to improve the deficiencies of the linearly collapsed two-group diffusion equations. More sophisticated approach is to use bilinear collapsing of the multi-group formulation to two group formulation. However, in this case bilinear collapsed cross-sections, which are currently not generated by the lattice physics codes and not used by the 3-D coupled codes, have to be utilized. For such bilinear collapsing the adjoint fluxes should be also collapsed according to their physical meaning as importance functions. For that reason, the accuracy of the above-described corrections are investigated, improved, tested and validated in this study.

The single assembly calculations should be performed in the same mode as the one used for generation of the linearly collapsed two group cross-sections. Using B_1 approximations (instead zero leakage) is preferable at least for the forward calculations. The second issue to be studied in this research is the choice of buckling to be used for the calculation of adjoint spectrum – zero or critical buckling. The obtained critical adjoint spectrum from B_1 calculations will be softer than the real one while the zero buckling adjoint spectrums will be harder than the real one.

One issue to be investigated is how many groups should be used for the calculation of the correction factors, i.e. for the correct representation of adjoint flux spectrum. These investigations consist of performing multi-group forward and adjoint spectral calculations for the material compositions corresponding to the homogenized nodes.

2.2 CODE DESCRIPTIONS

Prediction of a nuclear power plant's behavior under both normal and abnormal conditions has important ramifications for safety and economic operations. Such prediction is only possible using highly sophisticated computer codes given the complexity of nuclear power plants. Incorporation of full three-dimensional (3-D) models of the reactor core into system transient codes allows for a "best-estimate" calculation of interactions between core behavior and plant dynamics. Recent progress in computer technology has made the development of such coupled code systems (thermal-hydraulic and neutron kinetics) feasible. As input to these codes, a complete set of group constants

and kinetics parameters need to be generated by the lattice physics codes. The capabilities of the codes become a very important issue for the consistency of such reactor kinetics analyses. For this reason, this section is focused on the descriptions and the capabilities of the selected state-of-the-art nuclear codes to have meaningful study in this research. The basis of these selections are also described and justified in the following sub-sections.

2.2.1 Lattice Physics Code: TransLAT

The state-of-the-art computer code TransLAT [**3**] is selected for the lattice physics calculations of this study. TransLAT is used for the lattice physics calculations, in this research since it includes variety of effective delayed neutron fraction techniques such as k-ratio method and adjoint weighted method. While CASMO and HELIOS are more known codes the TransLAT is relatively new advanced lattice physics code, which is based partially on CPM-3, and utilizes the latest release of ENDF/B-VI nuclear data library. Since the code features in regard to the basic delayed neutron data and the available methods for evaluations of delayed neutron fractions meet our recommendations made on the basis of literature review summarized in the previous sections, TransLAT is selected to be utilized for this research.

The ***TransLAT*** software features the following general capabilities [**3**]:

a) ***TransLAT*** is advanced three-dimensional lattice physics burnup software that performs neutron flux, gamma-ray flux, and eigenvalue calculations for light

water reactor nuclear fuel assembly designs. ***TransLAT*** couples an arbitrary geometry modeling technique with integral transport theory methods to provide a flexible and highly accurate tool for predicting flux distributions and eigenvalues in light water reactor fuel assemblies. The ***TransLAT*** software system includes a cross-section data file based on the latest release of (currently it is release 5) **ENDF/B-VI,** which includes extended data representations to perform resonance treatments and isotopic burnup calculations of fuel and fission product chains and burnable absorber materials;

b) An important feature of ***TransLAT*** is the arbitrary geometry modeling capability, which allows the user to describe fuel assembly models of virtually any mechanical design and to any level of design detail. The geometry model described in ***TransLAT*** is solved explicitly in the flux calculations (i.e., there are no embedded assumptions for region or material homogenization which might bias calculated results). The arbitrary geometry modeling capability is also used to determine Dancoff correction factors and to support the determination of resonance effects for multi-annulus and sectored pin cell geometries by the spatial variation calculation. The flexible nature of the ***TransLAT*** geometry model, the arbitrary geometry Dancoff treatment and the spatial variation resonance treatment allows lumped fuel materials and burnable absorbers to be specified in regular or highly irregular geometry configurations;

c) Another important feature of ***TransLAT*** is the availability of two nuclear transport theory methods to solve flux and eigenvalue problems. The first method is based upon the Method of Collision Probabilities, which provides

traditional benchmark-quality results. The second method is based upon the Method of Characteristics, which provides production-quality results in a utility application environment. The transport methods are coupled to the arbitrary geometry model and provide an explicit solution for each region of each part in the solution geometry. The flux calculations may be performed in the micro-group energy group structure of the nuclear data file or, for burnup cases, in a few-group energy group structure specified by the user;

d) Flux calculations may be performed in any energy group structure. The reference calculation is performed in the micro-group energy group structure represented on the nuclear data file. Depletion cases may use any condensed energy group structure specified by the user.

e) Nuclear data for neutron and gamma-ray particles are automatically read from the nuclear data files. Nuclear data is provided for over 300 nuclides. Neutron cross-section data is provided in 97 energy groups over the energy range 0-10 MeV. Gamma-ray cross-section data is provided in 18 energy groups up to 10 MeV.

f) ***TransLAT*** performs a fundamental mode calculation, which accounts for neutron leakage effects. The leakage spectrum data is then available to calculate nuclide reaction rates and to perform isotopic depletion calculations. The user may optionally select to use the infinite spectrum or leakage spectrum data for most edit options.

g) ***TransLAT*** performs isotopic depletion calculations for each material region containing a burnable material. Over 200 nuclides are represented in the fuel

depletion chains. Special burnup chains are supported for burnable absorber materials including gadolinium, hafnium, erbium and silver-indium-cadmium. ***TransLAT*** supports three depletion modes to provide the user with the optimum approach for determining exposure effects. The three depletion modes, listed in the order of least to most accurate, are predictor-only, predictor-corrector, and time-averaged.

h) ***TransLAT*** features a sophisticated energy model, which calculates energy factors for seven energy terms. The ***TransLAT*** energy model accounts for all energy produced and deposited in the fuel assembly lattice, including fuel and non-fuel regions.

As it was stated before, our recommendation is to use 6 delayed neutron groups with variable lambdas based on the latest update of the delayed neutron parameters in the ENDF/B-VI (Progress in Nuclear Energy, Vol. 41, No. 1-4, pp. 71-107, 2002) [**15**]. TransLAT utilizes this version of the ENDF/B-VI library and has options for performing both of the utilized delayed neutron fraction evaluations – adjoint weighted and k-ratio methods.

2.2.2 PARCS Core Simulator

Purdue Advanced Reactor Core Simulator (PARCS) is a three-dimensional (3-D) reactor core simulator which solves the steady-state and time-dependent, multi-group neutron diffusion and SP_3 transport equations in orthogonal and non-orthogonal

geometries in order to predict the eigenvalue and the dynamic response of the reactor to reactivity perturbations such as control rod movements or changes in the temperature/fluid conditions in the reactor core [**29**][**30**].

The highlights of PARCS features can be listed as in the following [**29**].

- PARCS is coupled directly to the thermal-hydraulics system code, **T**RAC/**R**ELAP **A**dvanced **C**omputational **E**ngine (TRACE) [**31**][**32**] which provides the temperature and flow field information to PARCS during the transient calculations via the few group cross sections [**33**].
- PARCS has ability to perform *eigenvalue* calculations, *transient (kinetics)* calculations, *Xenon transient* calculations, *decay heat* calculations, *pin power* calculations, and *adjoint* calculations for commercial LWRs.
- Although PARCS has capability to calculate 3-D models of realistic physical reactor core it has various 1-D modeling features support faster simulations for a group of transients in which the dominant variation of the flux is in the axial direction, as for example in several BWR applications.
- The *coarse mesh finite difference* (CMFD) formulation is employed in PARCS to solve for the neutron fluxes in the homogenized nodes. The CMFD formulation provides a means of performing a fast core transient calculation by employing a non-linear iteration with local nodal calculation. The solution of the CMFD linear system is obtained using a Krylov subspace method.
- A transient fixed source problem is formed and solved at each time point in the transient.

- For spatial discretization, a variety of solution kernels are available to include the most popular LWR two group nodal methods, Advanced Nodal Method (ANM) and Nodal Expansion Method (NEM). NEM is also available in multi-group calculations.

PARCS is selected for performing kinetics calculations in this study. In addition to the features listed above, the reason for this selection is the high performance of PARCS simulator in numerous worldwide benchmark problems. In particular, PARCS was very well validated with the PBTT BWR benchmark [**34**].

2.2.3 TRACE/PARCS Coupled Code

System thermal-hydraulics codes have the capability to model the heat transfer and the hydraulic phenomena in a very detailed way. However, thermal-hydraulic codes may become cumbersome if neutronics models are directly embedded into these codes. Hence the recent developments in computer technology made parallel coupling with 3-D neutron kinetics codes with thermally-hydraulics codes possible.

The United States Nuclear Regulatory Commission (US NRC) uses computer models to study the phenomena associated with reactor safety issues. The reactor system analysis code TRACE (**T**RAC **R**ELAP5 **A**dvanced **C**omputational **E**ngine) is used to study the reactor coolant system under a wide variety of flow conditions including multi-phase thermal-hydraulics. Multi-dimensional time dependent power distributions are required for accurate simulation of some reactor transient or accident scenarios and the

PARCS (**P**urdue **A**dvanced **R**eactor **C**ore **S**imulator) multi-dimensional reactor kinetics code has been coupled to TRACE to provide this capability. TRACE coupled to PARCS has been validated previously for BWR transient analysis [**7**][**8**][**9**] [**34**]. The important features of the coupled TRACE/PARCS can be listed as [**33**]:

- The coupled TRACE/PARCS code utilizes an internal integration scheme in which the solution of the system and core thermal-hydraulics is obtained by TRACE and only the spatial kinetics solution is obtained by PARCS.
- PARCS utilizes the thermal-hydraulics solution data (e.g., moderator temperatures/densities and fuel temperatures) calculated by TRACE to incorporate appropriate feedback effects into the cross-sections.
- TRACE takes the space-dependent powers calculated by PARCS and solves for the heat conduction in the core heat structures.
- The TRACE and PARCS codes are locked into the same time step. For this implementation, the TRACE solution leads the PARCS solution by one time step.
- The normal termination of the coupled TRACE/PARCS code is controlled by TRACE. For reactor control, TRACE manages the control rod scram logic and communicates the corresponding trip signal to PARCS.
- PARCS controls all other features in the code except control rod scram logic.

Overall control of the coupled transient (e.g. convergence checks and trip initiation) is handled by TRACE. To accelerate the steady state initialization, a neutronic

calculation skipping strategy is used in which the PARCS calculation performed advances in TRACE.

2.3 PRELIMINARY SENSITIVITY STUDIES

It is important to predict the time dependencies of neutron flux that comprise the area of reactor kinetics or dynamics in reactor core. When a perturbation is made to the reactor properties, the steady state no longer holds, and the evolution of the neutron flux must be obtained from the time-dependent diffusion equation where kinetics parameters (delayed neutron fractions, decay constants, neutron lifetime, and inverse neutron velocities) are extensively utilized. Before developing, in the following chapters, the sophisticated and innovative methodologies for the kinetics parameters, this section presents some preliminary sensitivity studies performed by employing two well known benchmark problems: *Langenbuch, Maurer, and Werner* (LMW), and *Peach Bottom Turbine Trip* (PBTT). The intension of this sensitivity studies is to understand significance and importance of kinetics parameters in such transient problems.

In the first problem, PBTT, the impact of using spatially dependent nodal kinetics parameters as compared of using core average kinetics parameters is analyzed. The objectives of the PBTT studies are also to test and validate thermal-hydraulics/neutronics capability of the codes as well as to investigate significance of kinetics parameters on coupled 3-D calculations. The second benchmark problem, LMW, numerical studies are performed for different sets of kinetics parameters (delayed neutron fractions, decay constants and inverse velocities). Thus impact of the kinetics parameters on a numerical

benchmark problem which simulates operational transient involving rod movements can be investigated for each of these sets independently.

2.3.1 Peach Bottom Turbine Trip (PBTT) Problem

Turbine trip transients in a Boiling Water Reactor (BWR) are pressurization events in which the coupling between core space-dependent neutronics phenomena and system dynamics plays an important role [**6**][**7**][**8**][**9**]. In addition, the available real plant experimental data makes this benchmark problem very valuable. Over the course of defining and coordinating the BWR TT benchmark a systematic approach has been established by the Pennsylvania State University in order to validate best estimate coupled codes. This approach employs a multi-level methodology that not only allows for a consistent and comprehensive validation process but also contributes to the study of key parameters of pressurization transients. A consistent and comprehensive benchmark approach has been developed and the benchmark consists of three separate exercises, two initial states and four transient scenarios.

Peach Bottom Atomic Power Station Unit 2 is a General Electric (GE) designed BWR/4 with a nominal thermal power of 3,293 MW, a total core flow of 12,915 kg/s (102.5 x 10^6 lb/hr), a rated steam flow of 1,685 kg/s (13.37 x 10^6 lb/hr), and a turbine inlet pressure of 6.65 MPa (965 psia). Nuclear steam supply system (NSSS) has turbine-driven feed pumps and a two-loop M-G driven recirculation system feeding a total of 20 jet-pumps. There are totally four steam lines and each has a flow-limiting nozzle, main steam isolation valves (MSIVs), safety relief valves (SRVs), and a turbine stop valve

(TSV). The steam by-pass system consists of nine by-pass valves (BPVs) mounted on a common header, which is connected to each of the four steam lines.

There are 764 fuel bundles with an active fuel length of 365.76 cm (12 ft) in the core region. The fuel bundles consist of 576 original 7 x 7 fuel bundles with pitch/OD = 1.87452 cm / 1.43002 cm (0.738 in / 0.563 in) and 188 partially reload 8 x 8 fuel bundles with pitch/OD = 1.62560 cm / 1.25222 cm (0.640 in / 0.493 in). Additionally, core region includes 185 control rods (CRs). For the reactor protection system (RPS), the control systems for reactor pressure, recirculation flow, and feedwater flow and reactor water level are commonly used in reactors of this design.

Turbine trip test 2 (TT2) was initiated from steady-state conditions. PB2 was chosen for the turbine trip tests because it is a large BWR/4 with relatively small turbine by-pass capacity. During the test, the initial thermal power level was 61.6% rated 2030 MW; core flow was 80.9% rated 10,445 kg/s (82.9 x 10^6 lb/hr); and average range power monitor (APRM) scram setting was 95% rated power[1].

Peach Bottom Unit 2 Turbine Trip Test 2 starts with the sudden closure of the turbine stop valve (TSV) then the turbine by-pass valve begins to open. From a fluid flow phenomena point of view, pressure and flow waves play an important role during the early phase of the transient because rapid valve actions cause sonic waves, as well as the secondary waves, generated in the pressure vessel. In other words, the pressure oscillation generated in the main steam piping propagates with relatively little attenuation

---

[1] This scram set point by 95% power level was replaced in the benchmark specification by scram set to occur at 0.75 s of the transient in order to allow consistent comparison of results obtained by different participants' codes .[**6**]

into the reactor core. The induced core pressure oscillation results in dramatic changes of the core void distribution and fluid flow. The magnitude of the neutron flux transient taking place in the BWR core is strongly affected by the initial rate of pressure rise caused by pressure oscillation and has a strong spatial variation. The correct simulation of the power response to the pressure pulse and subsequent void collapse requires a 3-D core modeling supplemented by 1-D simulation of the remainder of the reactor coolant system. During the TT2 test, most of the important phenomena occur in the first five seconds of the transient. Therefore, the transient will be simulated for five-second time period. This approach simplifies the number of components required for performing the analysis of TT2. Basically, the transient begins with the closure of the TSV. At some point in time, the turbine BPV begins to open. The only boundary conditions imposed in the analysis should be limited to the opening and closure of the above valves.

For this study, the United States Nuclear Regulatory Commission (US NRC) version of **T**RAC/**R**ELAP **A**dvanced **C**omputational **E**ngine (TRACE) is coupled with Purdue University version of **P**urdue **A**dvanced **R**eactor **C**ore **S**imulation Code (PARCS). Thermal-hydraulics and neutronics models were developed according to the end of cycle of PB2 TT test conditions. Descriptions of both thermal-hydraulic and neutronic models are in the following.

2.3.1.1 PBTT TRACE Thermal-Hydraulics Model

The TRACE Peach Bottom model used here consisted of 67 components. The reactor was modeled using the vessel component with 4 radial rings and 14 axial levels.

Fuel assemblies were mapped into 33 thermal-hydraulic channels as shown in the Figure 2-1 in which the numbers indicate channel number assignments of the fuel assemblies and 'black box' corresponds to the reflector region. A thermal-hydraulic channel was not assigned to the reflector so that fixed reflector properties were used as provided in the final specifications. Each channel is also divided into 24 axial levels and the vessel model also used 3 separator (SEPD) components using the TRACE mechanistic separator option. The steam line was modeled using 2 TEE components and 3 VALVE components. The thermal-hydraulic nodalization diagram of TRACE is also provided in Figure 2-2.

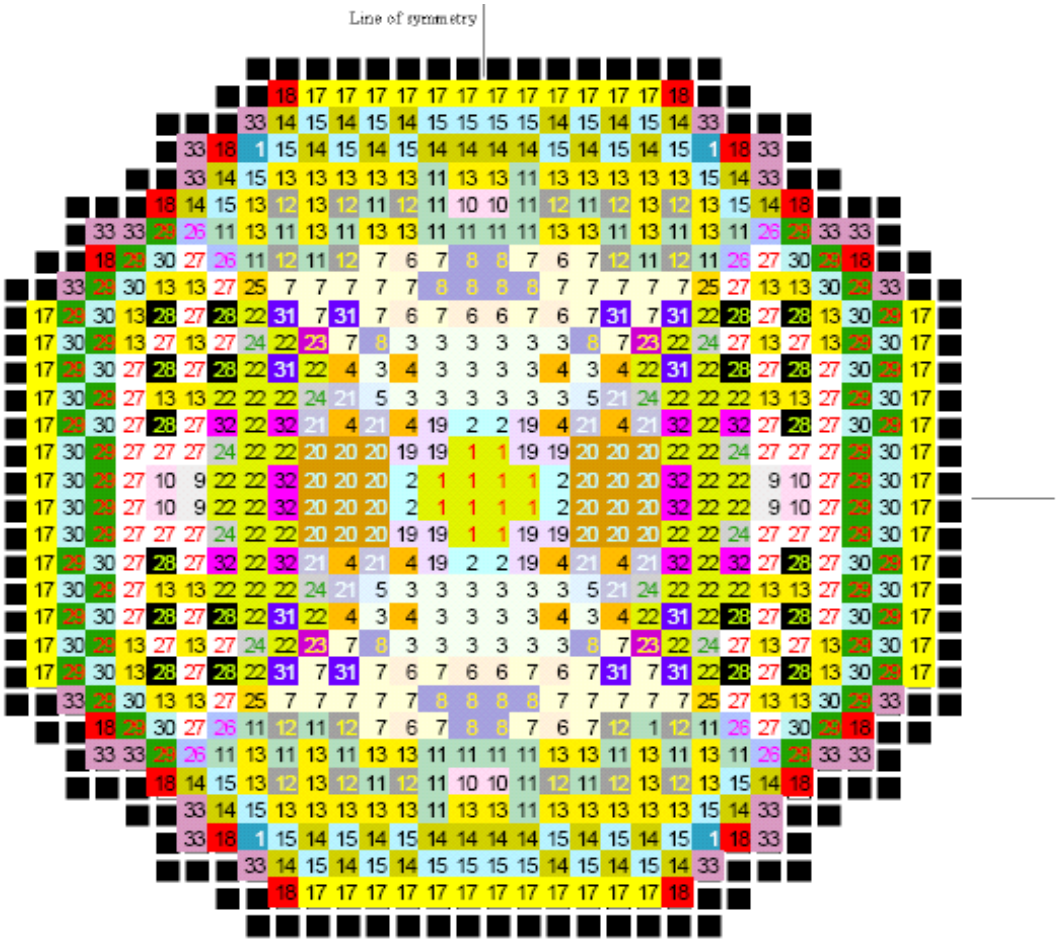

Figure 2-1: Thermal-Hydraulic 33-Channel Mapping for PBTT

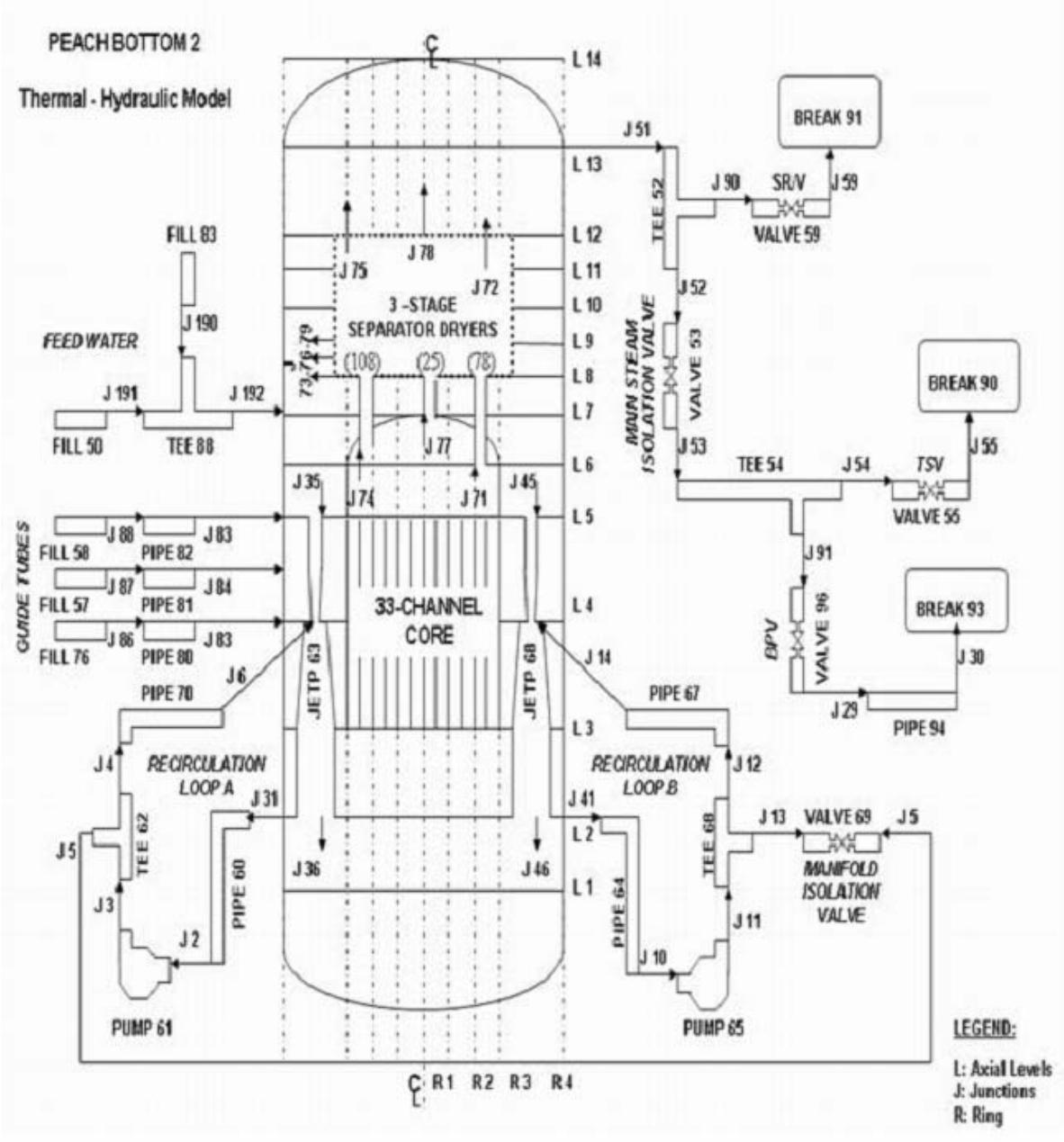

Figure 2-2: TRACE Thermal-Hydraulic Nodalization Diagram

2.3.1.2 PBTT PARCS Neutronics Model

The neutronics core model used in this benchmark is based on the end-of-cycle state of the Peach Bottom Unit 2. This is a BWR/4 consisting of 764 fuel assemblies and 185 control rods. At the time of the TT2 test, there were 576 7x7 and 188 8x8 fuel assembly types. All fuel assemblies have Gadolinium as a burnable poison. The PARCS model represents each of the 764 fuel assemblies as a single neutronics node. The active core height is 365.76 cm, which is modeled in PARCS with 24 axial layers. The thickness of the axial layers is 15.24 cm. At the top and bottom of the active core, there exist 15.24 cm-thick axial reflector regions. Full core geometry was modeled for the benchmark because the core is not symmetric.

The benchmark specifications provided for 432 sets of cross sections and kinetics parameters in the fuel region and 3 sets for reflector region (bottom, top, and radial reflector). The group constant data and kinetics parameters were provided as two data files, the first file is for unrodded compositions while the second one is for rodded compositions. Peach Bottom Unit 2 is equipped with local power range monitors (LPRM). Forty-three detector strings are provided for the in-core instrumentation with each string containing four LPRM located at four axial elevations in the core. In the cross section library, the microscopic fission cross sections are provided for the fissile material of the fission chambers, as well as the assembly detector factors, which are the ratio between the flux in the detector location and the average flux of the neutronic cell. An LPRM model was developed and implemented in PARCS to compare the calculations with the measured in-core detector signals.

2.3.1.3 PBTT Sensitivity Results and Discussion

The models given in the previous sections were validated in PBTT benchmark and published at the Reference [**34**]. It should be noted that the TRACE/PARCS overall results agree well with both static and transient plant measured data. This validation insures the studies given in this section. The purpose of the calculations performed in this section is to investigate the impact of using spatially dependent nodal kinetics parameters and core average kinetics parameters on the PBTT Benchmark problem. As it is mentioned in the previous section, effective delayed neutron fractions (beta) and decay constants (lambda) for six precursor families (6-group) are provided by the benchmark specification in the rodded and unrodded cross section libraries for each node. Also 6-group core average betas and lambdas are given in the specifications [**6**]. Six different sets of calculations were performed in this section. The calculation matrix is given at the Table 2-1.

Table 2-1: Calculation Matrix

Sets	Beta	Lambda
1	Local	Local
2A	Local	Core average
2B	Local	Core average input for ^{235}U from Keepin's data
3	Core average	Local
4A	Core average	Core average
4B	Core average	Core average input for ^{235}U from Keepin's data

The term "local" in this section refers to the spatially dependent nodal kinetics parameters that are provided by the PBTT Benchmark specifications [**6**]. Local values consist of 435 sets of parameters provided as a part of two data files; the first file is for unrodded compositions while the second one is for rodded compositions. The term "core average" refers to the core average kinetics parameters. The core average group wise decay constants and delayed neutron fractions are also provided in the PBTT Benchmark specifications and they are shown at the Table 2-2 .

Table 2-2: Core Average Kinetics Data from PBTT Specifications

Delayed Neutron Group	Lambda, (s^{-1})	Beta
1	0.012813	0.000167
2	0.031536	0.001134
3	0.124703	0.001022
4	0.328273	0.002152
5	1.405280	0.000837
6	3.844728	0.000214

In addition to the local and core average values from the PBTT Benchmark specifications, core average decay constants for ^{235}U from Keepin's data were used for the testing purposes. Keepin's Decay Constants for ^{235}U and their deviations from the core average values (Table 2-2) are provided at the Table 2-3. The sets given at the Table 2-1 were performed for two cases: best estimate case, and the extreme case (turbine trip transient without scram which is a design basis test case). The reason for repeating

the calculations with the extreme case is to understand the effect of different sets of kinetics parameters in case of scram is not initiated.

Table 2-3: Keepin's Decay Constants for ^{235}U

Group	1	2	3	4	5	6
Lambda, (s^{-1})	0.0124	0.0305	0.1110	0.3010	1.1400	3.0100
Deviation from core average (%)	-3.2	-3.3	-11.0	-18.9	-21.7	-11.1

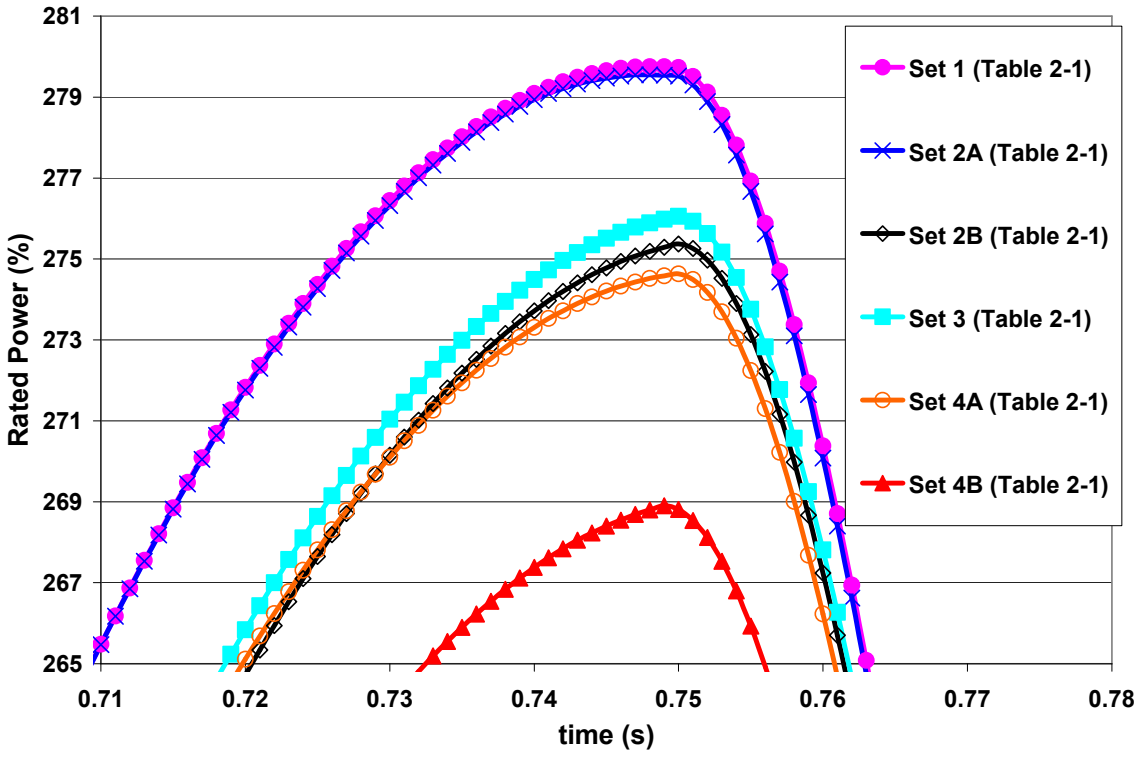

Figure 2-3: PBTT *Best Estimate* Core Power for All Sets from the Table 2-1

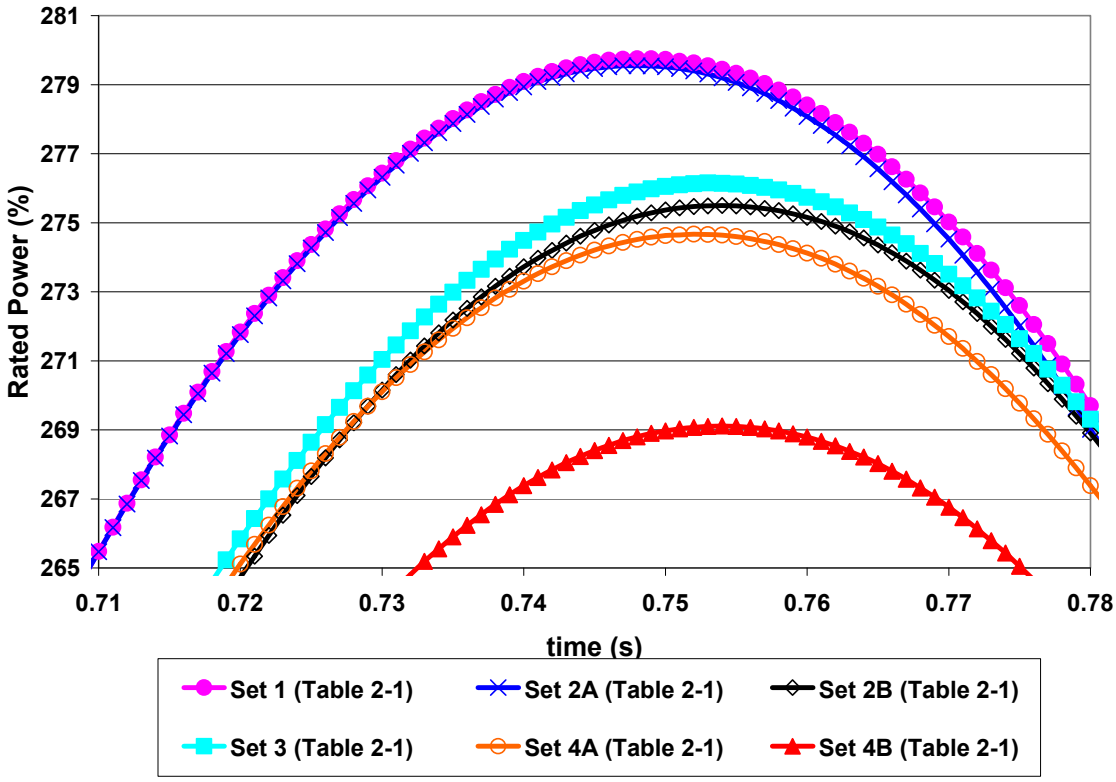

Figure 2-4: PBTT *Extreme Case (No Scram)* Core Power for All Sets from the Table 2-1

Table 2-4: Peak Time and Power for the Extreme Case (No Scram)

Sets	Time of Peak Power (s)	Peak Power (%)*
1	0.749	279.8
2A	0.748	279.6
2B	0.754	275.4
3	0.753	276.2
4A	0.752	274.7
4B	0.755	269.1

* Nominal power is 100 (%) and initial power of TT2 is 61.6 (%).

Figure 2-3 and Figure 2-4 present the core power results for the best estimate and extreme cases respectively. It should be noted that, in the following figures, turbine trip test (TT2) was initiated at 61.6% rated power (2030 MW). Although there are numerous output data available in PARCS and TRACE output files, only core power results are presented in this section for sake of simplicity. The peak time and peak power values are also given at the Table 2-4. It should be noted that the peak power during the TT2 measurement is 280.3% [**6**].

If Figure 2-3 and Figure 2-4 are compared, the effect of different kinetics parameters on the peak time become visible because scram is initiated at 0.75 of the transient problem time in all sets. It can be seen from Table 2-4 that the maximum deviation on the peaking time is less than 1%. The following remarks can be made if Figure 2-4 and Table 2-4 are analyzed.

The difference at the peak power between the sets 1 and 2A is 0.2% over the nominal value, and it is 2.5% between the sets 3 and 4A. This shows that the effects of lambdas are small when they are changed from local to average. This is consistent with the fact that the isotope dependence of the decay constants is not very pronounced If Keepin's data is used instead of average lambdas; the difference at the peak power becomes 4.2% for the sets 2A vs. 2B and 5.6% for the sets 4A vs. 4B. It should be noted that Keepin's data (Table 2-3) is dramatically different than the core average lambdas (Table 2-2). On the other hand, if the effects of beta are analyzed only, the difference at the peak power can be found as 3.6% for Set 1 vs. Set 3, 4.9% for Set 2A vs. 4A, and it is 6.3% for Set 2B vs. Set 4B. These are the effects of lambdas only when they are changed from local to average.

It is obvious that the deviations happen on the peak power values in case of betas changed only are significantly bigger than the deviations on the peak timing. If isolated effects of betas and lambdas on local vs. core average results are analyzed one can say that betas influenced the power values more effective than the lambdas. Therefore, usage of local kinetics parameter is recommended for this type of transient calculations.

In conclusion, the analysis of the PBTT experiment using TRACE/PARCS is presented in this section. PARCS neutronics model and TRACE thermal–hydraulics model are developed to model the Peach Bottom nuclear power plant and applied to the turbine trip experiment using the benchmark specifications. Sensitivity of kinetics parameters in particular delayed neutron fractions and decay constants on this type of transients is investigated.

2.3.2 Numerical Studies Using LMW Benchmark

The scope of this section is to investigate the effects of different sets of delayed neutron fractions on the numerical transient applications. Langenbuch-Maurer-Werner (LMW) benchmark problem [**5**] is one of the well known kinetics benchmark in this regard. LMW problem simulates operational transient involving rod movements. The transient of LMW benchmark is for a simplified large light water reactor and it is initiated by withdrawing of a bank of four partially inserted control rods at a rate of 3 cm/s. Then, a bank of five control rods is inserted with the same rate [**35**]. The total transient time is defined as 60 s. The core is reflected in both the radial and axial directions by 20 cm of water. There are 77 assemblies in one-eight-core symmetry. The

assemblies have x-y dimensions 20x20 cm and active height of 160 cm [**36**]. Detailed LMW model and the geometrical specifications are shown in the Figure 2-5, Figure 2-6 and Figure 2-7.

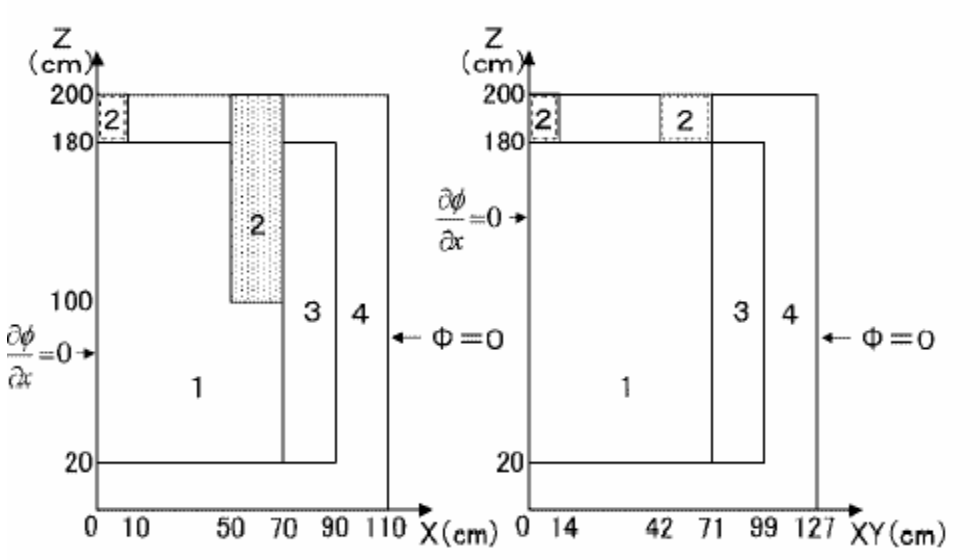

Figure 2-5: LMW Transient Problem Initial Rod Positions (Vertical)

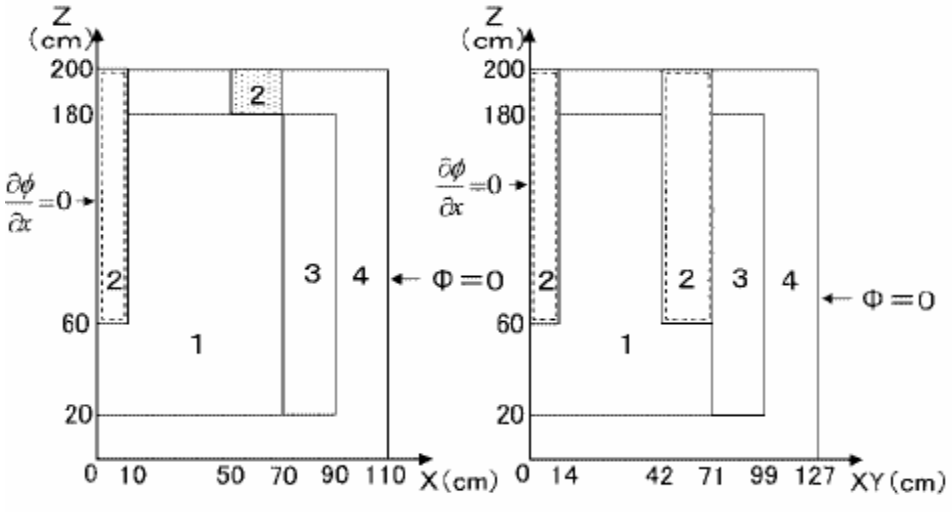

Figure 2-6: LMW Transient Problem Final Rod Positions (Vertical)

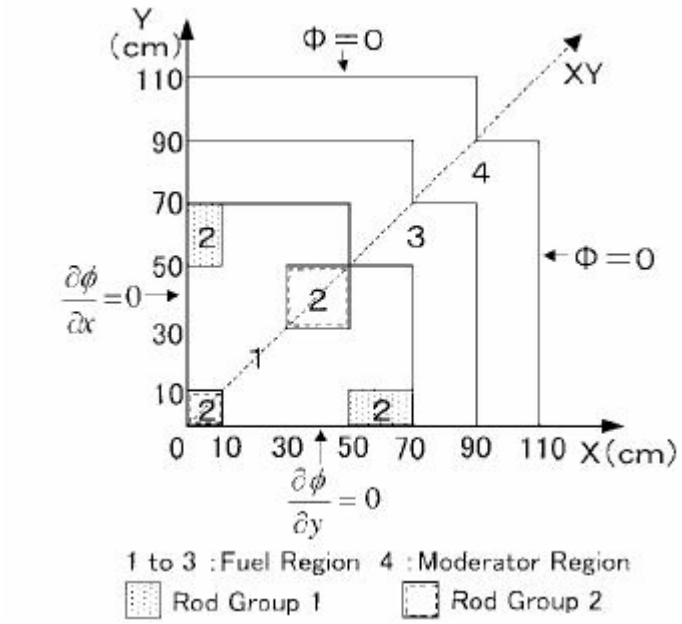

Figure 2-7: LMW Transient Problem (Horizontal Cross Section)

The control rods movement modeling has important discrepancies on the cross-sections. Since the spatially uniformed cross-sections for a given node cause errors when modeling the partially-rodded node as the volume weighted cross-sections of the fully-rodded and fully-unrodded cross-sections [**35**]. This is simply interpolation of the cross-sections. It is proposed in the Reference [**35**] that controlled and uncontrolled cross-sections should be weighted by the actual node axial flux distribution. Therefore, using this benchmark may bring some questions on the kinetics data generation because the variations of the results will not be clear unless true cross-section set is generated. However, it will provide a chance to understand how different sets of kinetics parameters have effects on the numerical transient problems.

The Pennsylvania State University version of Nodal Expansion Method (NEM) code is used in LMW benchmark calculations presented in this section. NEM is one of

the modern nodal methods, to solving the shape equations, in order to reduce the spatial discretization errors occurred in the conventional finite difference method.

2.3.2.1 LMW Sensitivity Results and Discussion

The first sensitivity analysis is performed on the delayed neutron fractions (betas) in this section. The lattice code, TransLAT has a capability to produce three different sets of delayed neutron fractions. The first method is based on the "direct" usage of the "physical" (raw) betas from nuclear data libraries. Therefore, this method is referred as "direct beta" (D) or "physical beta" in this thesis. As it was mentioned previously, a correction is necessary for the betas in order to take into account the importance of the delayed neutron spectrum in the transient calculations. The methods utilized these corrected betas are called as "beta effective" methods and TransLAT has the capability of producing betas with these two effective methods: One is called as "k-ratio beta effective" (k) and other is "adjoint weighted beta effective" (AW). The detailed analysis of these three methods is provided in the Chapter 3 since the purpose of the sensitivity analysis given in this section is to understand the effects of these three beta methods on LMW type of transient problem.

The three sets of total and six-precursor-family (6-group) betas (β) generated by TransLAT are given at the Table 2-5. Additionally, the percentage (%) changes of the effective betas from the direct betas are given at the Table 2-6. LMW problem is performed for the betas given at the Table 2-5 and power results are presented in Figure 2-8. Note that these calculations do not include thermal-hydraulics feedbacks.

Table 2-5: Total and 6-Group Betas for Different Methods

***β* Method**	**1**	**2**	**3**	**4**	**5**	**6**	**TOTAL**
Direct (D)	0.000256	0.001517	0.001392	0.003063	0.001097	0.000261	0.007586
k-ratio (k)	0.000245	0.001454	0.001335	0.002936	0.001052	0.000250	0.007272
Adjoint Weighted (AW)	0.000244	0.001446	0.001328	0.002921	0.001046	0.000249	0.007234

Table 2-6: Percentage (%) Differences of the Effective Betas from Direct Betas

%Method	**1 (%)**	**2 (%)**	**3 (%)**	**4 (%)**	**5 (%)**	**6 (%)**	**TOTAL**
100 x (k – D) / D	-4.14	-4.15	-4.09	-4.15	-4.10	-4.14	-4.13
100 x (AW – D) / D	-4.53	-4.68	-4.60	-4.64	-4.65	-4.64	-4.64

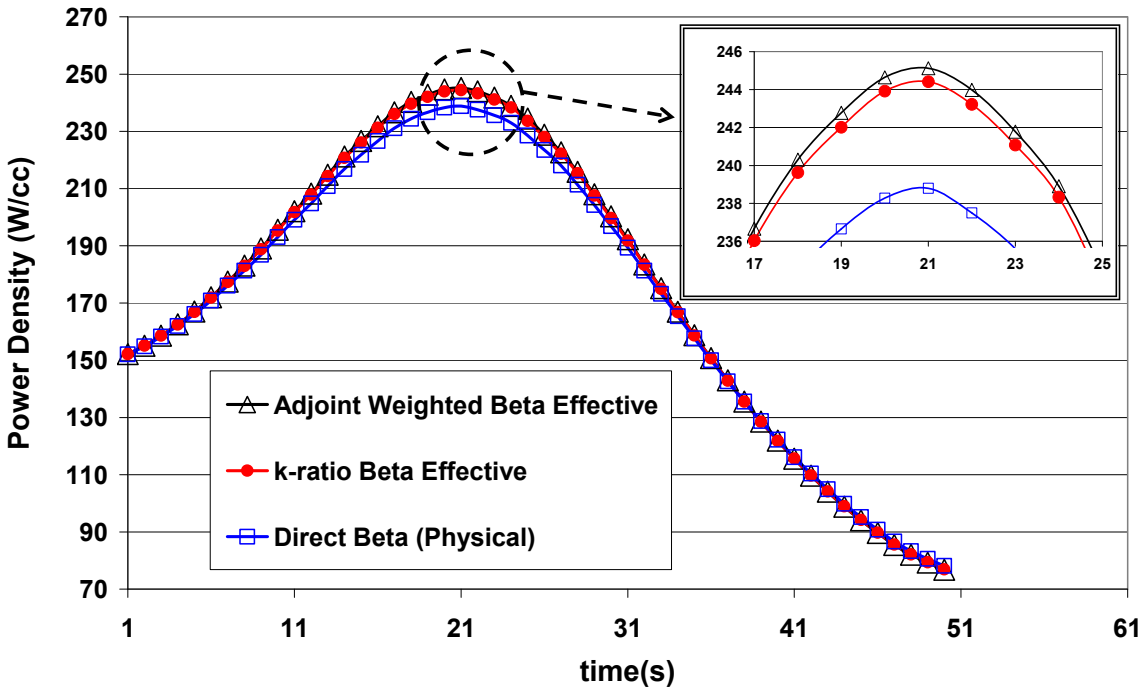

Figure 2-8: LMW Power Comparison for Different Beta Methods

The percentage (%) difference of the powers computed by using direct beta method from the powers computed by effective beta methods are given at the Table 2-7.

Table 2-7: % Changes of LMW Transient Power for Different Beta Effective Methods

t (s)	k-ratio (%) 100x(k-D)/D	Adjoint W. (%) 100x(D-AW)/D	t (s)	k-ratio (%) 100x(k-D)/D	Adjoint W. (%) 100x(D-AW)/D
1	0.06	0.06	**26**	2.03	2.38
2	0.14	0.11	**27**	1.88	2.15
3	0.20	0.21	**28**	1.91	2.12
4	0.34	0.37	**29**	1.60	1.85
5	0.45	0.50	**30**	1.44	1.72
6	0.59	0.65	**31**	1.31	1.56
7	0.73	0.82	**32**	1.15	1.19
8	0.87	0.98	**33**	1.02	1.16
9	1.02	1.18	**34**	0.82	0.91
10	1.19	1.34	**35**	0.63	0.65
11	1.36	1.52	**36**	0.43	0.46
12	1.50	1.69	**37**	0.18	0.28
13	1.65	1.86	**38**	0.01	-0.01
14	1.80	2.03	**39**	-0.19	-0.17
15	1.93	2.17	**40**	-0.28	-0.27
16	2.04	2.30	**41**	-0.40	-0.46
17	2.16	2.43	**42**	-0.62	-0.66
18	2.24	2.53	**43**	-0.75	-0.84
19	2.27	2.59	**44**	-0.88	-0.98
20	2.37	2.67	**45**	-1.05	-1.19
21	2.35	2.65	**46**	-1.17	-1.32
22	2.41	2.73	**47**	-1.27	-1.42
23	2.32	2.62	**48**	-1.40	-1.57
24	2.30	2.54	**49**	-1.48	-1.66
25	2.23	2.58	**50**	-1.57	-1.74

The results presented in this section are intended to provide a level of understanding for the impact of different beta methods on the LMW type reactivity-initiated transient problem. The significance and the importance of the effective delayed neutron fraction methods are discussed in the further chapters.

In this sensitivity analysis, it has been investigated that changes on the beta values have impact on the transient power. In particular, if the powers from direct beta and effective betas are compared as in the Table 2-7, one can say that approximately 4 to 5% changes on the beta values (Table 2-5) change LMW power about 2 to 3 % at the peak time (~22 s). Additionally, there is good agreement between the power solutions of the two effective beta methods (adjoint weighted vs. k-ratio). The adjoint weighted and k-ratio effective beta values differ about 0.5% from each other and this difference impact on the power results about 0.3% at the peak time.

Another sensitivity analysis is performed for the betas from each of the six precursor family groups in order to understand the isolated contributions of these families to the power density. The total contribution of these families can be seen from Figure 2-8.

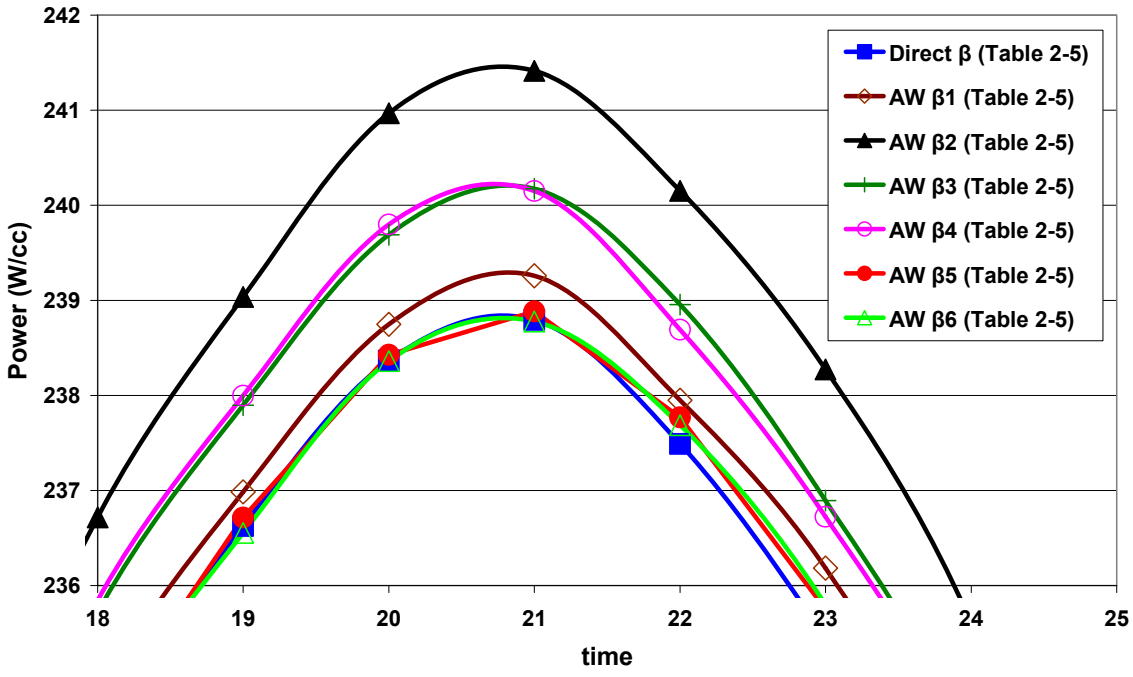

Figure 2-9: Isolated Effects of Group Wise Betas on LMW Power

In Figure 2-9, the effects of each of the six-group betas are isolated by changing them from direct beta to adjoint weighted beta effective one by one. For instance, B1 in Figure 2-9 refers to the power density results in case of only group 1 beta is changed from direct to adjoint weighted. The betas in the other five groups are still direct beta. Similarly, B2 refers to the power when only beta of the second group is changed from direct to adjoint weighted; and so on.

The effect of group 5 and group 6 betas (B5 and B6 in Figure 2-9 respectively) are insignificant if the effects of other groups are considered. The biggest contributor is group 2 (B2) and the contributions of group 3 (B3) and group 4 (B4) to power are approximately the same.

2.4 SUMMARY

This chapter provides a detailed analysis of literature addressing kinetics parameters with particular focus on delayed neutron data currently utilized in the modern nuclear computer codes. The studies in the level of nuclear data libraries show that there are numerous developments and improvements exist for the evaluation of delayed neutron data. However, this thorough analysis is somewhat lost in 3-D coupled transient calculations even though the kinetics data are accurate and elaborate. The reason for this is the fact that the codes use the processed information instead of nuclear data themselves. During this process, naturally, some approximations and methodologies as summarized in this chapter have been utilized to evaluate delayed neutron fractions. As a result of the review on these approximations, two important deficiencies are found in the

current techniques from the perspective of BWR design and code development. One deficiency is the assumption that the kinetics parameters to be dependent only on burnup (isotopic content). This assumption does not take into account the local instantaneous variations in the reactor core nodes. The other deficiency is the correction techniques (beta effective methods) which supposedly handle the fission emission spectra difference between prompt and delayed neutrons in two group applications. The adequacy and sufficiency of these corrections has never been tested thoroughly for BWR applications. Briefly, these flaws of the current methods emphasize the necessity of the innovations and improvements fulfilled in the following chapters.

In addition to the literature review on kinetics parameters, another review is performed to investigate the capabilities of the nuclear computer codes, which will be utilized as tools to validate the developments given in the further chapters. Out of the available computer codes, TransLAT for lattice calculations, PARCS for standalone kinetics calculations, and TRACE/PARCS for coupled thermal-hydraulics/neutronics analysis are selected for this research. The justification of this selection is provided with the capabilities of these codes in the second section of this chapter. This review also presents an extensive background which will be a basis for the code developments performed in the next chapters.

The sensitivity analysis section of this chapter is intended to provide some preliminary analyses on the kinetics parameters for the purpose of understanding the effects of delayed neutron data in reactor kinetics applications.

Chapter 3

CONSISTENT GENERATION AND MODELING OF DELAYED NEUTRON DATA

The goal of this thesis is to improve the three-dimensional (3-D) neutron kinetics modeling for coupled transient Boiling Water Reactor (BWR) applications. The reviews and studies presented in Chapter 2 reveal that new robust methods for consistent generation and modeling of delayed neutron data for such coupled thermal-hydraulics/neutronics simulations must be developed to achieve this goal. Once developed, these methods need to be validated by implementing them into the computer codes. This chapter mainly focuses on the method developments in this regard while implementations and validations of the developed techniques are given in the further chapters.

First section of this chapter provides more detailed reviews on the delayed neutron fraction methods. This introduction help to understand the motivation behind the studies performed in the further sections. The studies on enhancing the accuracy of the simplified k-ratio method are given, and the enhanced method is validated in the second section. In Section 3.3, a unique and very important analysis is performed for the state parameter effects on the delayed neutron fractions and delayed neutron importance factors, which are corrections applied to the nodal values of the delayed neutron fractions. The Section 3.4 presents a new methodology which provides an appropriate

functionalization of the state dependencies of the delayed neutron importance factor. One of the most important and innovative contributions of this thesis is given in this section.

3.1 METHODOLOGIES FOR DELAYED NEUTRON FRACTIONS

Delayed neutrons are considered together with prompt neutrons as total number of fission neutrons in the static reactor problems. However, from kinetics point of view, delayed neutrons have important effect on the time dependent neutron flux. It is previously pointed out that cross-section data, and delayed neutron (DN) data must be generated consistently. In order to investigate the deficiencies of the current methods, kinetics equations and delayed neutron fractions are analyzed carefully in the following sub-sections. Thus, this section will be a basis for the studies given in the next sections and will be reference to the specific terms and definitions used in this research.

In this study, "Direct Beta (β)" will refer to the fission rate averaged beta (i.e. physical beta), "k-ratio Beta Effective (β^{eff})" will refer to the physical beta adjusted by means of the importance factor (I) determined by k-ratio method, and "Adjoint Weighted Beta Effective (β^{eff})" will refer to the effective beta computed using adjoint spectrum weighting technique.

3.1.1 Overview on Kinetics Equations

The kinetics equations reflect the transient nature of the neutron balance equations when delayed precursors are included. The following multi-group equations [**37**] will be

useful for the further studies in order to understand the functions of the kinetics parameters in those equations. Multi-group kinetics equations are defined in Eq. 3.1 and Eq. 3.2.

$$\frac{1}{\upsilon_g}\frac{\partial}{\partial t}\Phi(\bar{r},t) = \underbrace{\nabla.D_g(\bar{r})\nabla\Phi_g(\bar{r},t)}_{leakage} - \underbrace{\Sigma_{ag}(\bar{r})\Phi_g(\bar{r},t)}_{loss\ by\ absorbtion} - \underbrace{\Sigma_{sg}(\bar{r})\Phi_g(\bar{r},t)}_{removal\ \ by\ scattering} + \underbrace{\sum_{g'=1}^{G}\Sigma_{sg'g}(\bar{r})\Phi_{g'}(\bar{r},t)}_{scattering\ \ in\ group\ \ g} + \underbrace{\chi_g^P}_{\substack{prompt\ \ neutron\\ fission\ \ spectra\\ in\ group\ \ g}}\underbrace{(1-\beta)}_{\substack{prompt\\ fraction}}\underbrace{\sum_{g'=1}^{G}\nu_{g'}\Sigma_{fg'}(\bar{r})\Phi_{g'}(\bar{r},t)}_{total\ \ fision\ \ production} + \underbrace{\chi_g^D}_{\substack{delayed\ \ neutron\\ fission\ \ spectra\\ in\ group\ \ g}}\underbrace{\sum_{d=1}^{N}\lambda_d C_d(\bar{r},t)}_{\substack{total\ \ delayed\\ source}} + \underbrace{S_g^{ext}}_{\substack{external\\ source}} \qquad \textbf{(3.1)}$$

$$\frac{\partial}{\partial t}C_d(\bar{r},t) = -\lambda_d C_d(\bar{r},t) + \underbrace{\beta_d}_{\substack{d^{th}\ part\\ of\ delayed\\ neutrons,\\ split\ by\\ decay\ const.}}\underbrace{\sum_{g'=1}^{G}\nu_{g'}\Sigma_{fg'}(\bar{r})\Phi_{g'}(\bar{r},t)}_{total\ fision\ production} \qquad \textbf{(3.2)}$$

g is multi energy group index and d is delayed neutron precursor group where total delayed neutron fraction can be defined as $\beta = \sum_d \beta_d$

It should be noted that the energy spectrum of the prompt fission neutrons, χ_g^P, is usually not the same as the energy spectrum of the delayed neutrons, χ_g^D in multi group equations.

As it was stated previously, delayed neutron spectrum is softer than the prompt neutron spectrum. For instance, while the average prompt neutron fission energy is approximately 2 MeV, the average energy of delayed neutrons is approximately 0.45 MeV. Therefore, all neutrons are born at the fast group in 2-group LWR applications. This means that the fast spectrum ($\chi_1^P = \chi_1^D$) is 1 and the thermal spectra are zero. In order to compensate this shortcoming of 2-group applications, delayed neutron fractions are adjusted to so-called effective delayed neutron fractions, which supposedly represent the impact of the difference between delayed neutron spectrum and prompt neutron spectrum.

3.1.2 Direct (Physical) Beta

The delayed neutron fraction (β) is the ratio of delayed neutron yield to the total neutron yield, which is composed of prompt and delayed neutrons. Modern lattice physics codes generate delayed neutron fractions for a given material composition and for a given energy group from nuclear database by employing summation and averaging them with the fission neutron production rate. This method will be called as *Direct Beta* or *Physical Beta* throughout this research. Direct beta method can be considered as a raw technique since it can not handle the spectrum effects in the evaluation of delayed neutron fractions. Direct beta can be calculated as in Eq. 3.3.

$$\beta = \sum_d \beta_d = \sum_d \left[\frac{\sum_i \beta_i a_{i,d} \sum_g \sum_j \nu \Sigma_{f,i,j,g} V_j \Phi_{j,g}}{\sum_i \sum_g \sum_j \nu \Sigma_{f,i,j,g} V_j \Phi_{j,g}} \right] \qquad \textbf{(3.3)}$$

d = delayed neutron precursor family group

g = multi-energy group index

i = fissionable nuclide index and j= cell (node) region index in volume V_j

β_i = total fraction of delayed neutrons from nuclide i

$a_{i,d}$ = the fraction of delayed neutrons from nuclide i related to delayed neutron group d

It should be noted that values of β_i and $a_{i,d}$ are obtained from nuclear data libraries in the lattice calculations where $\beta_{i,d} = \beta_i \, a_{i,d}$. As it was noted before this method, direct beta, does not take into account the difference between delayed and prompt neutrons fission spectra. To overcome this shortcoming, the following beta effective methods are used in the current applications.

3.1.3 Adjoint Weighted Beta Effective

In this method, the delayed neutron fraction is calculated according to the adjoint spectrum which is computed using the multi-group fundamental mode equation. This method provides more accurate estimate of reactivity because it uses adjoint flux as a weighting function in the derivation of kinetics equations by eliminating first-order variations in the flux spectrum [**21**]. The following paragraph from the Reference [**21**] explains the theory behind this methodology.

The adjoint spectrum can be obtained during the calculation of the fundamental mode real spectrum. Since the space dependency of the adjoint spectra is weak, the energy dependent adjoint spectra are calculated by simply transposing the cross section

matrix of the fundamental mode equation. Note that unlike the fundamental mode real calculation, the sum of multiplication of fission spectrum and adjoint spectrum is normalized to unity. Since the buckling of the system is already known from the fundamental mode real calculation, the adjoint equation needs to be solved only once. The real and adjoint spectra are then used to calculate the effective delayed neutron fraction. Since the energy of the delayed fission spectrum is lower than that of the prompt fission spectrum, delayed neutrons have a smaller chance to leak out of the system. This is taken into consideration in the kinetics equations by weighting the physical beta with the energy dependent adjoint spectra which quantifies the energy importance of neutrons in the system.

Adjoint weighted beta effective can be formulated as in Eq. 3.4

$$\beta_d^{eff} = \frac{\sum_i \beta_{i,d} \sum_g \nu\Sigma_{fg,i}\Phi_g \left(\sum_{g'} \chi_{d,g'}^D \Phi_{g'}^* \right)}{\sum_i \sum_g \nu\Sigma_{fg,i}\Phi_g \sum_{g'} \Phi_{g'}^* \left(\chi_{g'}^P (1-\beta_i) + \sum_d \chi_{d,g'}^D \beta_{i,d} \right)} \qquad \textbf{(3.4)}$$

Eq. 3.4 can be rearranged as shown in Eq. 3.5.

$$\beta_d^{eff} = \beta_d \frac{\sum_{g'} \chi_{g',d}^D \Phi_{g'}^*}{\sum_{g'} \chi_{g'} \Phi_{g'}^*} \qquad \textbf{(3.5)}$$

where $\chi_{g'}$ is the total fission spectrum, and total beta effective is:

$$\beta^{eff} = \sum_{d} \beta_{d}^{eff} \qquad (3.6)$$

It should be noted that the adjoint weighted beta effective method is superior to the k-ratio beta effective method since it explicitly treats the prompt and delayed neutron emission spectra in the evaluations of delayed neutron fractions.

3.1.4 k-ratio Beta Effective

A variant of the so-called *k*-ratio method is used in some lattice codes for the purpose of estimating the delayed neutron importance (effectiveness) factor. This method represents a first order approximation to a more rigorous method based on the adjoint solution to the steady-state transport equation. If applied correctly, the *k*-ratio method is capable of producing surprisingly accurate estimates of the importance factor. However, this would require at least one expensive *k*-eigenvalue calculation in addition to the normal steady-state k_{eff} calculation and would not offer any advantage over the more rigorous approach based on the adjoint flux, unless the adjoint flux calculation itself is very cumbersome (as in the case of Monte Carlo methods).

As a result a simplification of the *k*-ratio approach is adopted in lattice codes that do not have access to an adjoint calculation (i.e., PHOENIX, HELIOS). This simplification avoids any additional lattice calculations and utilizes a standard reaction rate edit to compute the *k*-ratio. The edit is performed over a specified energy range that is supposed to cover the influence range of the delayed neutron emission spectrum. In most lattice codes an upper energy for this range is hard-wired to a value of about

roughly 0.45 MeV. It seems that the common source for this energy choice (i.e., 0.45 MeV) as well as the description of the simplified *k*-ratio method can be tracked to an old technical note related to the AEBUXY code [**25**].

In a general way, k-ratio beta effective can be calculated by multiplying direct beta with k-ratio (or simplified k-ratio) method as shown in Eq. 3.7

$$\beta^{eff} = \frac{k_D}{k}\beta \tag{**3.7**}$$

The definition of the *k*-ratio method can be stated as in Eq. 3.8.

$$\frac{k_D}{k} = \frac{\int_0^{E_D} dE\, \chi^D(E) \int_0^{E_D} dE' \nu \sum_f (E')\psi(E')}{\int_0^{E_D} dE \left(\sum_a (E) + D(E)B^2\right)\psi(E)} \frac{\int_0^{\infty} dE \left(\sum_a (E) + D(E)B^2\right)\Phi(E)}{\int_0^{\infty} dE\, \chi(E) \int_0^{\infty} dE' \nu \sum_f (E')\Phi(E')} \tag{**3.8**}$$

where B^2 is a buckling representing leakage effects, $\chi^D(E)$ and $\chi(E)$ are the delayed neutron and the total neutron emission spectra, and E_D represents the upper energy boundary of the delayed neutron emission spectrum. Note that, the upper case "*D*" referred to term "delayed" in this thesis. Clearly, the fission spectra are normalized to unity since they represent probability density distributions and their integral values can therefore be dropped from the above expression. The flux spectra obtained from the two eigenvalue calculations are not the same and it is by assuming that they are the same that the *simplified k*-ratio method is obtained by Eq. 3.9.

$$\left(\frac{k_D}{k}\right)_{simplified} = \frac{\int_0^{E_D} dE' \nu \sum_f (E')\Phi(E')}{\int_0^{E_D} dE \left(\sum_a (E) + D(E)B^2\right)\Phi(E)} \frac{\int_0^{\infty} dE \left(\sum_a (E) + D(E)B^2\right)\Phi(E)}{\int_0^{\infty} dE' \nu \sum_f (E')\Phi(E')} \tag{**3.9**}$$

Here E_D is interpreted as some cut-off energy defining the energy range over which the delayed neutron multiplication factor (i.e., k_D) should be edited and traditionally it has been set at about 0.45 MeV. The accuracy of the simplified *k*-ratio method will be tested in the Section 3.3 and enhanced by adjusting the value of the upper energy for the delayed neutron range to a somewhat higher generic value than the traditional 0.45 MeV value.

3.1.5 Importance Factor

Importance factor (called as effectiveness factor in some literature) can be defined as a correction applied to the direct betas to compensate the inherent deficiency of the two-group model which can not explicitly capture neutron emission spectrum effects. It is simply a factor defining the relation between direct beta and effective beta.

There are two importance factor formulas since there are two beta effective methods in the current delayed neutron fraction evaluation methods. Eq. 3.3 and Eq. 3.5 yields the *adjoint weighted (AW) importance factor* as given at Eq. 3.10 while Eq. 3.3 and Eq. 3.9 yields the *simplified k-ratio importance factor* as presented at Eq. 3.11.

$$I_{AW} = \frac{\beta^{eff}}{\beta} = \frac{\sum_g \chi_g^D \Phi_g^*}{\sum_g \chi_g \Phi_g^*} \qquad (\mathbf{3.10})$$

$$I_{k-ratio} = \left(\frac{k_D}{k} \right)_{simplified} \qquad (\mathbf{3.11})$$

Importance factor is the key parameter of this study, and it is extensively used as a kernel in the analyses and developments presented in the further sections and chapters. It is shown in the further sections that the importance factor is not only utilized to capture the spectrum effects but also utilized to represent instantaneous local variations in the reactor core nodes.

Fundamentally, adjoint weighted importance factor is a better approximation than the simplified k-ratio beta effective method. However, some lattice codes have no such availability of the adjoint weighted method. For this reason, the study given in the next section seeks the possibility of enhancement on the simplified k-ratio method.

3.2 ENHANCING THE ACCURACY OF THE SIMPLIFIED K-RATIO METHOD

k-ratio method is used in some lattice codes for the purpose of estimating the delayed neutron importance factor (also known as the delayed neutron effectiveness factor). This method represents a first order approximation to a more rigorous method based on the adjoint solution to the steady-state transport equation. If applied correctly, the *k*-ratio method is capable of producing surprisingly accurate estimates of the importance factor. However, this would require at least one expensive *k*-eigenvalue calculation in addition to the normal steady-state k_{eff} calculation and would not offer any advantage over the more rigorous approach based on the adjoint flux, unless the adjoint flux calculation itself is very cumbersome (as in the case of Monte Carlo methods). As a result a simplification of the *k*-ratio approach is adopted in lattice codes that do not have

access to an adjoint calculation. This simplification avoids any additional lattice calculations and utilizes a standard reaction rate edit to compute the *k*-ratio. The edit is performed over a specified energy range that is supposed to cover the influence range of the delayed neutron emission spectrum. In most lattice codes an upper energy for this range is hard-wired to a value of about 0.45 MeV.

In this section numerical results are presented that show how the accuracy of the simplified *k*-ratio method may be enhanced by adjusting the value of the upper energy for the delayed neutron range to a somewhat higher generic value than the traditional 0.45 MeV value. While geared towards lattice physics code applications, this modification may make the simplified *k*-ratio method attractive for use in Monte Carlo applications as well.

3.2.1 Methodology Development

The calculation of the effective delayed neutron fraction, β^{eff}, or alternatively the delayed neutron importance factor, $I=\beta^{eff}/\beta$, is quite standard in industrial lattice codes. These parameters are normally processed for assembly-size radial homogenization areas (nodes) and passed on to a nodal core transient simulator via specialized interfaces. In most nodal transient codes the (node-wise) β^{eff} is expected to be placed on the nodal cross-section data files since these codes are primarily two-group diffusion-theory codes (because of the two-group approach they require β^{eff} and not β as discussed in the Sections 3.3 and 3.4 as well as Reference [**38**]). In the work presented at Sections 3.3 and 3.4 and Reference [**39**], it has been proposed to pass the (nodal) importance factor *I* and

the fundamental delayed neutron fraction β to the simulator so as to cater for both multi- and two-group transient applications. This is discussed in a more detailed way in the Chapter 4 (also in the Reference [**40**]).

The determination of the delayed neutron importance factor requires the solution of the adjoint transport equation in the lattice code if the strict point kinetics definition of β^{eff} is to be followed. This is done in some lattice codes (e.g., TransLAT), but in a few others (e.g., PHOENIX and HELIOS), an adjoint solution is not available and a simpler approach is adopted to compute the importance factor. The method referred to is widely known as the *k*-ratio method. In its most general form this method approximates the importance factor by the ratio of two k_{eff} eigenvalues, the one obtained by using the delayed neutron fission spectrum and the other obtained by using the total fission spectrum in the solution of the steady-state transport equation. Since this would require two instead of just one costly eigenvalue solution (more would be required if the delayed neutron emission spectra associated with each precursor family were to be used to generate an importance factor for each family), a further simplification is introduced in the lattice code procedures for determining the importance factor. This simplification avoids any additional lattice calculations and utilizes a reaction rate edit to compute the *k*-ratio from the results of the standard k_{eff} calculation case (the one using the total fission spectrum). The edit is performed over a specified energy range that is supposed to cover the influence range of the delayed neutron emission spectrum. In most lattice codes (e.g., TransLAT, PHOENIX and HELIOS) an upper energy for this range is hard-wired to a value close to 0.45 MeV, which is often the upper energy boundary of the discrete energy group that brackets the average emission energy for delayed neutrons (roughly 0.45

MeV). It should be noted one more time that the common source for this energy choice (i.e., 0.45 MeV) as well as the description of the simplified *k*-ratio method can be tracked to an old technical note related to the AEBUXY code [**25**]. More recently, a theoretical basis for the *k*-ratio method was proffered by Spriggs and his co-workers [**22**].

The definitions of the k-ratio and simplified k-ratio methods are given at Eq. 3.8 and Eq. 3.9 respectively. The delayed neutron multiplication factor, k_D, Eq. 3.9 can be rewritten in a discrete form as shown in Eq. 3.12.

$$k_D = \frac{\sum_{g=E_D}^{G} \nu \Sigma_{fg} \Phi_g}{\sum_{g=E_D}^{G} \Sigma_{ag} \Phi_g + \sum_{g=G_D}^{G} D_g B^2 \Phi_g} \qquad (\mathbf{3.12})$$

where g is energy group index, G is the total number of energy groups in the micro-library (i.e. G=97 in TransLAT), $(\nu \Sigma_{fg} \Phi_g)$ is fission rate for group g, $(\Sigma_{ag} \Phi_g)$ absorption rate for group g, and $(D_g B^2 \Phi_g)$ leakage rate for group g. E_D is interpreted as some cut-off energy defining the energy range over which the delayed neutron multiplication factor (i.e., k_D) should be edited and traditionally it has been set at about 0.45 MeV. However, the influence range of delayed neutrons extends to about 1 MeV, which might be an indication that too low a cut-off energy was selected for the simplified *k*-ratio method as implemented in some well-known lattice codes.

In this section it is shown that the simplified k-ratio method is capable of yielding accurate estimates of the delayed neutron importance factor provided that a proper choice is made for the upper energy boundary E_D of the delayed neutron source range. Such a value is found by inspection of lattice calculation results in which this energy boundary is

varied in the reaction rates edit phase. It is demonstrated that a somewhat higher value than the traditional 0.45 MeV is required to obtain a level of accuracy that is essentially independent of the assembly type or the state conditions that are modeled. In other words, it is shown that a generic value of the delayed neutron energy cut-off can be found and such a value is proposed.

3.2.2 Improved Calculation Procedure

In order to evaluate the performance of the simplified *k*-ratio method a lattice physics code with an adjoint flux calculation capability is needed to determine reference delayed neutron importance factors. The TransLAT code was therefore chosen for this purpose. TransLAT computes both the precursor family dependent and the total delayed neutron importance factors for a homogenization region as described in the previous section:

$$I_d = \frac{\beta_d^{eff}}{\beta_d} = \frac{\sum_g \chi_{g,d}^D \Phi_g^*}{\sum_g \chi_g \Phi_g^*}; \qquad I = \frac{\sum_d I_d \beta_d}{\sum_d \beta_d}$$

where β_d^{eff} is the effective delayed neutron fraction for precursor family *d* defined according to the standard definition using the adjoint flux spectrum. In the simplified *k*-ratio method the delayed neutron importance factor *I* is approximated by

$$I_{k\text{-}ratio} = (k_D/k)_{simplified}.$$

While the *k*-ratio method is available in TransLAT, the numerical results presented in this work were obtained in a separate procedure to compute $I_{k\text{-}ratio}$. This procedure simply

utilized the multi-group reaction rates produced by TransLAT. In this way the value of E_D could be easily manipulated without impacting on the TransLAT code itself.

The optimization of the cut-off energy E_D involved minimizing the error of $I_{k\text{-}ratio}$ relative to I. Both the forward and the adjoint flux spectra are computed by TransLAT in its input library multi-group structure (97 energy groups). A fundamental mode solution for an infinite (homogenized) multiplying medium is used for this. While the buckling may be input to TransLAT, a critical buckling search was performed for the purpose of optimizing the value of E_D. This was done since the delayed neutron importance factor is essentially defined for a critical system and, moreover, because it has been shown (see [**22**]) that the *k*-ratio method performs well for near-critical systems. Therefore it would be prudent to perform our optimization of the simplified *k*-ratio method also for near-critical systems. In this regard, inducing criticality via a buckling eigenvalue rather than via a multiplication factor eigenvalue (k_{eff}) is deemed to produce a more physical (realistic) fast neutron spectrum (both forward and adjoint) since, for a given material constitution, leakage is the mechanism that establishes criticality and in the fast energy range leakage has a fundamental mode character due to the long mean free path of fast neutrons. And it is precisely the fast energy range (above 10 keV) that is of interest for the determination of the delayed neutron importance factor.

Non-critical (non-leakage) cases are subsequently analyzed in order to demonstrate that the "optimization" performed for critical systems is acceptable also for non-critical systems.

3.2.3 Results and Discussion

The results presented here are generated for two 8x8 BWR assembly types: one (*Assembly Type 1*) with a large central water rod and with 11 Gd-loaded fuel pins of different enrichments; and the other (*Assembly Type 2*) with two small water rods and with significantly higher enriched fuel than the first one. Calculations are performed at a variety of conditions as shown in Table 3-1 for both assembly types. As noted, the optimization effort involve fundamental mode (critical buckling) TransLAT calculations (in 97 energy groups) followed by simple editing of reaction rates using different values for the cut-off energy E_D. The results depicted in Figure 3-1 shows the deviations of the simplified k-ratio importance factor from the adjoint weighted one as a function of the cut-off energy for the traditional cut-off energy (about 0.45 MeV) and the other the cut-off energy that would be a clear candidate for an optimized *k*-ratio method.

Table 3-1: Calculation Matrix for Assembly Type 1 and Assembly Type 2

Case Id	Fuel Temp. (K)	Mod. Temp. (K)	Void Frac. (%)	Burnup (GWd/t)	Control Rod
1	540	540	0	0	unrodded
2	540	540	0	0	rodded
3	800	559	40	14	unrodded
4	800	559	40	14	rodded
5	800	559	80	60	unrodded
6	800	559	80	60	rodded

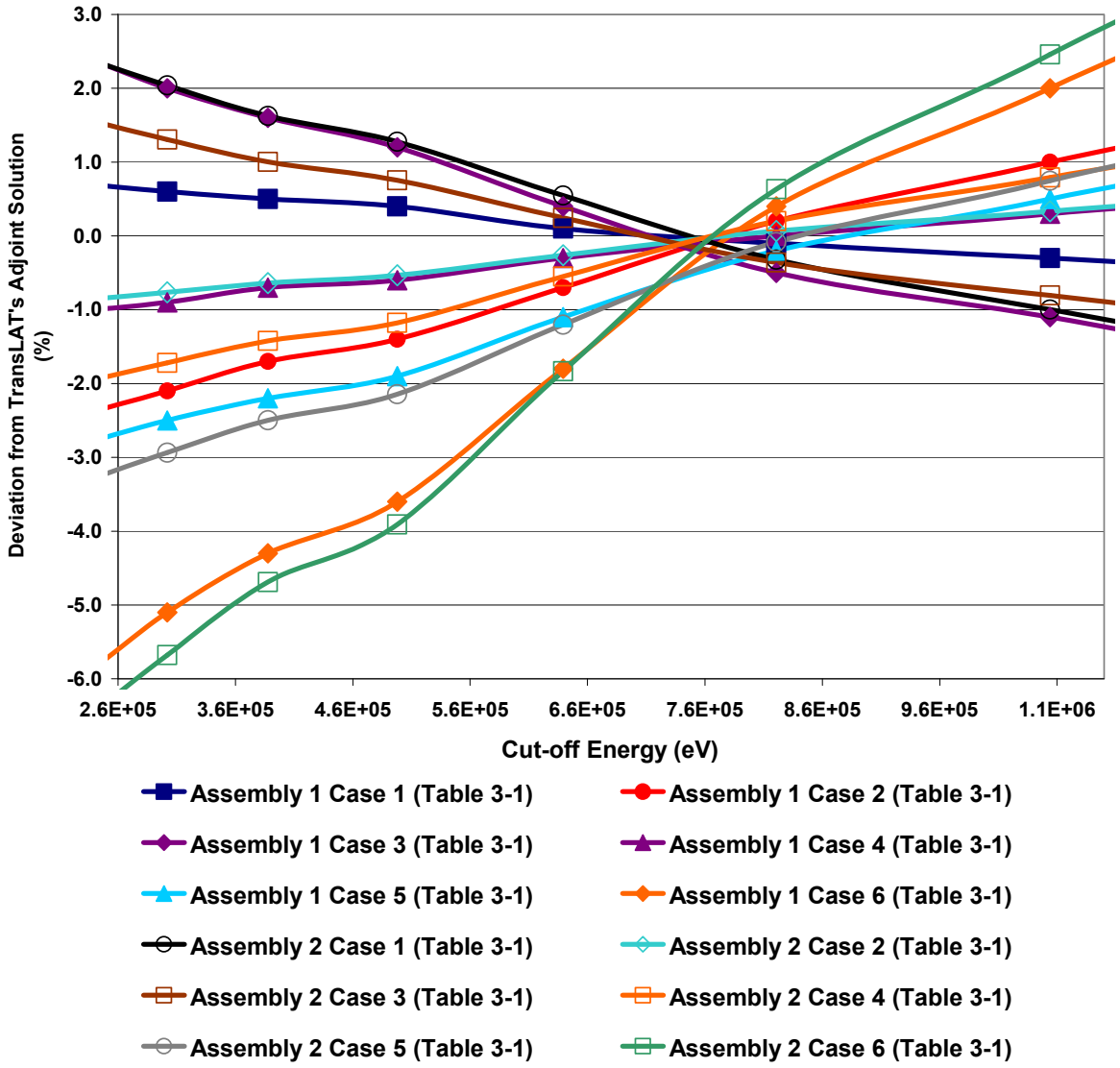

Figure 3-1: Relative Error (%) in the k-ratio Importance Factor (Critical Buckling)

As it can be seen in Figure 3-1, the optimal cut-off energy would appear to be approximately 0.77 MeV and the nearest group boundary in the TransLAT cross-section library (see Appendix) is then 0.821 MeV (this also being a common boundary in many lattice codes).

The average error and the standard deviation around this average as obtained with a cut-off energy of 0.77 MeV are -0.15% and ±0.15%. Using 0.821 MeV instead, these values become -0.01% and ±0.33%. With the traditional 0.45 MeV cut-off the average error is 0.97% and the standard deviation is ±1.73%. It is clear that adjusting the cut-off energy upwards to around 0.77 MeV constitutes a significant improvement in the performance of the simplified *k*-ratio method for critical systems: both the average error and the standard deviation is more than halved.

In order to check that changing the cut-off energy will not deteriorate the estimate of the delayed neutron importance factor for non-critical (non-leakage) systems, the TransLAT calculations were rerun with zero bucklings (specified as input bucklings). For these cases the simplified *k*-ratio method yielded an average error of -0.33% and a standard deviation of ±0.35% with the 0.77 MeV cut-off while with the traditional 0.45 MeV values of -0.18% and ±0.37% were obtained. Thus, even for non-critical cases (k_{eff} ranged from 0.680 to 1.039) the upwards adjustment of the cut-off can be considered an improvement. It is concluded that adjusting the cut-off energy upwards to around 0.77 MeV is generally acceptable for all cases.

Another effort is performed to understand leakage effects on the k-ratio method. It is found that simplified k-ratio importance factors from the zero buckling calculations are less sensitive to cut-off energy boundary than the critical buckling ones. This observation yields this work to investigate the cause what makes critical buckling importance factors more sensitive to cut-off energy than zero buckling results. For this reason, the behavior of delayed neutron multiplication factor (k_D) was analyzed as shown in Figure 3-2. Here, simplified delayed neutron multiplication factors are calculated from reaction rate edits of

TransLAT for three cases: the zero buckling, critical buckling with leakage, and critical buckling without leakage. The results are illustrated with diffusion coefficient in Figure 3-2.

It is found that the critical buckling k_D is very close to the zero buckling k_D when leakage rate is not taken into account. This shows that flux spectrum does not play the major role on the simplified delayed neutron multiplication factor calculations but that it is the leakage rate because the diffusion coefficient has strong energy dependence compared to that of fission or absorption rate.

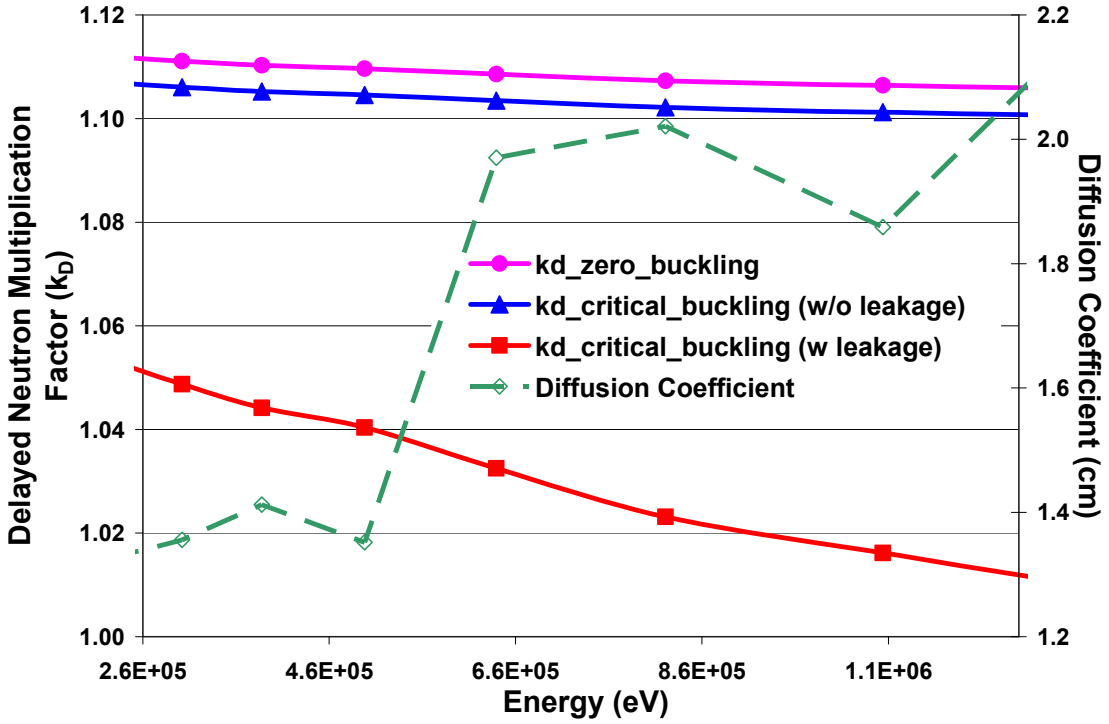

Figure 3-2: Leakage Effects on Delayed Neutron Multiplication Factor

In order to evaluate the significance of the observed improvement in the delayed neutron importance factor in actual transient applications, a simple BWR mini-core kinetics benchmark was constructed as a test case. This mini-core consisted of a 6x6 matrix of identical fresh BWR assemblies with a fuel active height of 366 cm (see Figure 3-3).

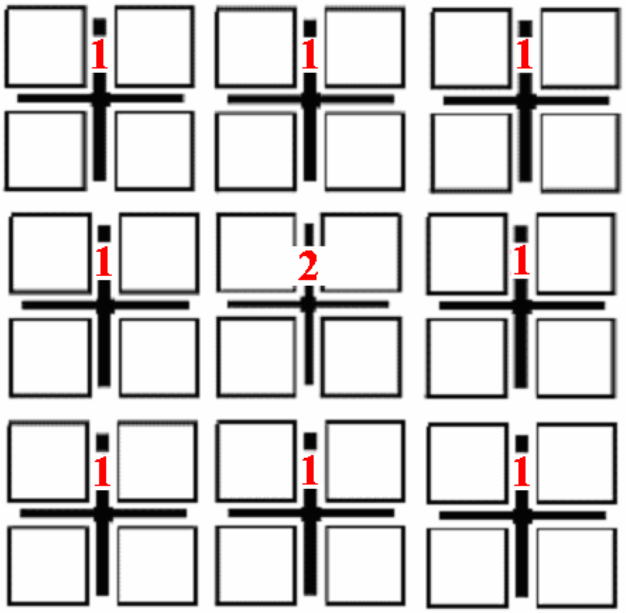

Figure 3-3: Mini core cross-sectional view and control rod grouping

Reflective radial boundary conditions and vacuum axial boundary conditions are applied. Cross sections and kinetics data were generated by TransLAT and passed on to the 3-D nodal transient code PARCS, which was used to simulate a reactivity insertion transient. For the transient simulation the initial core state (steady-state) was chosen at typical hot-zero-power (HZP) conditions with the central control rod fully inserted and the peripheral eight control rods fully withdrawn. No thermal-hydraulic feedback is

modeled in this problem and a reasonable power transient evolution is attained simply by control rod movement. The transient is initiated by withdrawing the central control rod (# 2 in Figure 3-3) at a speed of 3.81 cm/s and after 12s into the transient the peripheral rods (#1 in Figure 3-3) are inserted at a speed of 7.62 cm/s.

The impact of varying the delayed neutron importance factor around the given default value of 0.961 (as computed by TransLAT) is illustrated in Figure 3-4. It is noted that the transient is initiated at 1% of the nominal power. The power axis in Figure 3-4 presents percentage (%) power values over the nominal (100%) value.

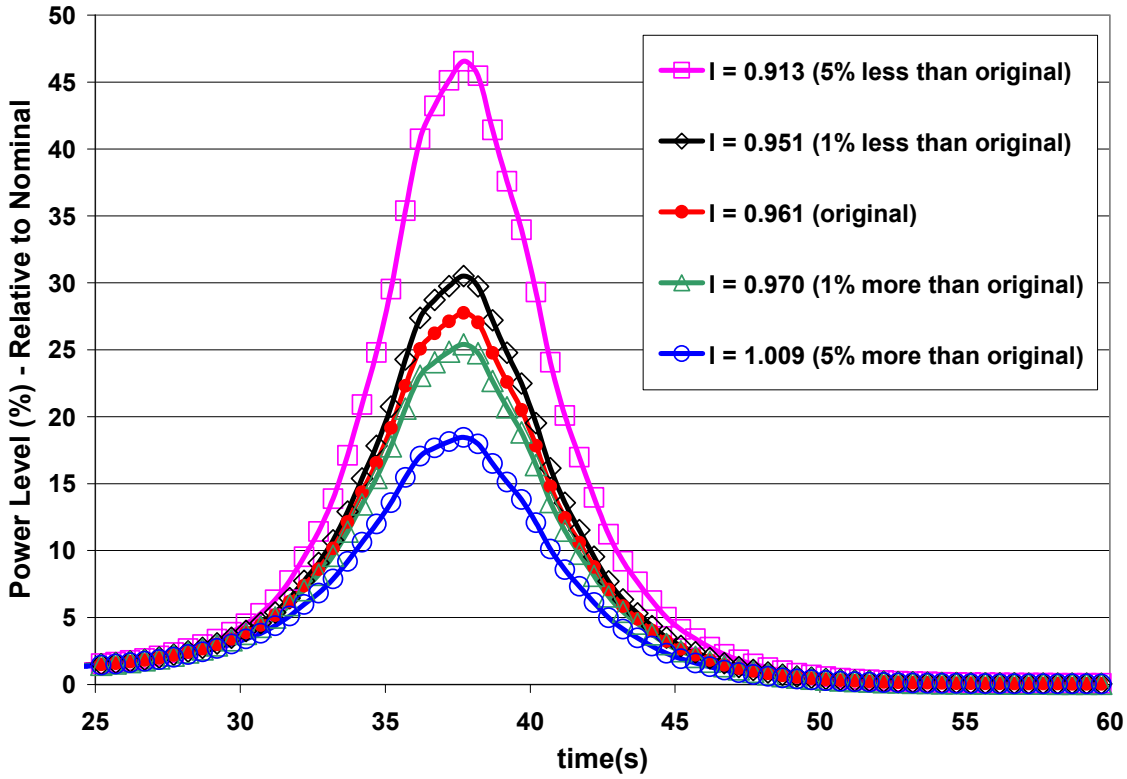

Figure 3-4: Sensitivity of Transient Power (%) Evolution to Importance Factor (I)

The variation of 1% around the original value (0.961) is assumed to represent the range of results that could be expected with the simplified *k*-ratio method employing a 0.77 MeV cut-off energy while the variation of 5% is likewise intended to represent the range of results that could be expected with the traditional 0.45 MeV cut-off. It is seen that a variation of 1% causes a 2-3% change (over the nominal) in the power peak value while a 5% variation causes a 10-20% change (over the nominal) in the power peak value. From this one might deduce that adjusting the cut-off energy E_D from its traditional value of 0.45 MeV to a somewhat higher value of around 0.77 MeV could reduce the error in the peak power value that would be obtained with the "traditional" simplified *k*-ratio importance factor by as much as a factor 5. This fact motivates such a trivial improvement to the simplified *k*-ratio method.

3.2.4 Conclusion to Proposed k-ratio Method

Through numerical experimentation a generic value could be determined for the upper energy boundary of the delayed neutron source range that should be used in the so-called simplified *k*-ratio method for estimating the delayed neutron importance factor for a homogenized near-critical fuel medium. A value of about 0.77 MeV, which is somewhat higher than the traditional 0.45 MeV that is used in some lattice codes, is recommended for this cut-off energy. With this cut-off the *k*-ratio method approximates the exact importance factor (as computed by means of an adjoint-weighting method) with an accuracy of better than 1% for a wide range of conditions and fuel designs. This is an improvement compared to the traditional cut-off for which the accuracy is normally no

better than 1-4% for a critical BWR assembly. This improvement was found to be of significance in certain types of reactivity insertion transients.

In conclusion, it has been shown that with a proper choice of the delayed neutron source range the simplified *k*-ratio method can be very effective in estimating the delayed neutron importance factor. This may make this very simple method attractive for use in applications other than lattice physics calculations, such as in the Monte Carlo method, for instance.

3.3 EVALUATION OF THE EFFECT OF STATE PARAMETERS

It is a fact that current nodal codes are mostly based on the 2-group calculations in which both prompt fission neutrons and delayed neutrons are born in the fast group. As a consequence of this fact, delayed neutrons have a much lower probability of causing fast fissions than prompt neutrons because their average energy is below fast fission threshold which is at about 1 MeV. Other important consequence is that the delayed neutrons have lower probability of leaking out of the system since they have lower energies and they travel shorter distances between collisions with material. These two consequences (lower fast fission factor and higher non-leakage probability for delayed neutrons) can not be directly accounted for in a 2-group model.

In order to compensate for this shortcoming of 2-group nodal applications, delayed neutron fractions (betas) are usually adjusted by a so called importance factor (*I*) which supposedly represents the impact of the difference between delayed neutron

spectra and prompt neutron spectra. That is an adjusted beta (β^{eff}) which is used instead of the physical beta (β). The relation between physical beta and effective beta is:

$$\beta^{eff} = I\,\beta$$

In a small reactor with highly enriched fuel, the increase in the non-leakage probability may dominate the decrease in the fast fission factor. So, importance factor can be greater than unity (1). On the contrary, in a large reactor with low enriched fuel, the decrease in the fast fission factor can dominate the increase in the fast non-leakage probability which can make importance factor smaller than unity. It is also expected that the delayed neutron importance factor can be greater than unity (1). This is true in the case of high leakage and low absorption conditions. Therefore, importance factors are usually less than unity for the LWR in the early steps of the exposure history since burnable poisons in BWRs and boron concentration in PWRs [**21**] dominate the neutron leakage effects. This issue is also discussed in the following sub-section.

Usually, the calculation of the importance factor coincides with the calculation of the nodal cross-section data. The standard cross-section modeling for coupled 3-D steady state and transient simulations are based on the data generated in the so-called base and branch calculations using a lattice physics code. The developed in this way cross-section history and instantaneous dependence models are based on burnup and feedback parameters (i.e. fuel temperature, void fraction, control rod). Needless to say, the kinetics data must be consistent with these cross-section generation techniques. For this purpose, the study described in this section was carried out with focus on the analyses of state parameter effects on delayed neutron fractions and importance factor by performing

history and branch calculations. TransLAT is used for the lattice physics calculations since it includes both widely used techniques such as k-ratio method and adjoint weighted method. In this study, an 8x8 BWR assembly (with 11 Gd fuel pins of different enrichments and with a large central water rod) shown in the Figure 3-5 is utilized at a variety of conditions that are typically employed in industry to functionalize nodal data. These included depletion at a number of void conditions (so-called void histories) and depletion at a number of fuel temperature conditions (Doppler histories) combined with instantaneous branches in fuel temperature, coolant voiding and buckling (user-specified input values).

The state conditions given at the Table 3-2 are used in the reference (base) lattice calculations.

Table 3-2: Reference (base) State Conditions

Void Fraction:	40 %
Void Fraction at By-pass:	0 %
Fuel Temperature*:	900 K
Moderator Temperature*:	560 K
Control Rod Position:	Fully Unrodded

* Temperatures are volume averaged values

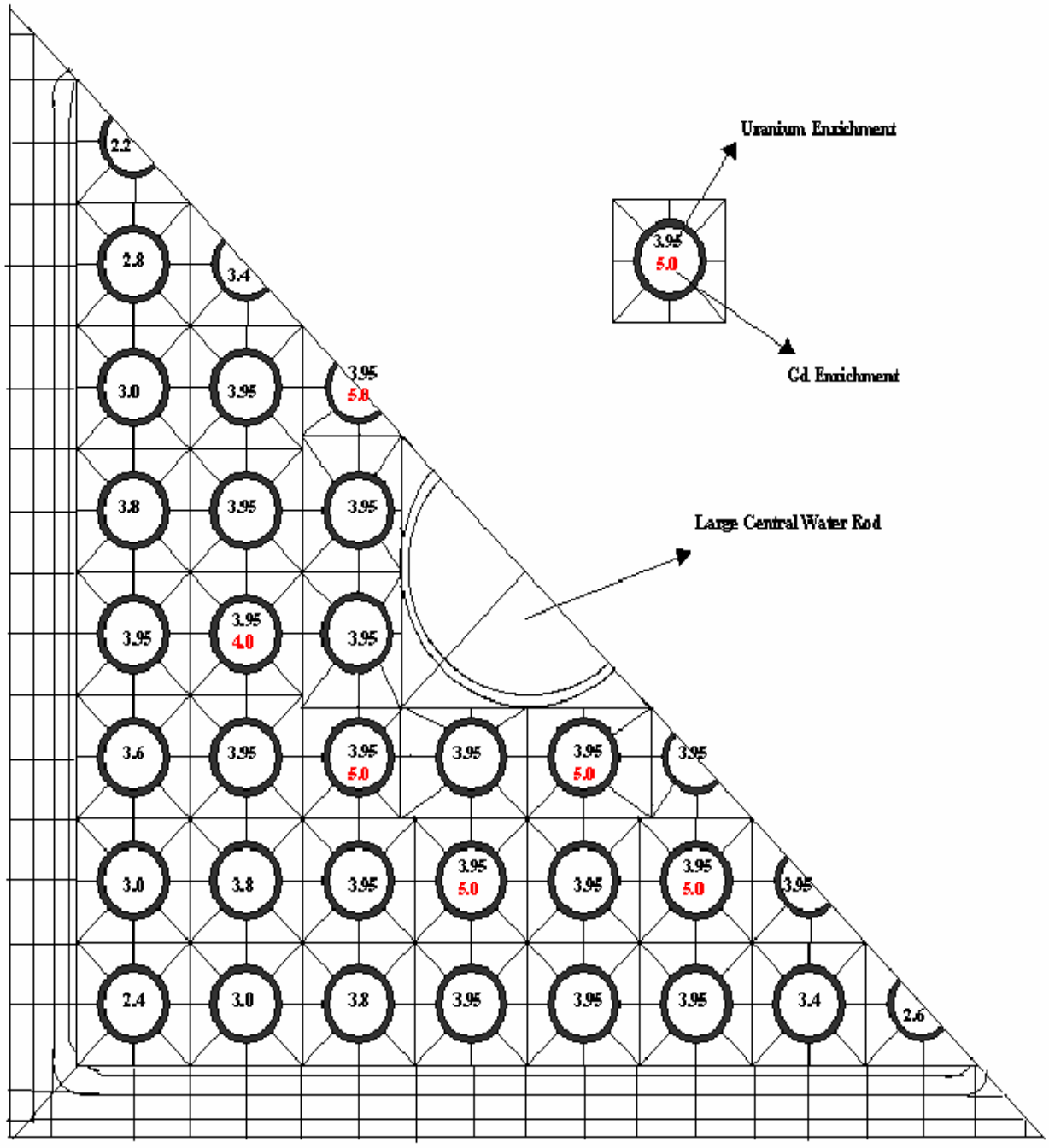

Figure 3-5: 8x8 BWR Assembly Model for Calculations with TransLAT

As it was mentioned previously, the standard cross section modelling for coupled 3-D steady state and transient simulations are based on the data generated in the so-called

exposure history (base) and instantaneous branch calculations using a lattice physics code. These exposure history and instantaneous calculations are usually dependent to burnup and local feedback parameters (i.e. fuel temperature, moderator temperature, void fraction, and control rod insertion for BWRs).

In the following sub-sections, very similar to cross section modeling, the state parameter effects on the delayed neutron fractions and importance factors are extensively investigated. In particular, exposure (burnup), void fraction, fuel temperature (Doppler) and control rod dependencies are analyzed in the next four sub-sections respectively. Buckling effects on the delayed neutron fractions and importance factors are studied subsequently. In addition to history (base) calculations, various instantaneous branch calculations perturbed from reference base case are performed for the feedback parameters to seek the possibility of having computationally efficient 2-D off-line delayed neutron generation and modeling.

3.3.1 Burnup Effect

The reference assembly (Figure 3-5) with the base conditions given above is run with TransLAT up to 6 MWd/t burnup step. The Figure 3-6 shows the total delayed neutron fractions (beta) for direct beta, k-ratio beta effective and adjoint weighted beta effective methods during this period.

The adjoint weighted beta effective and k-ratio beta effective results agree quite well over the entire exposure range as shown in Figure 3-6. If beta values are compared for 0-exposure and 6 MWd/t exposure steps, it can be seen that direct beta varies 12%

during the period of 6 MWd/t exposure while the effective betas vary 10%. On the other hand, if direct beta results are compared to effective beta results, maximum deviation, which happens at 0-exposure is found to be 5%. It should be noted that critical buckling search option of TransLAT is used these calculations.

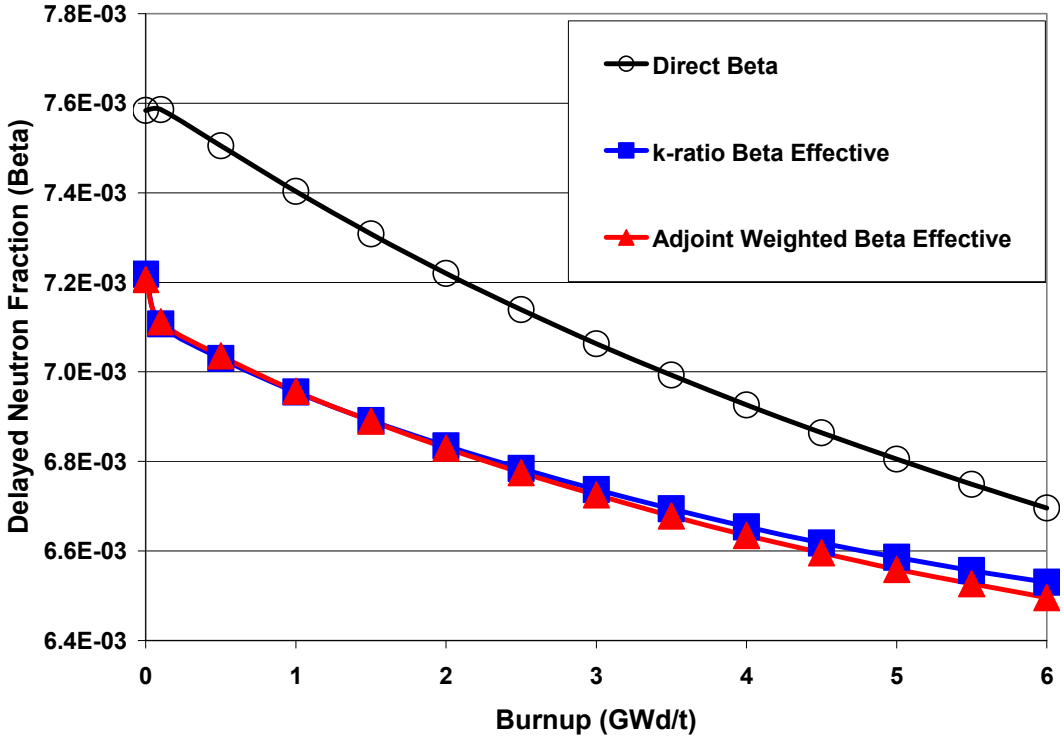

Figure 3-6: Burnup Dependency of Delayed Neutron Fractions

The exposure dependency of k-ratio and adjoint weighted importance factors are shown in the Figure 3-7. For both k-ratio and adjoint weighted importance factors, there is roughly 4% variation between the 0.1MWd/t and 6MWd/t exposure steps. However, if the two importance factors compared with each other, maximum deviation occurs at the 6 MWd/t and it is about 0.5% which can be considered insignificant. Note that, the sharp variation during early exposure stage (approximately 0-0.1MWd/t) that can be seen from

the above figures is due to Xe-135 buildup. It can be said that importance factor is less exposure dependent (4%) than the betas (10%) since betas are strongly depend on the isotopic content.

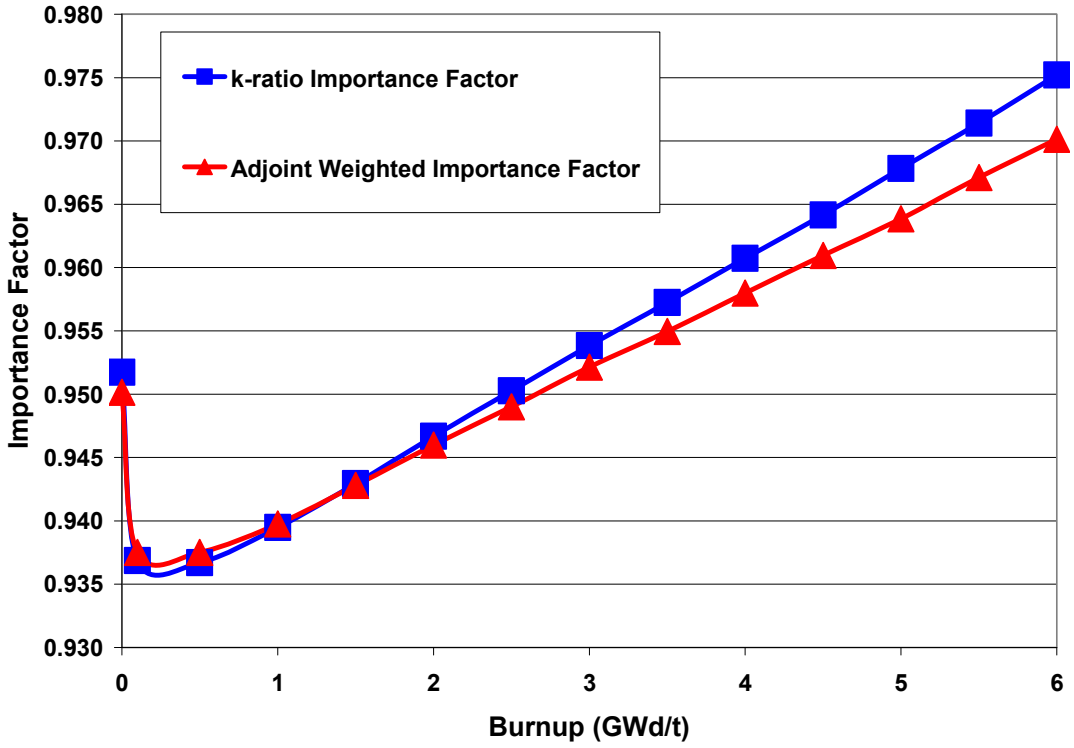

Figure 3-7: Importance Factor as a Function of Burnup

The Table 3-3 presents the values of delayed neutron fractions and importance factors, which are graphically represented in with above figures. Last column of the Table 3-3 shows the absolute percentage difference between k-ratio importance factor and adjoint importance factor for each burnup step.

Table 3-3: Burnup Dependence of Betas and Importance Factors

	Delayed Neutron Fraction			Importance Factor		
Exposure (MWd/t)	**Direct**	**k-ratio**	**Adjoint Weighted**	**k-ratio**	**Adjoint Weighted**	**Adj. vs. k-ratio**
0.0	7.58E-03	7.26E-03	7.24E-03	0.9583	0.9558	0.26%
0.1	7.58E-03	7.15E-03	7.15E-03	0.9434	0.9431	0.03%
0.5	7.50E-03	7.08E-03	7.08E-03	0.9431	0.9428	0.03%
1.0	7.41E-03	7.00E-03	7.00E-03	0.9456	0.9451	0.06%
1.5	7.32E-03	6.94E-03	6.94E-03	0.9489	0.9479	0.10%
2.0	7.23E-03	6.89E-03	6.88E-03	0.9524	0.9508	0.17%
2.5	7.15E-03	6.84E-03	6.82E-03	0.9558	0.9537	0.22%
3.0	7.08E-03	6.79E-03	6.78E-03	0.9593	0.9568	0.27%
3.5	7.01E-03	6.75E-03	6.73E-03	0.9626	0.9595	0.33%
4.0	6.95E-03	6.71E-03	6.69E-03	0.9662	0.9626	0.37%
4.5	6.89E-03	6.68E-03	6.65E-03	0.9697	0.9656	0.42%
5.0	6.83E-03	6.65E-03	6.62E-03	0.9731	0.9685	0.47%
5.5	6.78E-03	6.62E-03	6.58E-03	0.9768	0.9717	0.53%
6.0	6.72E-03	6.59E-03	6.55E-03	0.9805	0.9747	0.60%

In addition to the above discussed case, the burnable poison (BP) effect on the importance factor is analyzed to show importance factor can be greater than unity in the case of low absorption conditions. For this purpose, Gd, enrichment in the assembly is reduced dramatically. In original (reference) case, there are 11 Gd pins with five of them have 4% Gd enrichment and six of them with 5% enrichment. In reduced BP case enrichments of the Gd in all the pins are set to 1%. Figure 3-8 shows the importance factor for reduced (1%) Gd case.

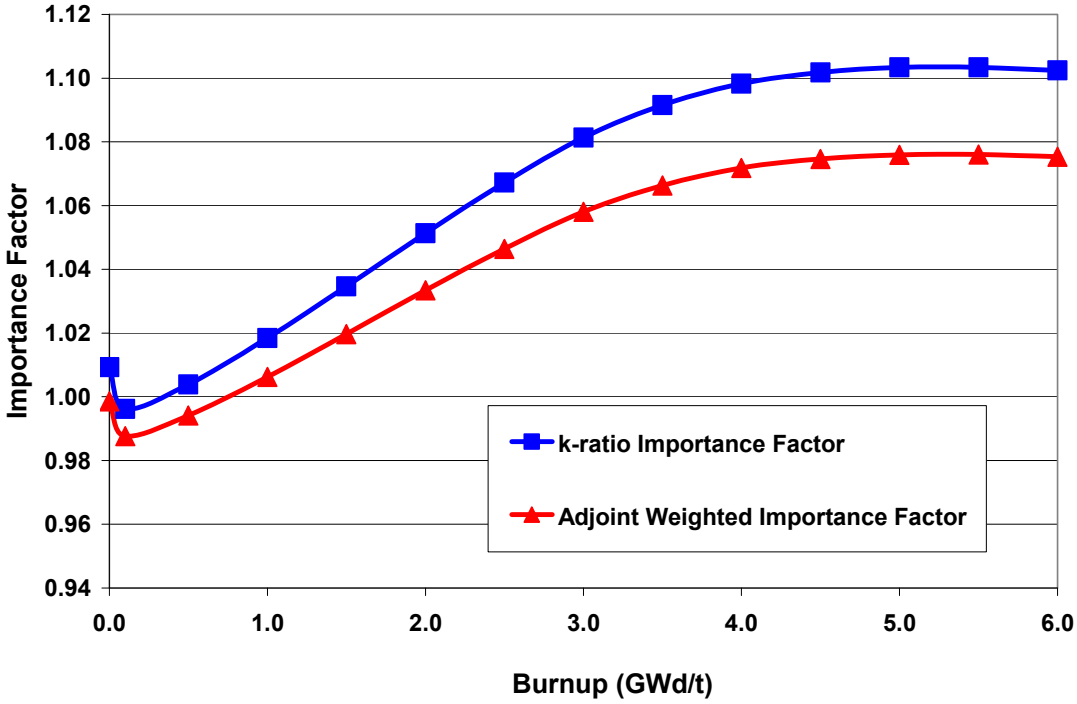

Figure 3-8: Importance Factor for reduced (1%) Gd enrichment case

3.3.2 Moderator Void Feedback

Moderator void feedback effect on the delayed neutron fractions and the importance factors is analyzed by changing void fraction in the BWR fuel assembly. Firstly, historical void cases are run for the void fractions, 0%, 20%, 40%, 60%, 80% and 100%. Then, by taking the 40% void history case as a reference base case, instantaneous branch calculations (0%, 20%, 60%, 80% and 100%) are performed for the each exposure step (given at Table 3-3) separately. For the sake of simplicity, direct beta, adjoint weighted beta, and adjoint weighted importance factors are presented in this part.

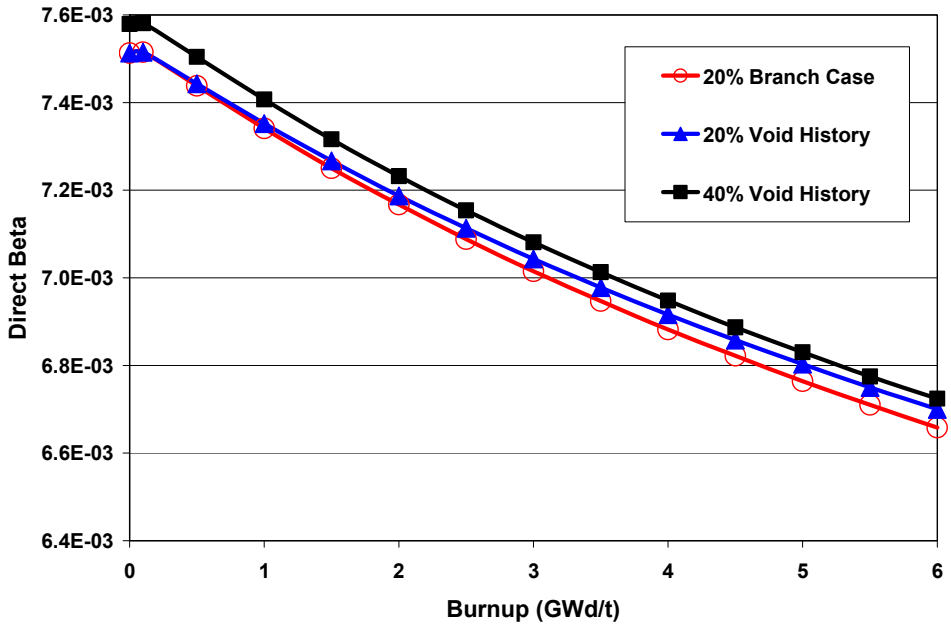

Figure 3-9: Direct Beta for the 20% Void Fraction Branch

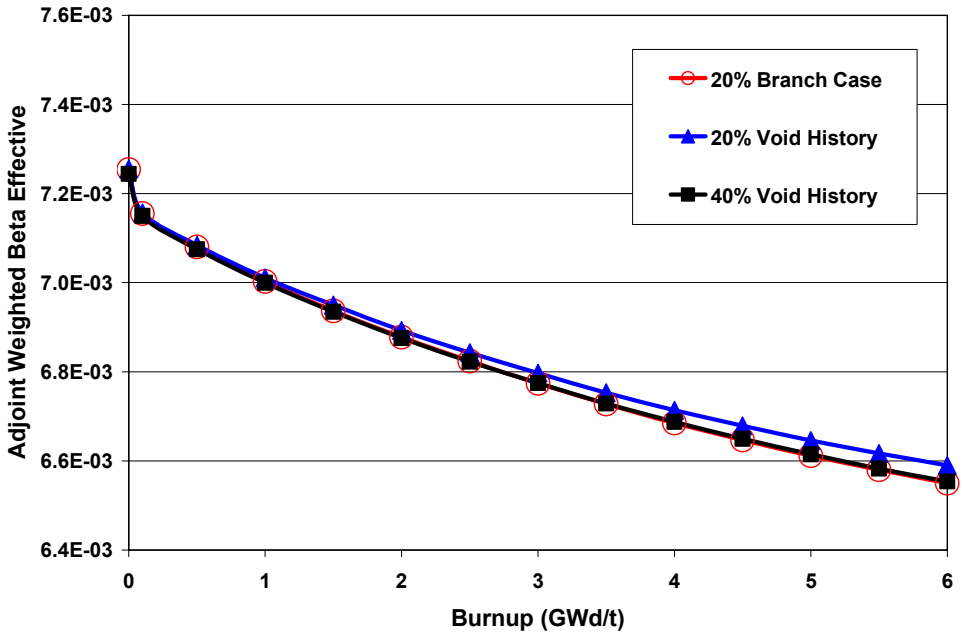

Figure 3-10: Adjoint Weighted Beta Effective for the 20% Void Fraction Branch

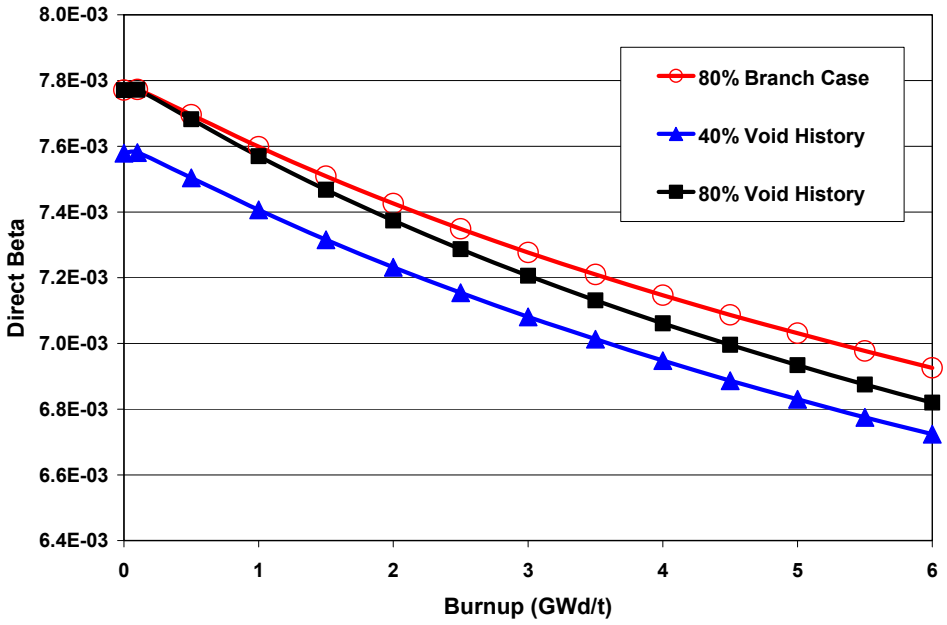

Figure 3-11: Direct Beta for the 80% Void Fraction Branch

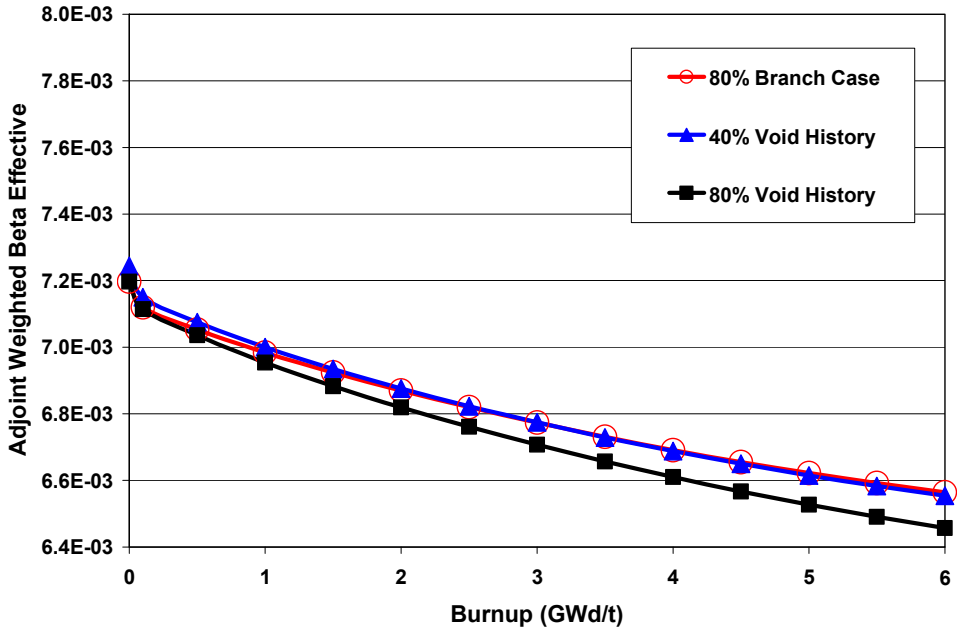

Figure 3-12: Adjoint Weighted Beta Effective for the 80% Void Fraction Branch

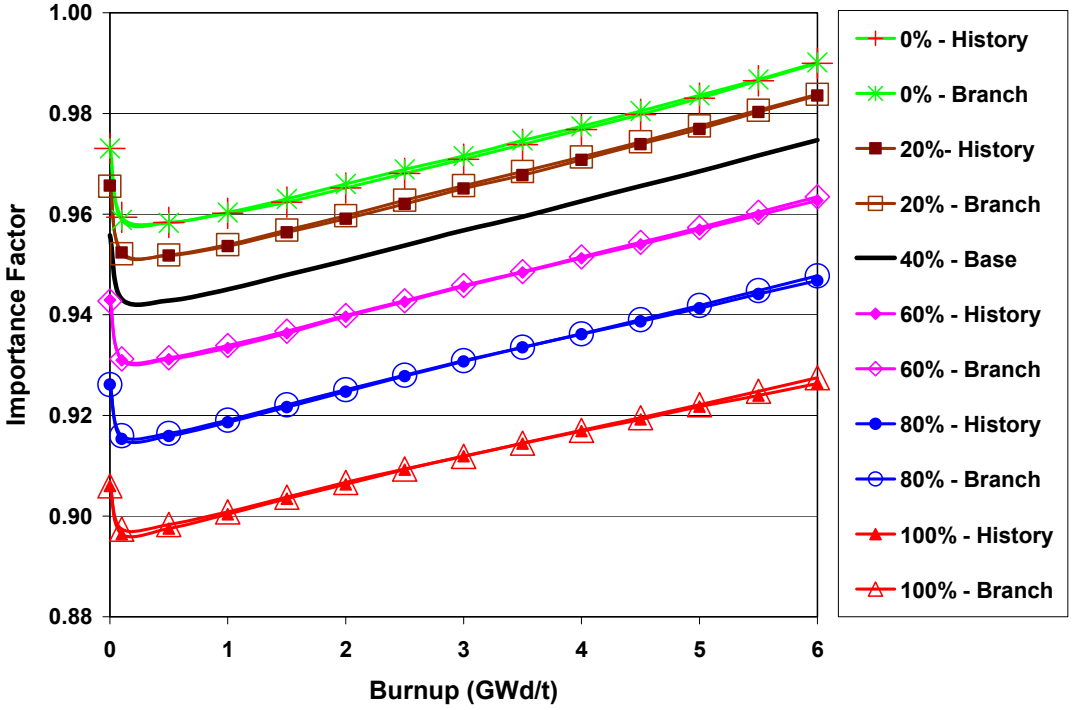

Figure 3-13: Importance Factors for all Void Fraction Cases

For each burnup step, 20% void instantaneous branch calculations are performed from 40% history base case. 20% void history, 20% branch and 40% void history direct beta results are shown in Figure 3-9 while adjoint weighted beta effective results are given in Figure 3-10. Another example of this analysis is given in Figure 3-11 and Figure 3-12 for the 80% void fraction. Figure 3-13 presents the adjoint weighted importance factors as a function of burnup for all void fraction history and instantaneous branch cases (from 40% base case).

The following conclusions can be made for the moderator void feedback analysis performed in this part.

- The void effect on direct beta and adjoint weighted beta effective is from 3 to 4 percent smaller than exposure effect.
- Void history effect is smaller than the instantaneous void effect for betas.
- Importance factor (***I***) is quite insensitive to void history but changes significantly with instantaneous void (5% to 8%). In fact, the instantaneous void dependence is more significant (approximately two times) than exposure dependence.
- In particular, there are some deviations between different void fraction cases for all exposure steps. For example, if 0% and 20% cases are compared the deviation on ***I*** is about 1% and if 0% and 100% cases are compared the deviation ***I*** is about 8% for all exposure steps.
- Importance factor varies roughly 4% for all void cases during the exposure if the deviations are calculated from minimum and maximum values of the importance factors.
- It can be also seen that the importance factor results are quite linear in exposure after the Xenon reaches equilibrium, which coincides with approximately 0.1 MWd/t exposure step, in these calculations.
- Additionally, these linear void fraction lines remain almost parallel to each other during the entire exposure history, which implies that even the void dependence is linear.

3.3.3 Fuel Temperature (Doppler) Feedback

Similar to the void fraction analysis, fuel temperature dependency is analyzed for exposure history and instantaneous branch cases. In this part, 900K fuel temperature case is used as reference base case. Although various fuel temperatures (from room temperature to 2400 K) are tested for this study, only 600K and 1500K are given in the figures for the sake of simplicity. Figure 3-14 and Figure 3-15 present direct beta and adjoint weighted beta effective results respectively. In these figures, 600K branch and history cases are compared with the reference 900K history case. This analysis is repeated for 1500K fuel temperature case in Figure 3-16 and Figure 3-17. Adjoint weighted importance factors of these cases are given in Figure 3-18.

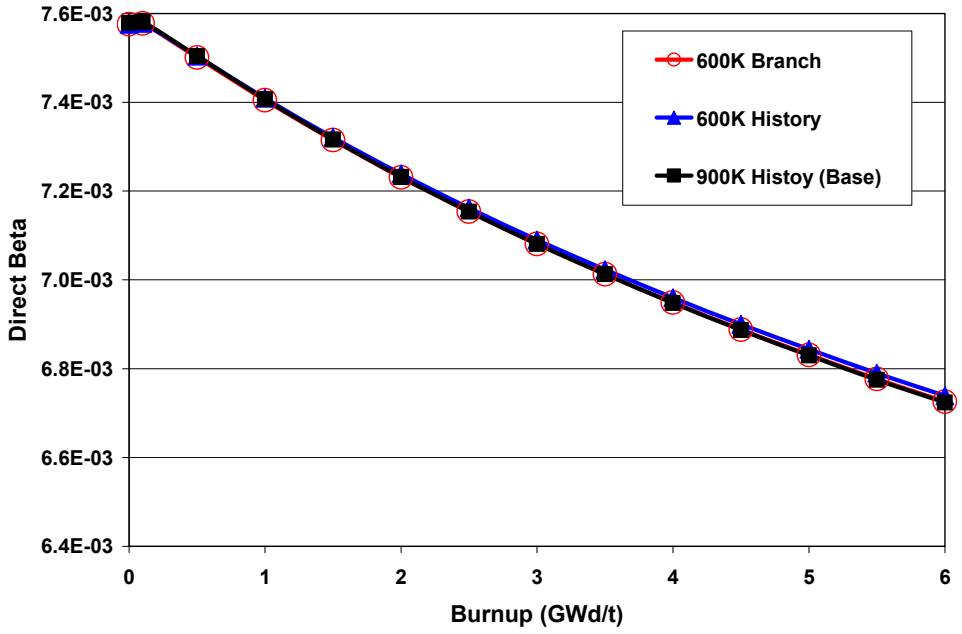

Figure 3-14: Direct Beta for the 600K Fuel Temperature Branch

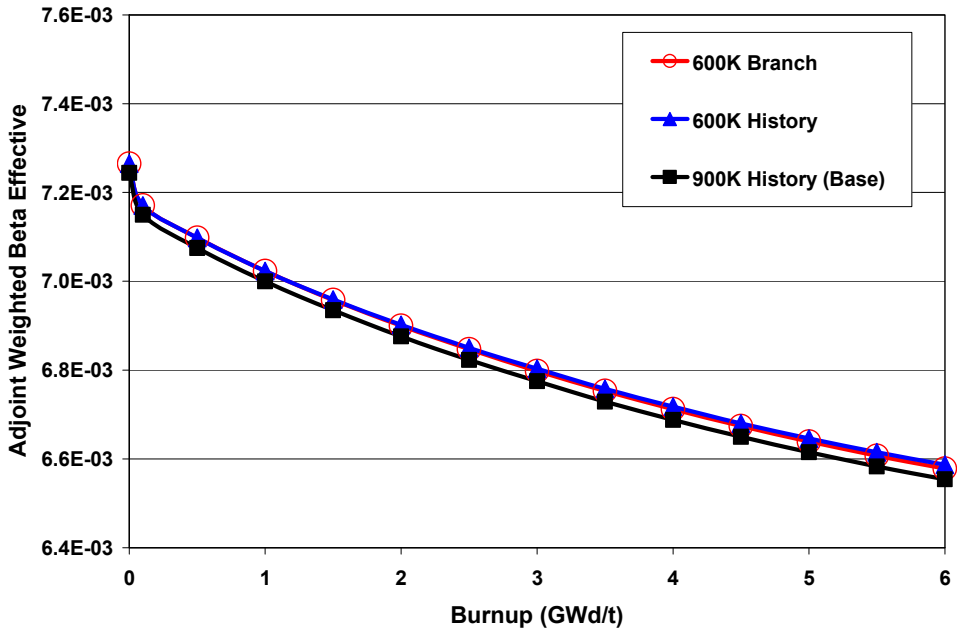

Figure 3-15: Adjoint Weighted Beta Effective for the 600K Fuel Temperature Branch

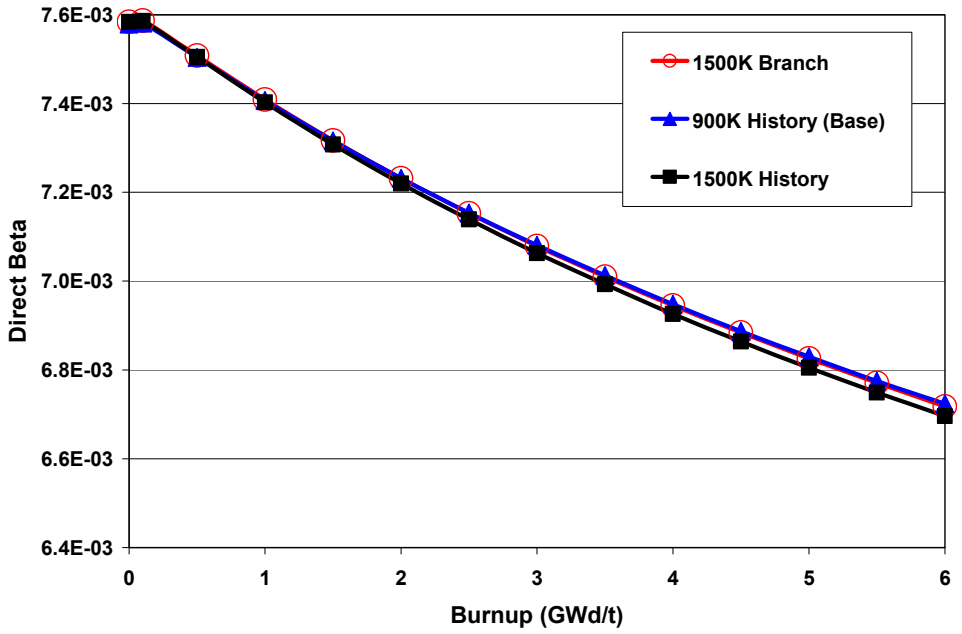

Figure 3-16: Direct Beta for the 1500K Fuel Temperature Branch

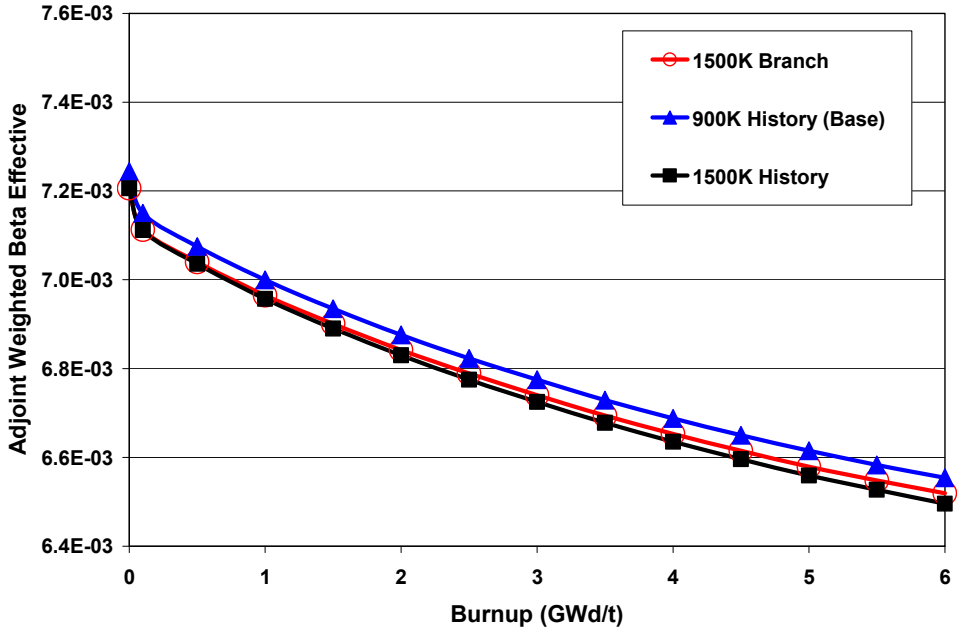

Figure 3-17: Adjoint Weighted Beta Effective for the 1500K Fuel Temperature Branch

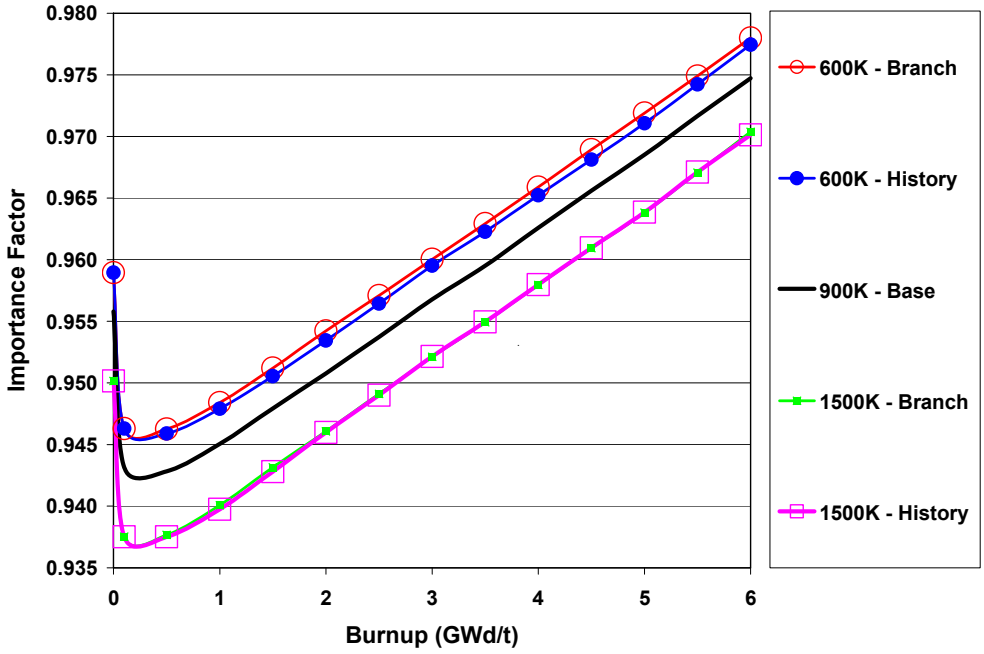

Figure 3-18: Adjoint Weighted Importance Factor for Fuel Temperature Cases

As shown in the above figures, the deviation due to different fuel temperatures is less than 0.1% which can be considered insignificant. In other words, it can be assumed that betas are not sensitive to fuel temperatures. While the importance factors vary up to 3% during the exposure, maximum temperature effect on importance factors is less than 1%. It can be considered that instantaneous branch calculations are independent from the exposure histories. It can be seen that, the importance factor results are quite linear after the Xe-equilibrium just like the void fraction cases which are described in the previous section. Similarly, these linear lines remain almost parallel to each other during the entire exposure range.

3.3.4 Control Rod Feedback

Control rod feedback effects on the betas and importance factors are investigated by performing un-rodded and rodded assembly calculations. The base case here is unrodded assembly with the system state parameters described in the introduction part of this section. Exposure history calculations are performed for both rodded and unrodded assembly. Unrodded to rodded assembly branch calculations are performed for each exposure step.

Figure 3-19 and Figure 3-20 present direct beta and adjoint weighted beta effective respectively. In these figures, exposure histories for rodded and unrodded assembly results are given with results from unrodded to rodded branch case. Figure 3-21 shows the adjoint weighted importance factors from unrodded history, rodded history and rodded branch cases.

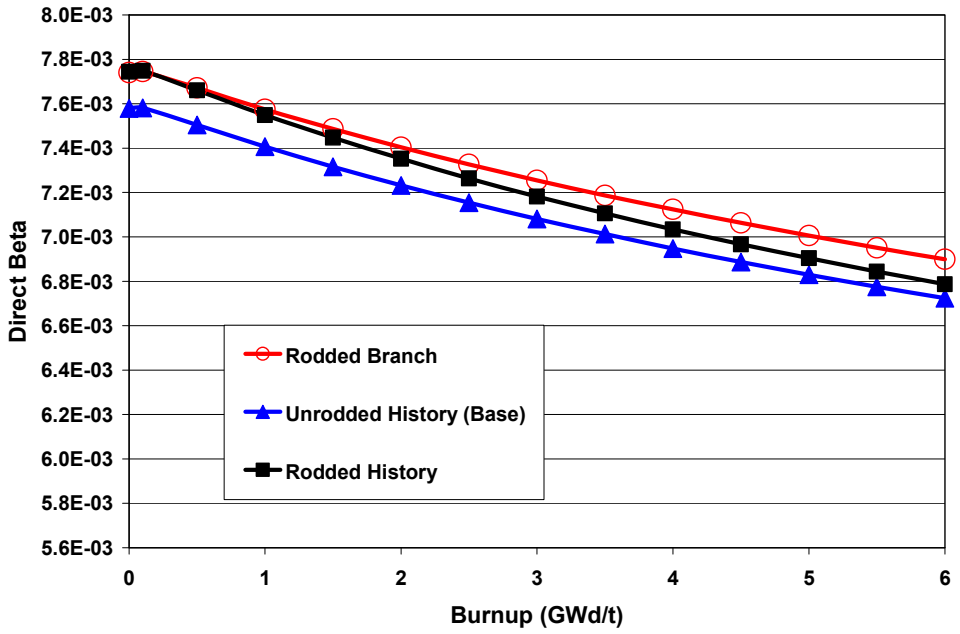

Figure 3-19: Direct Beta for Control Rod Branch

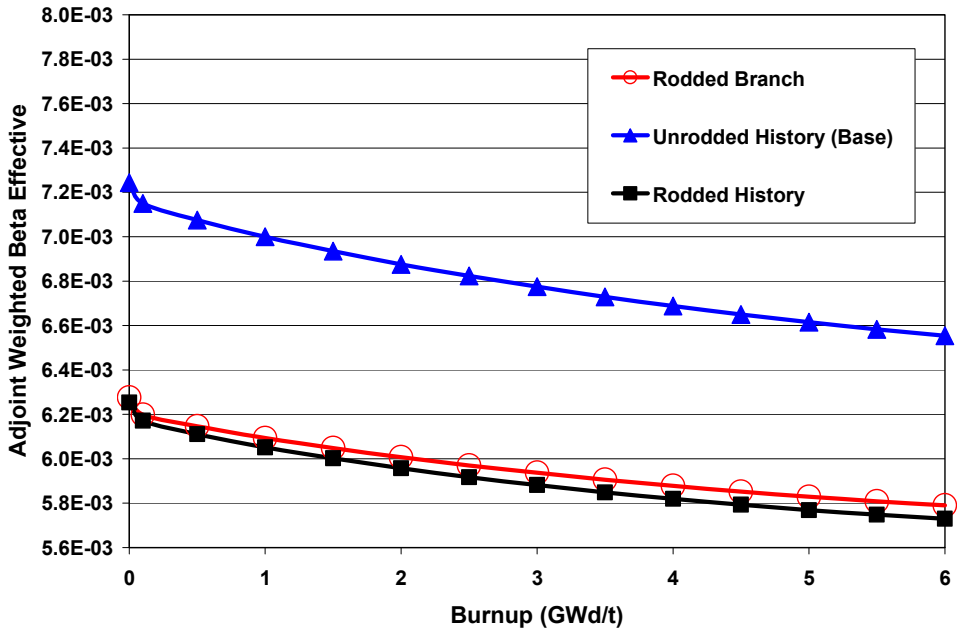

Figure 3-20: Adjoint Weighted Beta Effective for Control Rod Branch

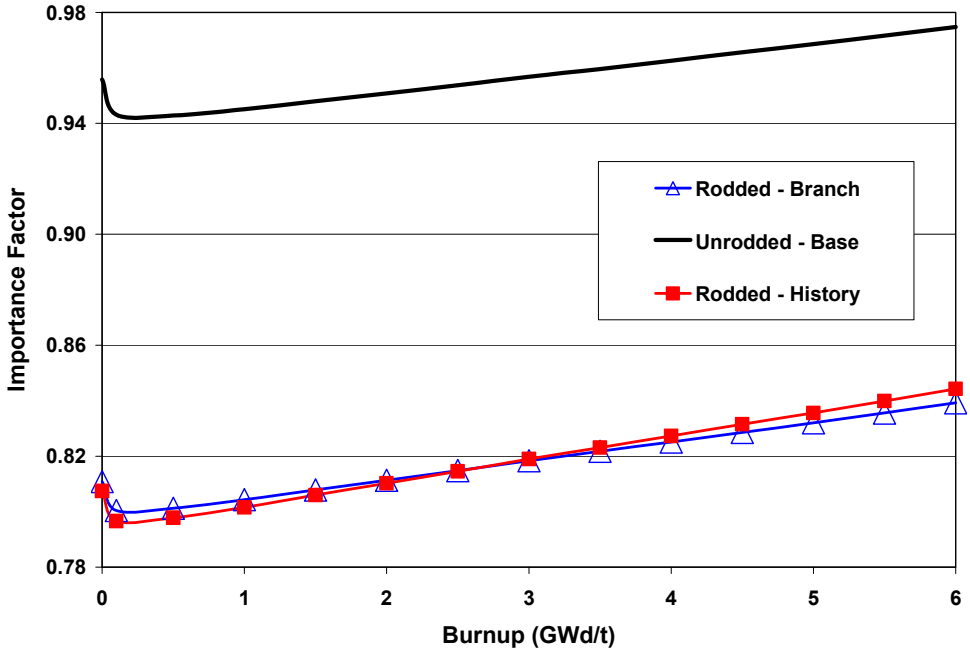

Figure 3-21: Adjoint Weighted Importance Factor for Control Rod Branch

It is found that instantaneous control rod insertion effects on adjoint weighted beta effective and importance factors are quite more significant than the exposure history effects. Moreover, instantaneous control rod insertion is not effective on the direct beta since control rod insertion phenomena is a spectral effect which can not be captured by direct beta method. During the exposure, while the maximum deviation between the rodded and unrodded cases is 3% for direct betas, the maximum deviation between the rodded and unrodded cases is 14% for adjoint weighted effective betas. Consequently, the maximum deviation between the importance factors of rodded and unrodded cases is about 15%. Here, it must be noted that the control rod has an important impact on the effective delayed neutron fractions, and this impact is not taken into consideration in most of the 3-D applications. This phenomenon will be extensively analyzed in the Chapter 4.

3.3.5 Effect of Different Buckling Options

In this part, the study is focused on the understanding of the effects of the different buckling options on the delayed neutron fractions and importance factors. The works presented in the previous sub-sections are performed by utilizing critical buckling search option in TransLAT. The critical buckling search allows taking into account the neutron leakage by the addition of a homogeneous leakage term in the multiplication form of diffusion coefficient and buckling terms (DB^2). In the following figures, exposure dependence of direct beta (Figure 3-22), k-ratio beta effective (Figure 3-23), adjoint weighted beta effective (Figure 3-24), k-ratio importance factor (Figure 3-25), and adjoint weighted importance factor (Figure 3-26) are presented for various buckling options (critical, zero, and input). Only two input buckling (-1.3100E-03 cm^{-2} and 4177E-03 cm^{-2}) are shown below for the sake of simplicity.

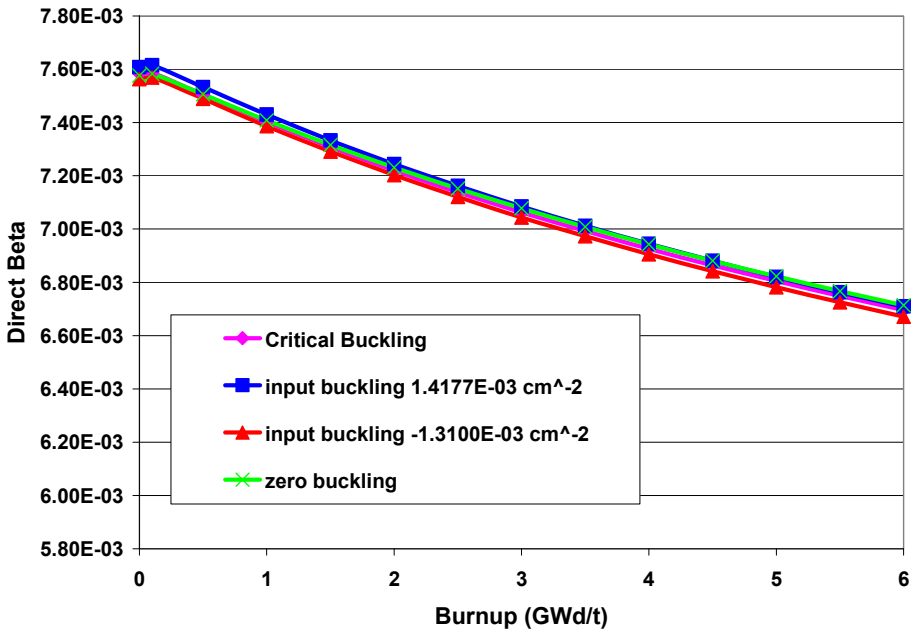

Figure 3-22: Direct Beta for Different Buckling Options

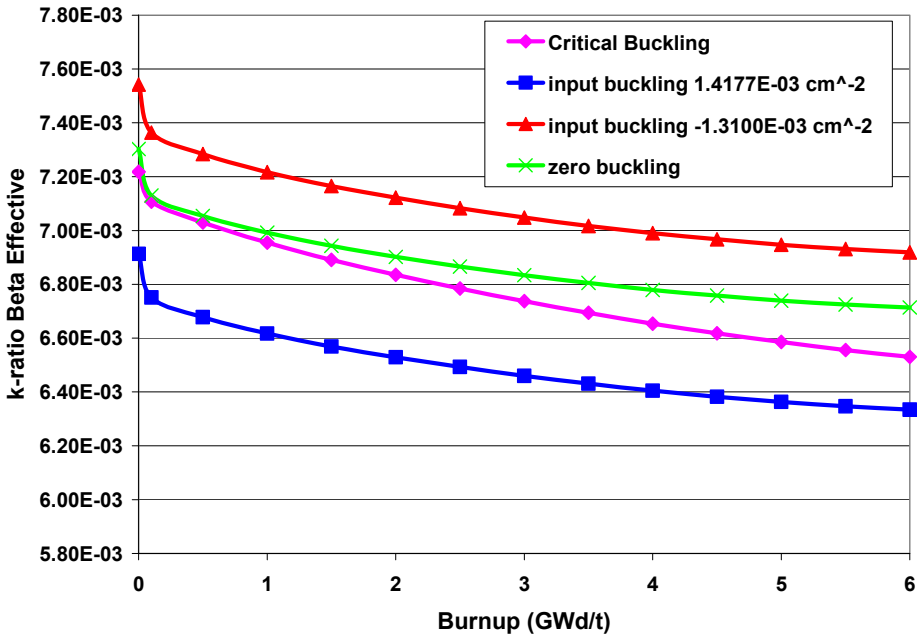

Figure 3-23: k-ratio Beta Effective for Different Buckling Options

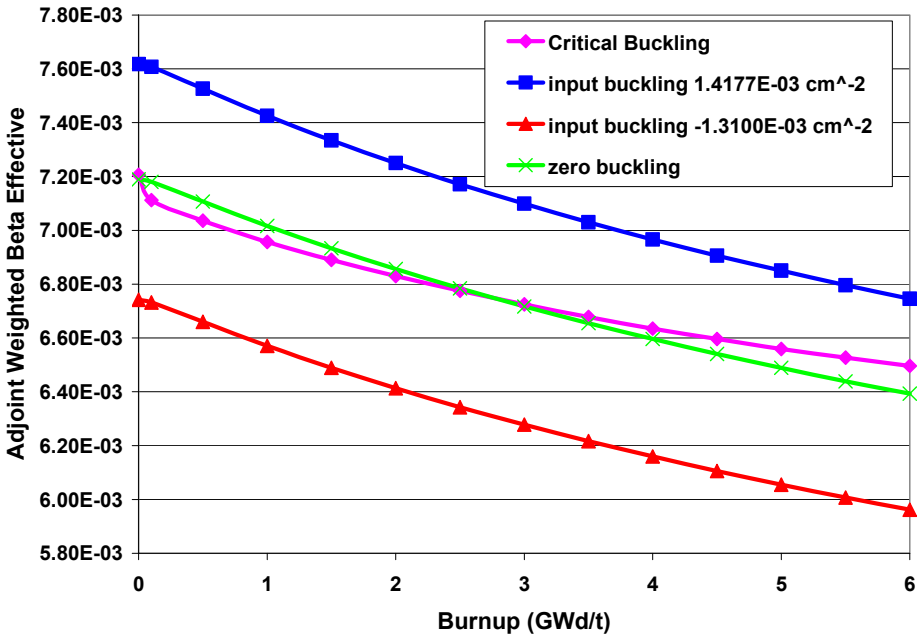

Figure 3-24: Adjoint Weighted Beta Effective for Different Buckling Options

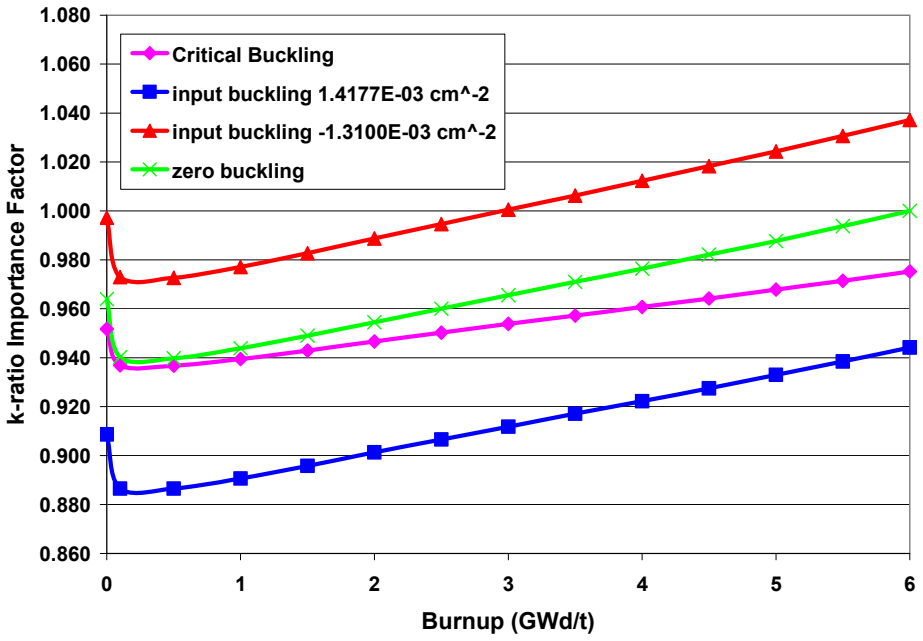

Figure 3-25: k-ratio Importance Factor for Different Buckling Options

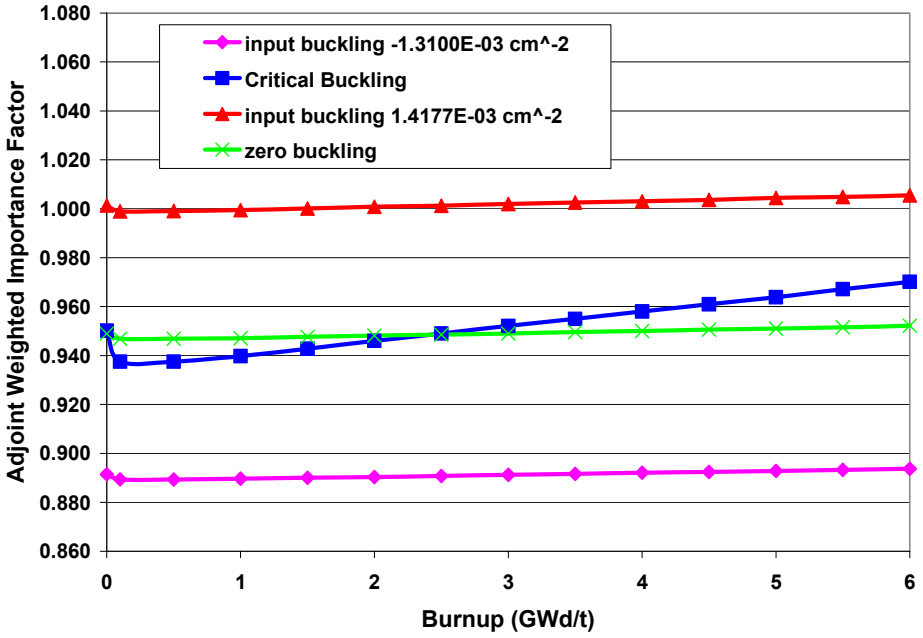

Figure 3-26: Adjoint Weighted Importance Factor for Different Buckling Options

In general, betas have tendencies to decrease during the exposure. Beta can be defined simply as the contribution of delayed neutrons to the total neutrons and it is a fact that ^{239}Pu (which has beta value of approximately 0.0024) is produced while ^{235}U (which has beta value of approximately 0.0065) is depleted during the exposure. This yields the direct lattice average beta to decrease during the exposure. On the other hand importance factor slightly increase during the exposure due to spectrum change after Pu build-up. Since the number of neutrons per fission is increased during the exposure due to the Pu buildup, the fast leakage is increased. Therefore, the importance of the delayed neutrons is increased due to the spectrum effect. Note that the critical buckling value is 1.716678E-04 cm^{-2} at the beginning (0 GWd/t) of the exposure history and 5.697006E-04 cm^{-2} at the end (6 GWd/t).

Figure 3-22 shows that different buckling options have no effect on the direct beta results during the exposure history. However, buckling has strong effect on the k-ratio and adjoint weighted betas as shown in Figure 3-23 and Figure 3-24. For the input buckling cases, the adjoint weighted importance factors (Figure 3-26) are almost constant during the exposure. As shown in Figure 3-25, the k-ratio importance factors are not constant during the exposure and there is approximately up to 8% difference during the exposure.

3.3.6 Conclusions to State Parameter Effects

State parameter effects on delayed neutron fractions and delayed neutron importance factors are comprehensively analyzed in this section, so far. Study is mostly

focused on the effects of exposure (burnup), buckling and feedback (void, Doppler, control rod etc.) parameters.

It is understood that the exposure dependence of the delayed neutron fractions and the importance factor is important in case of critical buckling search. In all cases, the importance factor is less exposure dependent than direct delayed neutron fractions. Importance factors' deviation from unity means that a representation of a correction is required.

The void exposure history effect on the delayed neutron fractions is smaller than the effect of instantaneous void variations. It is also seen that the importance factor is quite insensitive to the void history. The conclusions from moderator void feedback effects on betas and importance factor are valid for the fuel temperature (Doppler Effect) effects. However, it is important to note that the impact of the void fraction changes on the importance factor for a specific exposure step is significantly higher than the impact of the fuel temperature changes.

The importance factor is quite insensitive to the control rod history while instantaneous control rod insertion is very important for the effective delayed neutron fractions and the importance factor, but not so much for the direct beta.

It is observed that the direct betas are sensitive to exposure, spectral, and control history (since this determines the isotopic content) while the importance factors and subsequently effective betas are sensitive to the instantaneous thermal-hydraulics and control effects.

It is found that the importance factor is strongly affected by the spectrum itself. It is also proposed that the usage of adjoint weighted importance factor rather than k-ratio

importance factor is more accurate since delayed neutron spectrum effects are directly accounted for the adjoint weighting formulas.

For a diversity point of view, the analysis performed in this section is repeated for a quite different BWR assembly type, different lattice physics code (CASMO-3) and various burnable poison (BP) concentrations; however, the results can not be presented here for the sake of simplicity. Cross term effects are also analyzed for the feedback parameters. It is proved that the conclusions of this section are still valid for these diverse calculations.

Overall, the analysis performed in this section shows that the state dependence of the delayed neutron importance factor derived from BWR assembly lattice calculations can be investigated consistently. It should be noted that this analysis is a quite original study that shows the importance factor has a potential to be represented by lumped state parameters. Hence, the next section is going to focus on developing an appropriate functionalization of the state dependencies of the delayed neutron importance factor.

3.4 PARAMETERIZATION OF THE DELAYED NEUTRON IMPORTANCE FACTOR

Thermal reactor core calculations are customarily performed with three-dimensional two-group (one thermal and one fast neutron energy group) nodal diffusion methods. Steady-state multi-group transport theory calculations on heterogeneous single assembly domains subject to reflective boundary conditions are normally used to prepare the equivalent two-group spatially homogenized nodal parameters. For steady-state

applications the equivalent nodal parameters are theoretically well-defined but for transient applications the definition of the nodal delayed neutron precursor data is somewhat unclear. The fact that delayed neutrons are emitted at considerably lower energies than prompt neutrons and that this difference cannot be accounted for in a two-group representation (all fission neutrons are born in the fast group) is of particular concern. To compensate for this inherent deficiency of the two-group model a correction is customarily applied to the nodal values of the delayed neutron fractions [**21**]. This correction is computed during lattice calculations [**16**] and takes the form of the ratio between the importance (adjoint flux) weighted effective delayed neutron fractions and the regular flux weighted delayed neutron fractions for each precursor family *d* as given in Eq. 3.13.

$$I_d = \frac{\beta_{eff,d}}{\beta_d} = \frac{\dfrac{\int_V \left\{ \sum_{g'} \left(\sum_i \chi^D_{g',d,i} \left[\sum_g \beta_{i,d,g} \nu \Sigma_{fg,i} \Phi_g \right] \right) \Phi^*_{g'} \right\} dr}{\int_V \left\{ \sum_{g'} \left(\sum_i \chi_{g',i} \left[\sum_g \nu \Sigma_{fg,i} \Phi_g \right] \right) \Phi^*_{g'} \right\} dr}}{\dfrac{\int_V \left\{ \sum_i \left[\sum_g \beta_{i,d,g} \nu \Sigma_{fg,i} \Phi_g \right] \right\} dr}{\int_V \left\{ \sum_i \left[\sum_g \nu \Sigma_{fg,i} \Phi_g \right] \right\} dr}} \approx \frac{\int_V \left\{ \sum_{g'} \chi^D_{g',d} \Phi^*_{g'} \right\} dr}{\int_V \left\{ \sum_{g'} \chi_{g'} \Phi^*_{g'} \right\} dr} \quad \textbf{(3.13)}$$

where *i*= fissionable nuclide, *g*= neutron energy group, *V*= node volume, $\chi^D_{g',d,i}$ = delayed neutron emission spectrum, $\chi_{g',i}$ = total neutron emission spectrum, $\beta_{i,d,g}$ = delayed neutron fraction (precursor family wise direct betas for each nuclide per energy group),

$\nu\Sigma_{fg,i}$ = fission-neutron production cross-section, $\Phi^{*}_{g'}$ = adjoint flux and $\Phi_{g'}$ = regular forward flux. The correction factor I_d is known as the (adjoint weighted) delayed neutron importance factor for precursor family *d*.

The previous section revealed that the equivalent nodal data, including the delayed neutron importance factors I_d must be functionalized in terms of a number of state parameters such that the nodal data that are consistent with reigning local conditions can be utilized during global core calculations. Common state parameters that are used for nodal data include fuel and moderator temperatures, moderator densities and fuel exposures. In this section the state dependence of the delayed neutron importance factors is investigated with a view of determining an appropriate functionalization.

Standard lattice calculations are utilized to show that the state dependence of delayed neutron importance factors can be represented in terms of two parameters only.

3.4.1 Description of the Methodology

The TransLAT code is used to perform lattice calculations for an 8x8 BWR assembly (with 11 Gd fuel pins of different enrichments and with a large central water rod, see Figure 3-5) at a variety of conditions that are typically used in industry to functionalize nodal data. These included depletion at a number of void conditions (so-called void histories) and depletion at a number of fuel temperature conditions (Doppler histories) combined with instantaneous branches in fuel temperature, coolant voiding and buckling (user-specified input values). Void history cases were run both with fixed input bucklings (no critical buckling search) and with a critical buckling search. Instantaneous

buckling branch cases were performed only for the reference history case (reference buckling=0, reference void fraction (α) = 40%, reference fuel temperature (T_f) =900K).

Table 3-4: Calculation Matrix for Importance Factor Parameterization Study

#	History (depletion) Calculations with Critical Buckling	History (depletion) Calculations with Zero Buckling
1	α=0%, T_f =900K	α=0%, T_f =900K
2	α=20%, T_f =900K	α=20%, T_f =900K
3	α=40%, T_f =900K	α=40%, T_f =900K
4	α=60%, T_f =900K	α=60%, T_f =900K
5	α=80%, T_f =900K	α=80%, T_f =900K
6	α=100%, T_f =900K	α=100%, T_f =900K
7	T_f =600K, α=40%	T_f =600K, α=40%
8	T_f =1500K, α=40%	T_f =1500K, α=40%
9	T_f =2000K, α=40%	T_f =2000K, α=40%
#	**Instantaneous Branch Calculations (Branch from History Cases)**	
8	α=0%	
9	α=20%	
10	α=40%	
11	α=60%	
12	α=80%	
13	α=100%	
20	T_f =600K	
21	T_f =1500K	
22	T_f =2000K	
23	α=20% and T_f =600K combined	
24	α=80% and T_f =1500K combined	
#	**Instantaneous Buckling Branch Calculations (Branch from Reference History Case)**	
25	Buckling = -8.9E-04 cm^{-2}	
26	Buckling = 1.8E-03 cm^{-2}	
27	Buckling = -1.3E-03 cm^{-2}	

Table 3-4 summarizes the cases relevant to the results presented here. It should be mentioned that auxiliary calculations with a number of different assembly designs are also used to confirm the conclusions of this study.

The results given in this section are for the total importance factor (Eq. 3.14) since this serves to purposes of this study adequately (the I_d exhibits the same state dependencies as I):

$$I = \frac{\sum_d \beta_{eff,d}}{\sum_d \beta_d} \qquad (\mathbf{3.14})$$

3.4.2 Results and Discussion

Figure 3-27 illustrates the exposure dependence of importance factor (I) for a number of history cases with zero buckling and critical buckling searches (cases 2, 3, and 5 of Table 3-4). Also included are the instantaneous buckling branch cases (cases 25 to 27 of Table 3-4). It is immediately noted that the critical buckling search induces the significant exposure dependence of importance factor (I) and that leakage itself rather than fuel exposure should be considered as a state parameter for I. Here it is proposed to use the relative fast-group leakage rate (Eq. 3.15) for this purpose;

$$\frac{L_1}{(\sum_{r1} \Phi_1)} \qquad (\mathbf{3.15})$$

where $\Sigma_{r1} = \Sigma_{S21} + \Sigma_{a1}$. and $L_1 = (D_1 B^2 \Phi_1)$. This relationship is shown to be reasonable in the left hand side of Figure 3-28 where all buckling branch cases of the reference history case are plotted.

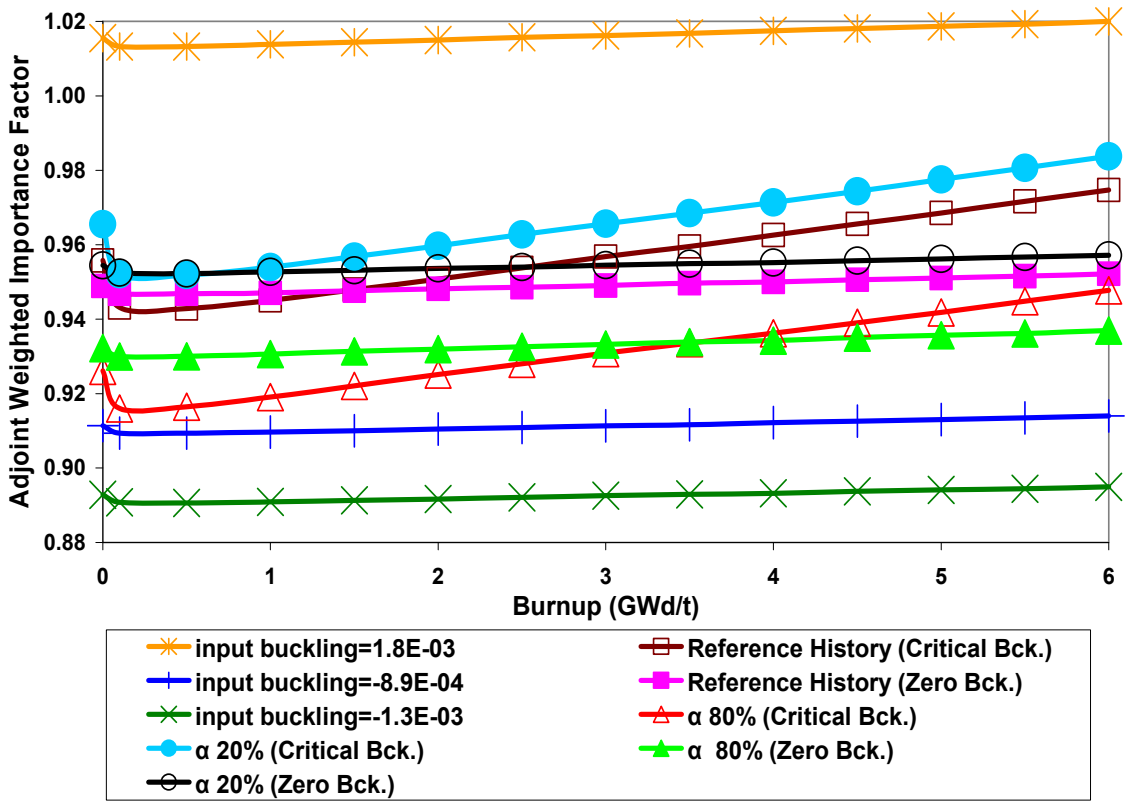

Figure 3-27: Exposure Dependence of the Delayed Neutron Importance Factors

Figure 3-27 also illustrates the dependence of importance factor on the void history, but this figure is misleading since it is actually a dependence on instantaneous void that is seen here. A detailed comparison of the various history and instantaneous branch cases reveals that history conditions are essentially irrelevant and that the instantaneous void dependence is dominant as far as importance factor is concerned. This is expected since coolant density variations induce large changes in neutron moderation

and resonance absorption in the fast energy range and this in turn has a significant impact on the multi-group adjoint spectrum. Since these changes are essentially spectrum changes that affect the competition between fast fission and the fast neutron removal processes, it is proposed to represent the state dependence (other than leakage) by the ratio given in Eq. 3.16.

$$\frac{\nu \Sigma_{f1}}{(\Sigma_{r1} \Phi_1)} \tag{3.16}$$

This is shown to be reasonable in the right hand side of Figure 3-28 where all zero buckling cases (history and branch cases) are plotted.

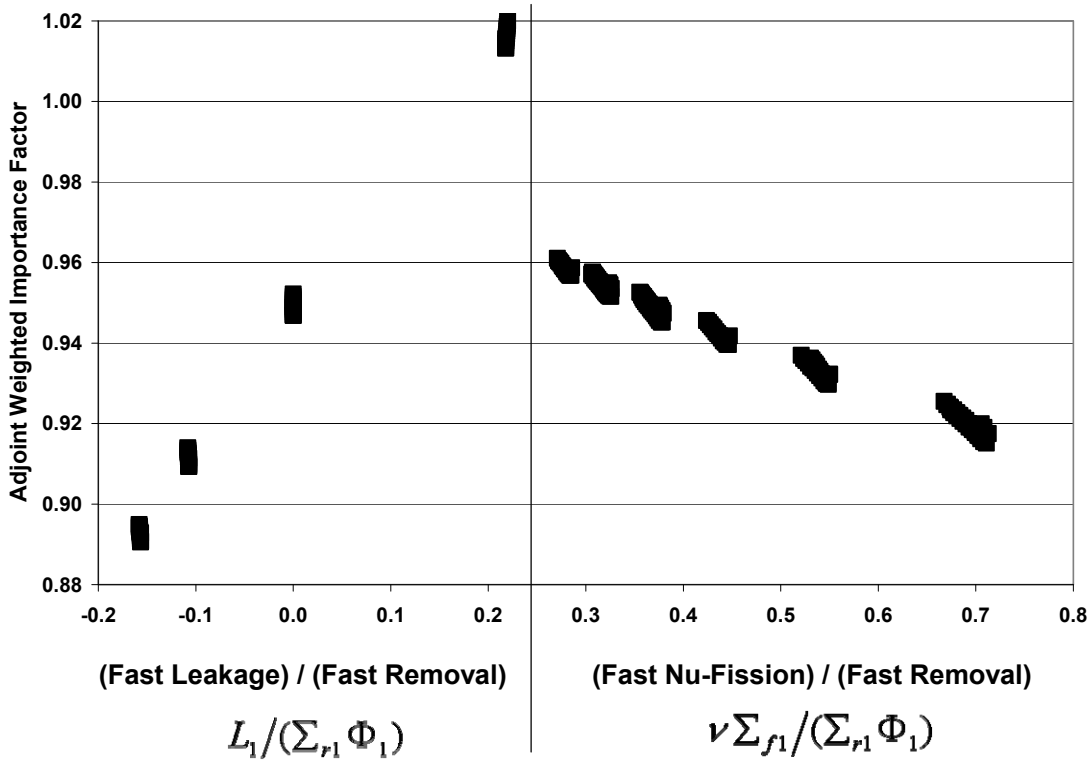

Figure 3-28: State Representation of the Delayed Neutron Importance Factor

Thus, the state dependence of *I* is thus proposed to be represented by Eq. 3.17.

$$I\left(\frac{\nu\Sigma_{f1}\Phi_1}{\Sigma_{r1}\Phi_1},\frac{L_1}{\Sigma_{r1}\Phi_1}\right)\approx A_0+A_1\left(\frac{\nu\Sigma_{f1}\Phi_1}{\Sigma_{r1}\Phi_1}\right)+A_2\left(\frac{L_1}{\Sigma_{r1}\Phi_1}\right) \qquad (\mathbf{3.17})$$

To demonstrate the adequacy of this representation, reference history case and its associated instantaneous branch cases (excluding buckling branches) are used to determine the expansion coefficients A_0 and A_1 by means of a least squares fit (yielding R^2=0.9984). Further A_2 (yielding R^2=0.9993) was determined from the instantaneous buckling branch cases (all other state parameters fixed at reference values) for this same history case.

The performance of this model is also tested against the entire data base represented by the cases in Table 3-4. The maximum relative error is of the order of 0.7%, which is excellent considering that the variation of importance factor around its base value (zero-buckling, 40% void history case) is of the order of 13% (8% if buckling branches are excluded).

3.4.3 Conclusion on Parameterization of Importance Factor

Several representation methods (spectral index) for the delayed neutron importance factor have been developed and tested in consistent with the recent cross section generation methods. Fast flux to thermal flux ratio given in Eq. 3.18, and fast

removal and leakage to fast absorption ratio given in (Eq. 3.19) are two examples of these representations methods.

$$SI^{*} = \left(\frac{SI - SI^{base}}{SI^{base}} \right) \tag{3.18}$$

Where $SI^{base} = \frac{\Phi_1^{base}}{\Phi_2^{base}}$ fast flux to thermal is flux ratio for the base case, and $SI = \frac{\Phi_1}{\Phi_2}$ is fast flux to thermal flux ratio for the instantaneous branch state.

$$\frac{\sum_{r,1} + DB^2}{\sum_{a1}} \tag{3.19}$$

Out of all tested methods only the method given by Eq. 3.17 has provided the best representation for the delayed neutron importance factor. In conclusion, the state dependence of the delayed neutron importance factor derived from BWR assembly lattice calculations is investigated in this section, and shown to be well represented by two lumped state parameters. These two parameters are the nodal fast fission to fast removal ratio and the nodal fast leakage to fast removal ratio. The numerical results also indicated that the main contributor to the exposure dependence of the delayed neutron importance factor is not fuel depletion itself but rather the critical buckling search that is usually performed during lattice depletion calculations.

3.5 SUMMARY

The studies presented in this chapter indicate that the state conditions have important effect on the delayed neutron importance factor; in addition to this, it is possible to generate delayed neutron data in consistent with the current cross section generation techniques for 3-D BWR simulations.

The deficiencies of the delayed neutron fraction methods utilized in the current applications are analyzed carefully, and improved methods are proposed. Enhancing the accuracy of simplified k-ratio method is one of these improvements. It has been shown that with a proper choice of the delayed neutron source range, the simplified *k*-ratio method can be very effective in estimating the delayed neutron importance factor. This enhancement validated by utilizing 3-D core simulator shows the importance of this improvement for the lattice codes which has no capability to calculate adjoint weighted delayed neutron fractions.

The state dependence of the delayed neutron importance factor derived from BWR assembly lattice calculations are extensively investigated for burnup, buckling, and local feedback parameters (i.e. fuel temperature, moderator void fraction, and control rod insertion). It has been showed that the state parameters play important role on the delayed neutron importance factor in such BWR calculations.

The state parameter study yield that the state dependence of delayed neutron importance factors can be represented in terms of two lumped parameters: nodal fast fission to fast removal ratio, and the nodal fast leakage to fast removal ratio. Thus, a

brand new technique named parameterization of the delayed neutron importance factor is developed in this chapter.

Needless to say, a robust computational platform is needed to test the accuracy and feasibility of the methods developed and proposed in this chapter. In this aim, the studies in the following chapter focus on the code modifications and methods implementations.

Chapter 4

IMPLEMENTATIONS OF THE METHODS

A fundamentally appropriate approach to test the accuracy of the importance factors would be to solve the nodal kinetics equations in a sufficient number of energy groups to explicitly capture neutron emission spectrum effects. But this would require the availability of a multi-group nodal transient code as well as a lattice code to generate the appropriate multi-group nodal data for the simulator. One such simulator is the PARCS nodal transient code, which is widely used and recognized as representative of the current state-of-the-art. Unfortunately, a proper nodal data preparation path between PARCS and a lattice code, TransLAT is not available. This deficiency also exists in the other lattice and diffusion codes. Even though several industrial lattice codes could be considered as candidates, most of them are tailored to producing two-group nodal data and would require modifications to produce multi-group prompt and delayed neutron emission spectra.

This chapter intends to establish a computational platform which makes possible an investigation of the accuracy and efficiency of the parameterization method developed in the previous chapter. In regard to this, the study firstly focuses on the capabilities of the lattice physics code, TransLAT, and the neutron kinetics code, PARCS. After the deficiencies of these codes are determined and mended, then the delayed neutron parameterization method is implemented. Finally, the code modifications and implementations are verified in this chapter.

In particular, the first section presents TransLAT code improvements which will lead to generate delayed neutron data to be used later in the nodal kinetics calculations consistently.

The PARCS nodal transient code capabilities for BWR multi-group transient applications are analyzed, and the PARCS code modifications are given in the second section. These code modifications and improvements are required to have fully consistent two-group and multi-group applications. In addition to these, the delayed neutron parameterization technique is implemented into the PARCS code, and this implementation is described in this section

Numerical results are described and presented in Section 4.3 and Section 4.4 respectively both to verify the proper functioning of these modifications and to illuminate the impact of various nodal kinetics data approximations in a selected transient calculation. Particularly, the significance of blending rodded and unrodded kinetics data in partially rodded nodes is demonstrated. It is also confirmed that the use of delayed neutron importance factors in two-group calculations notably reduces the differences between two-group and multi-group kinetics calculations.

4.1 IMPROVEMENTS TO LATTICE PHYSICS CODE

In this thesis, TransLAT is utilized to perform lattice calculations because it includes all the standard features of an industrial lattice code and in addition offers an adjoint spectrum solution method for computing delayed neutron importance factors. Furthermore, the TransLAT cross-section and kinetics data are based on the latest

releases of the ENDF/B-VI data files. The basis of this selection is provided in the Section 2.2.1 in a detailed way.

Although the TransLAT code produces most of the nodal kinetics parameters (e.g. inverse velocities, effective delayed neutron fractions, and delayed neutron precursor decay constants) it does not produce prompt and delayed neutron emission spectra as part of its output data. This presents an obstacle to using the code as a nodal data generator for multi-group nodal transient codes. For this reason, TransLAT is modified in this section to edit node-average delayed and prompt neutron emission spectra based on the following equations (Eq. 4.1, Eq. 4.2, Eq. 4.3, Eq. 4.4, and Eq. 4.5):

$$\chi^{D}_{h,d,i} = \sum_{g \in h} \chi^{D}_{h,d,i} \tag{4.1}$$

$$\chi^{D}_{h,d} = \frac{\sum_{i} \chi^{D}_{h,d,i} \beta_{i,d} \sum_{j} S^{i,j}}{\sum_{i} \beta_{i,d} \sum_{j} S^{i,j}} \tag{4.2}$$

$$\chi^{D}_{h} = \frac{\sum_{d} \chi^{D}_{h,d} \beta_{i,d}}{\sum_{l} \beta_{d}} \tag{4.3}$$

$$\chi^{P}_{h,i} = \sum_{g \in h} \chi^{P}_{g,i} \tag{4.4}$$

$$\chi_h^P = \frac{\sum_i \chi_{h,i}^P (1 - \sum_d \beta_{i,d}) \sum_j S^{i,j}}{\sum_i (1 - \sum_d \beta_{i,d}) \sum_j S^{i,j}} \quad \textbf{(4.5)}$$

In the above, *i* is an actinide index, *g* is a micro-group index, *h* is a macro-group index, *j* is a region index, *D* indicates "delayed", *P* indicates "prompt", *d* is a delayed neutron precursor family index, β is a total delayed neutron fraction where delayed neutron group-wise beta is given in Eq. 4.6.

$$\beta_d = \frac{\sum_i \beta_{i,d} \sum_j S^{i,j}}{\sum_i \sum_j S^{i,j}} \quad \textbf{(4.6)}$$

Here the source term can be defined as $S^{i,j} = V_j \sum_g \nu \Sigma_{fg,i,j} \Phi_{g,j}$

TransLAT has also been modified to compute node-average delayed neutron precursor family dependent importance factors (Eq. 4.7) directly (instead of leaving this to an external operation) from the ratio.

$$I_d = \frac{\beta_d^{eff}}{\beta_d} = \frac{\sum_g \chi_{g,d}^D \Phi_g^*}{\sum_g \chi_{g,d} \Phi_g^*} \quad \textbf{(4.7)}$$

where β_d^{eff} is the effective delayed neutron fraction for family *d* defined according to the standard definition using the adjoint flux spectrum (see the Reference [**21**]). The total importance factor is also computed by TransLAT as given in Eq. 4.8.

$$I = \frac{\sum_d I_d \beta_d}{\sum_d \beta_d} \qquad (\mathbf{4.8})$$

Figure 4-1 shows the 97-group fission spectra for each delayed neutron precursor family and prompt fission spectrum for a typical BWR assembly (given in Section 3.3) as generated by TransLAT using the input fine-group library for single unrodded assembly calculations with reflective boundary conditions. The energy group structures of the 97-group fission spectra can be found in the Appendix. The results in Figure 4-1 are the examples of the TransLAT modifications described in this section.

As a demonstration of the features added to TransLAT the (total) delayed and prompt fission spectra produced as output by the code are tabulated in Table 4-1 for a selected 6-group structure. The data tabulated here are for the unrodded state of the BWR assembly type given in Section 3.3. The difference in the neutron emission spectra of prompt and delayed neutrons is clearly seen in Figure 4-1 and at the Table 4-1.

Total and six precursor family group-wise importance factors are shown in Figure 4-2 and Figure 4-3 from k-ratio and adjoint weighted TransLAT calculations respectively.

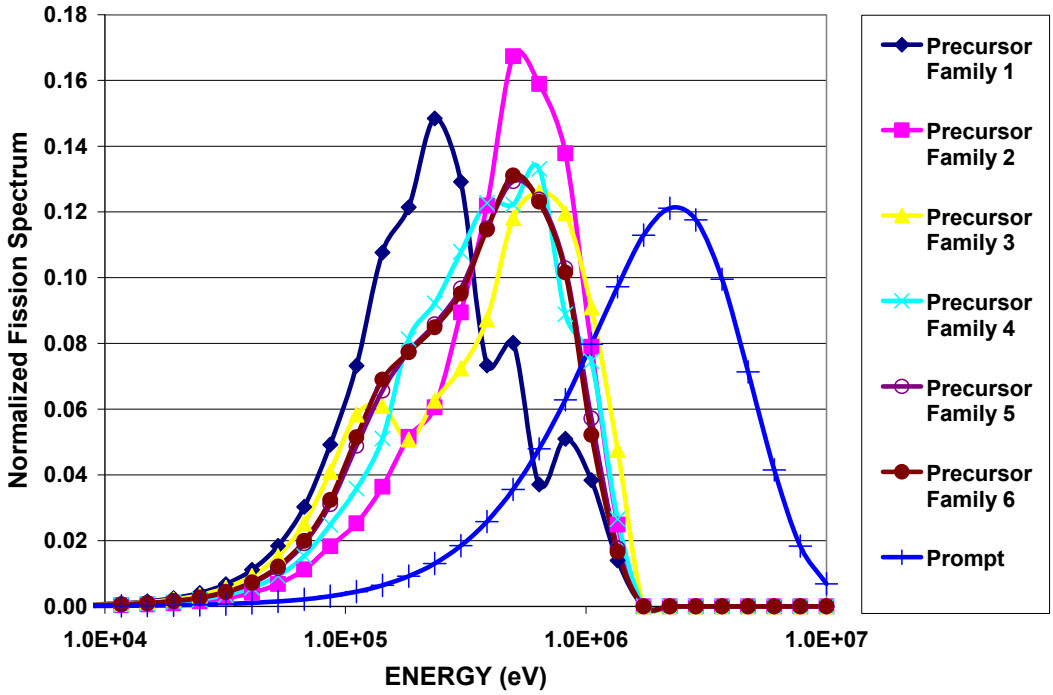

Figure 4-1: Prompt and 6-group Delayed Neutron Fission Spectra

Table 4-1: 6-Group Fission Spectra and Energy Group Structure

Group	Prompt Spectrum	Total Delayed Spectrum	Energy Boundaries (eV)
1	4.747E-01	0.000E+00	1.000E+07 – 1.738E+06
2	4.384E-01	4.658E-01	1.738E+06 – 3.877E+05
3	8.620E-02	5.321E-01	3.877E+05 – 1.503E+04
4	7.188E-04	2.090E-03	1.503E+04 – 3.928E+00
5	4.541E-11	1.108E-10	3.928E+00 – 6.250E-01
6	0.000E+00	0.000E+00	6.250E-01 - 0.000E+00

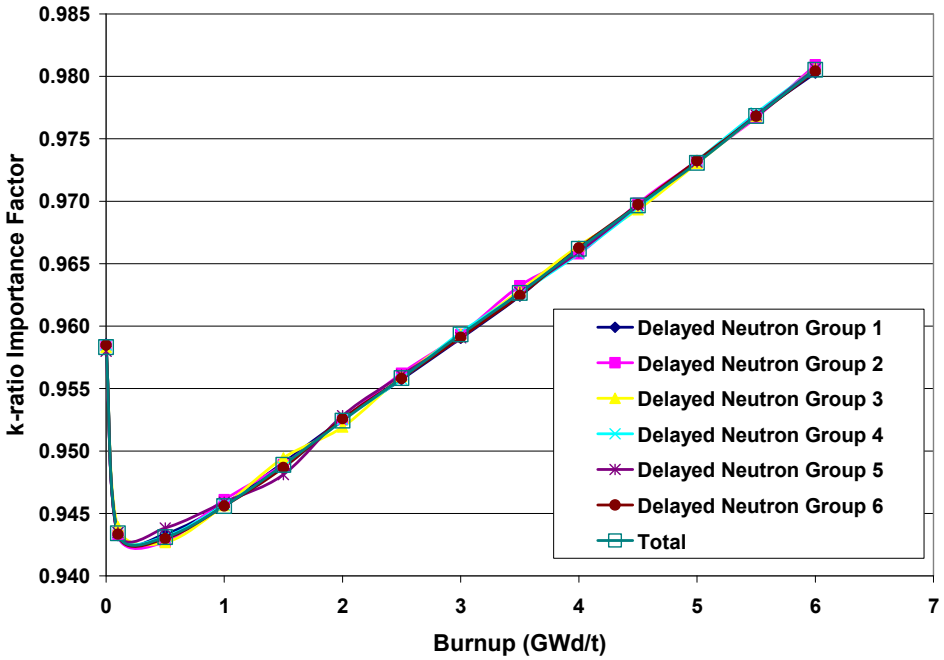

Figure 4-2: k-ratio Importance Factors for Total and Each Delayed Neutron Group

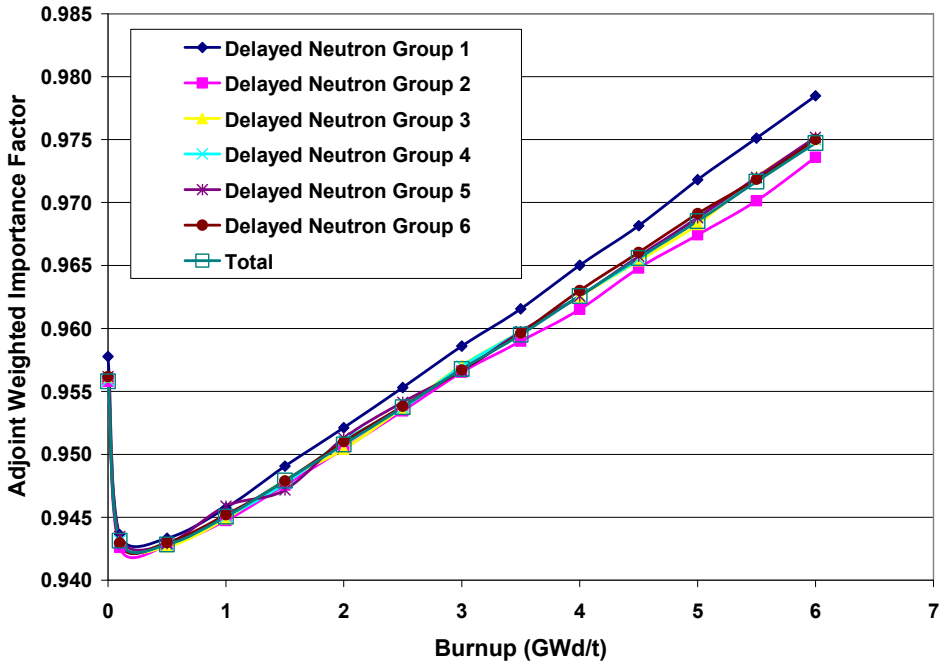

Figure 4-3: Adjoint Weighted Importance Factors for Total and Each Delayed Neutron Group

At present only the total importance factor I is passed on to PARCS for utilization in two-group kinetics calculations, the reason being that it is found from Figure 4-2 and Figure 4-3 that the delayed neutron precursor dependency is very weak (<0.3%) and that $I_d \approx I$ for both k-ratio and adjoint weighted importance factors.

In addition to the delayed neutron fractions β_d, the macroscopic prompt and delayed fission spectra (χ_h^p and χ_h^D) and the total importance factor, flux-weighted inverse decay constants for each precursor family and flux-weighted inverse neutron speeds for each macro energy group are calculated by TransLAT and passed on to PARCS.

4.2 IMPROVEMENTS TO NEUTRON KINETICS CODE

In the standard input cross-section model of PARCS the nodal parameters, including the kinetics parameters, are allowed to be dependent on exposure and a number of instantaneous state parameters. In Chapter 3 it is proposed to treat the delayed neutron importance factor as a separate nodal parameter because its state dependence could be simplified considerably relative to that needed for a direct state-dependent tabulation of effective delayed neutron fractions. Since the delayed neutron importance factor has not thus far been treated as a nodal parameter by PARCS, it had to be modified to do so. The code was therefore modified to construct the total importance factor per node (or per sub-node in partially rodded nodes) according to the state dependence proposed in the Eq. 4.9.

$$I \approx A_0 + A_1\left(\frac{\nu\sum_{f1}\Phi_1}{\sum_{r1}\Phi_1}\right) + A_2\left(\frac{L_1}{\sum_{r1}\Phi_1}\right) \qquad \textbf{(4.9)}$$

The fuel type dependent (and control rod dependent) constants A_0, A_1 and A_2 are provided in the nodal cross section library while the node-wise (not per subnode) fast reaction and leakage rates are calculated by PARCS at the initial steady state as well as at each time step during a transient simulation. PARCS thus also requires modifications to read (from the nodal cross section library) the mentioned coefficients and to compute the noted nodal reactions rates (using node-average cross sections and the nodal solution fluxes). Furthermore, the code is changed such that the importance factors are used in two-group transient calculations to modify the "physical" delayed neutron fractions, the latter being extracted in the usual way (per node or per subnode) from the nodal cross section library at relevant local conditions.

It is found in PARCS that a control rod cusping model (an axial homogenization correction for partially rodded nodes) was implemented only in the two-group analytic nodal model and not in the multi-group nodal expansion method (NEM). Since (two-group) numerical analyses had shown the cusping correction to be important, it was decided to implement it also in the NEM procedure and to apply it to all nodal cross-section data, including radial side discontinuity factors and kinetics parameters (delayed neutron fractions, precursor decay constants and neutron speeds). The cusping correction (Eq. 4.10) takes the form of a flux-volume weighting correction to the purely volume weighted rodded and unrodded data in a partially rodded node:

$$\Delta\sum^{node} = \frac{\sum^{unrod} h^{unrod}}{h^{node}}\left[\frac{\Phi^{unrod}}{\Phi^{node}} - 1\right] + \frac{\sum^{rod} h^{rod}}{h^{node}}\left[\frac{\Phi^{rod}}{\Phi^{node}} - 1\right] \qquad (\mathbf{4.10})$$

Here h^{node} is the height of the node while h^{unrod} represents the height of the unrodded part (unrodded subnode) of a partially rodded node. Φ^{node} is the node average flux and Φ^{unrod} is the average "heterogeneous" neutron flux in the unrodded part as computed for a simple one-dimensional three-node problem with the partially rodded node (with two sub-nodes) as the central node. Likewise for the rodded subnode data. When the heterogeneous flux is assumed to be flat, the cusping correction vanishes. Due to the flux depression in the partially rodded region the cusping correction reduces the control rod worth relative to that obtained without the cusping correction.

It should be noted that in addition to the cusping correction to the node-average data, axial side discontinuity factors are normally also computed as part of the axial homogenization procedure. However, such a calculation has as yet not been implemented to PARCS for the multi-group NEM case (it already exists for the two-group analytic nodal model).

During the course of these code modifications it is discovered that PARCS does not have a model for side-dependent discontinuity factors in the event that the standard cross-section model is used. It handles side-dependent discontinuity only if the specialized cross-section models for certain pre-defined transient benchmark problems are run. Since the standard cross-section model is the one that is to be used in real world

cases, this deficiency is mended by appropriate code changes. This capability is essential for BWR applications.

4.3 MINI-CORE TRANSIENT BENCHMARK

The 3-D nodal transient calculations presented in this chapter are performed for a BWR control rod movement transient scenario, which demonstrates the impact of delayed neutron parameters. For transient scenario, the mini-core model consisting of a 6x6 matrix of identical fresh BWR assemblies (given in Section 3.3) with a fuel active height of 365.75 cm (see Figure 4-4 and Figure 4-5) are developed for PARCS calculations.

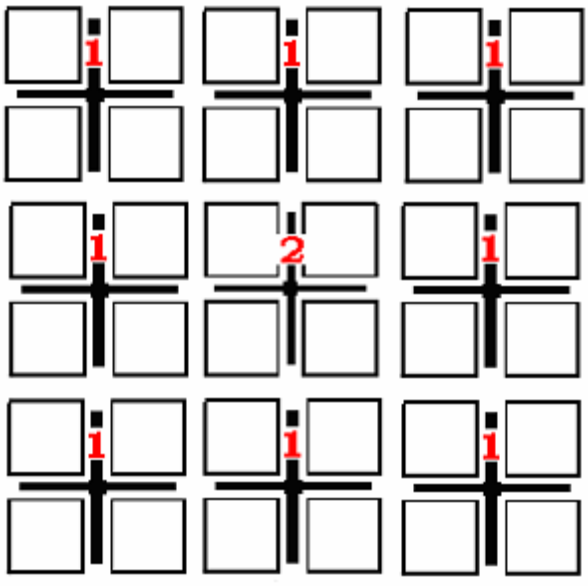

Figure 4-4: Mini core cross-sectional view and control rod grouping

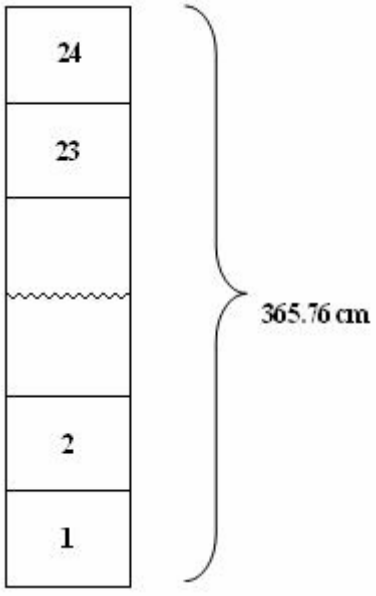

Figure 4-5: Axial representation of a single assembly

Reflective radial boundary conditions and vacuum axial boundary conditions are applied. For the transient simulation the initial state (steady-state) was chosen at typical hot-zero-power conditions with the central control rod bank (# 2 in Figure 4-4) fully inserted and the peripheral eight control rod banks fully withdrawn (# 1 in Figure 4-4). No thermal-hydraulic feedback is modeled in this problem and a reasonable power transient evolution is attained simply by control rod movement.

The transient is initiated by withdrawing the central control rod (# 2 in Figure 4-4) at a speed of 3.81 cm/s and after 12 s into the transient the peripheral rods (#1 in Figure 4-4) are inserted at a speed of 7.62 cm/s. The simplicity thus achieved facilitates a clear and meaningful comparative analysis of 6-group vs. 2-group kinetics calculations.

4.4 VERIFICATION OF THE IMPLEMENTATIONS

In this section, the results illustrating the impact of the modifications implemented in TransLAT and PARCS are presented. The multi-group NEM solver of PARCS was exclusively used both in the two-group and the six-group calculations reported here for a simple BWR mini-core kinetics benchmark. The six-group energy structure with prompt and total delayed neutron fission spectra are given at the Table 4-1. It should be noted that this six-group energy structure does not represent a reference multi-group case. An extensive study for the selection of reference multi-group structure is given in the next chapter. Here the study only focuses on the numerical tests which will be employed for the purpose of the verification of the code modifications given in this chapter.

As a test of the functionality of the TransLAT and PARCS combination, several steady-state calculations of the mini-core problem are performed and results are reported at the Table 4-2.

Table 4-2: Mini-Core Steady-State Results: Comparison of TransLAT and PARCS

Boundary Conditions	**Code**	**Groups**	**Rodded** All Rods In k_{eff}	**Un-rodded** All Rods Out k_{eff}	**Central Rod In** with DFs k_{eff}	**Central Rod In** w/o DFs k_{eff}
Reflective Everywhere	TransLAT	97	0.827458	1.038651		
	PARCS	2	0.827458	1.038652		
	PARCS	6	0.827458	1.038652		
Reflective Radially and Vacuum Axially	PARCS	2	0.824436	1.034801	1.019213	1.017646
	PARCS	6	0.824477	1.034833	1.018916	1.017326
	PARCS	Δk_{eff} (6 - 2 group)	4 pcm	3 pcm	-30 pcm	-32 pcm
	PARCS	$\max_n(\lvert\Delta P_n\rvert)$ (6 - 2 group)			1.0%	1.1%

In the above cases where the original axial boundary conditions were changed from vacuum to reflective and all rods are either inserted or withdrawn a direct comparison between TransLAT and PARCS results is possible (because a unit assembly configuration is attained). The fact that PARCS yields identical results to TransLAT for these cases irrespective of the number of energy groups used in PARCS simply confirms

that the nodal data preparation by TransLAT and utilization of such data by PARCS is consistent and proper. When the vacuum axial boundary conditions are re-instated and all rods are again either inserted or withdrawn, a single assembly case with uniform axial leakage is modeled. In this case the 2-group and 6-group PARCS results agree very well, which might be taken as a further indication that nodal data are properly utilized. The case where the central rod is inserted illustrates the utility of radial discontinuity factors and here it is seen (last two columns in Table 4-2) that they do affect the results significantly (about 160 pcm in k_{eff}). However, the impact on the difference between 2-group and 6-group results is negligible (for this problem, at least).

To test the implementation (in the NEM solver of PARCS) of the axial homogenization (cusping correction) method for partially rodded nodes, the BWR mini-core transient calculation is performed for each of the cases listed in Table 4-3. The 2-group calculations are performed with three choices for the delayed neutron fractions: "beta physical" implies that the fission-rate weighted betas (for each precursor group) produced by the lattice code and tabulated as a function of state parameters are used, "beta effective" implies that the adjoint spectrum weighted betas produced by the lattice code were used and "importance factor" implies that the delayed neutron importance factor as reconstructed according to Eq. 4.9 is multiplied into the "physical" betas.

The cases where "unrodded" kinetics parameters are used in all nodes irrespective of their control rod status are interesting from the point of view that such an application is quite common in many 3-D transient codes. The cases labeled with an "a" represent the status in PARCS prior to the changes reported in this thesis, with the exception of the radial discontinuity factor implementation. The results for all these cases are presented in

Figures 4-6 through 4-9. It should be noted that in all cases radial discontinuity factors were used.

Table 4-3: Mini-core transient cases to test axial homogenization procedure in PARCS

CASE ID					
6-group Beta Physical	**2-group Beta Physical**	**2-group Beta Effective**	**2-group Importance Factor**	**XS & DF axial smearing**	**Kinetics data axial smearing**
1a	2a	3a		Volume	Unrodded
1b	2b	3b		Flux-volume	Unrodded
1c	2c	3c		Volume	Volume
1d	2d	3d	4d	Flux-volume	Volume

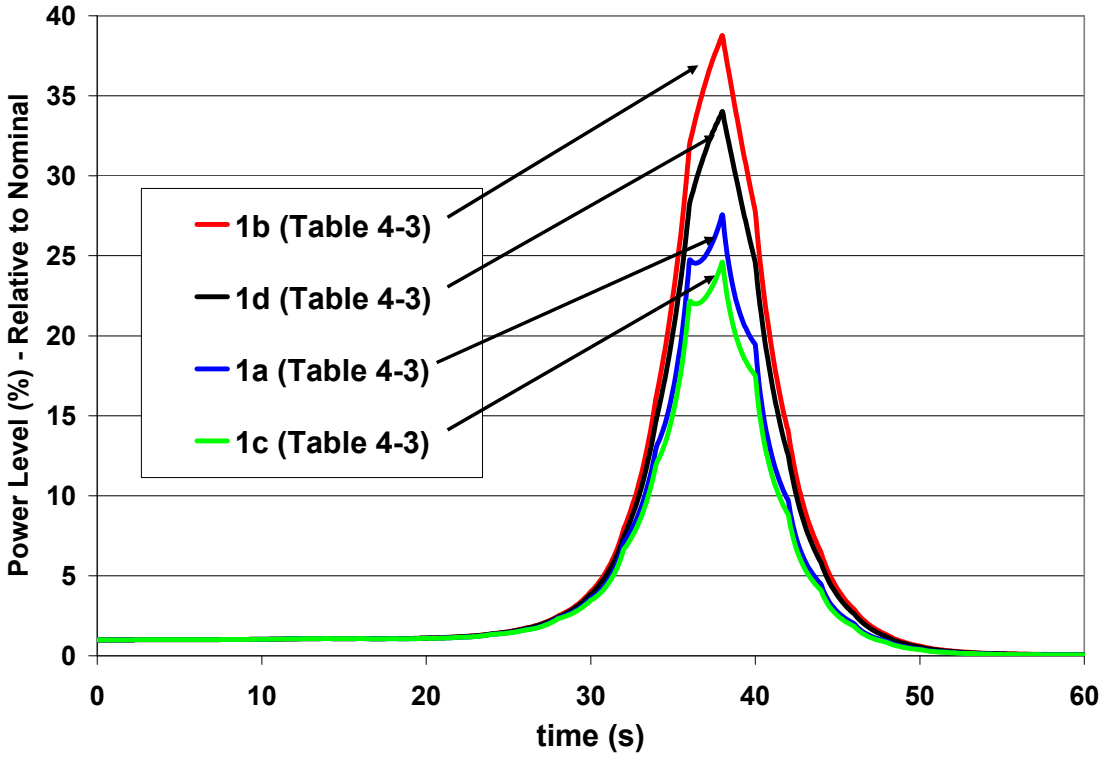

Figure 4-6: Power Comparison for 6-group

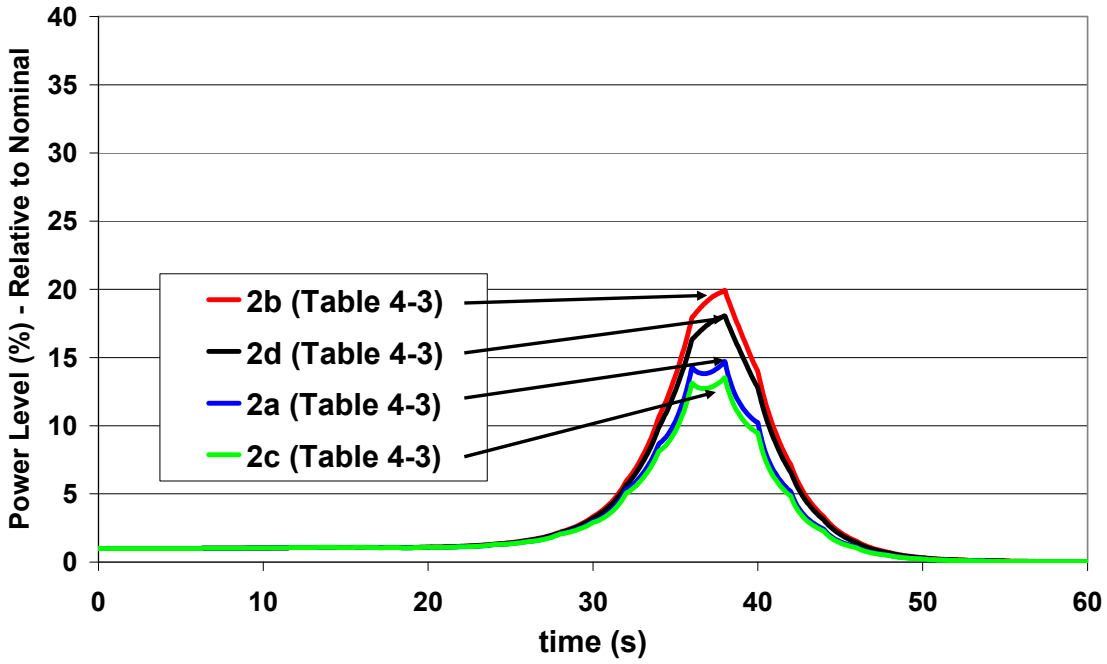

Figure 4-7: Power Comparison for 2-group with physical delayed neutron yield fractions

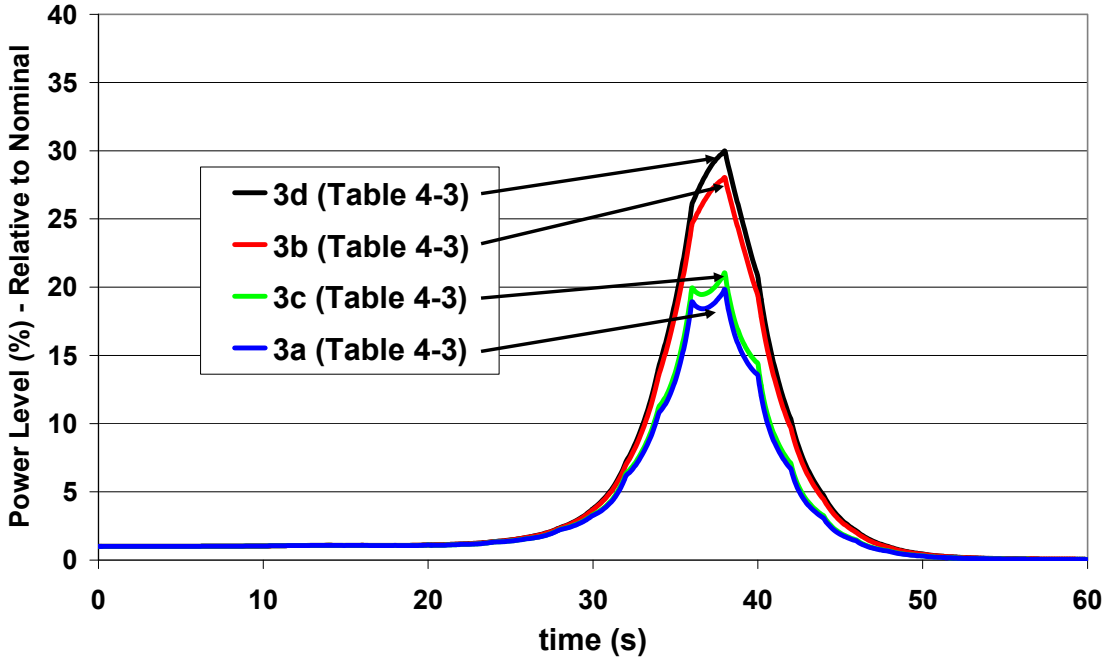

Figure 4-8: Power Comparison for 2-group with effective delayed neutron yield fractions

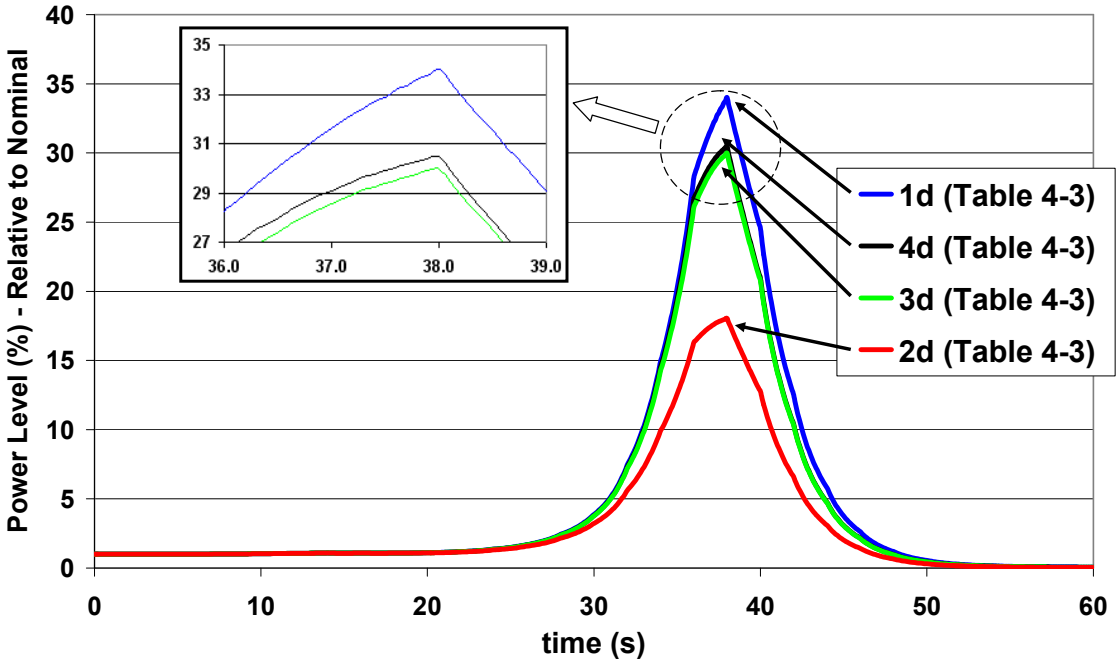

Figure 4-9: Power Comparison for 6- and 2-groups

The following discussions can be made:

1. Using both rodded and unrodded (instead of just unrodded) kinetics parameters has a modest affect on the power peak value (compare "a" to "c") that should certainly not be neglected if the peak value itself and/or the integral of the power evolution is important.
2. The cusping correction to the nodal cross-sections and radial discontinuity factors in partially rodded nodes is very significant (it reduces rod worth) and affects both the power peak value and the half-width of the power evolution curve (compare "a" to "b").
3. The cusping correction to the kinetics data appears to be somewhat insignificant (the difference between cases "a" and "c" is roughly the same as between cases

"b" and "d" and in the same direction) thus indicating that volume smearing of rodded and unrodded kinetics data suffices.

4. The use of effective betas in 2-group calculations dramatically reduces the difference between 2-group and 6-group results (see Figure 4-7) and since the 6-group case represents the delayed neutron emission spectrum explicitly, this must be taken as strong support for the standard practice of using effective betas in 2-group transient calculations. It is also noted that the use of the delayed neutron importance factor nearly reproduces the results obtained with the effective beta (compare case 3d and 4d) and this is an indication that the importance factor methodology has been implemented correctly; it is actually expected that these two approaches should yield different results since the importance factor method accounts for actual local leakage (or spectrum) effects whereas the effective beta method does not.

5. The impact of smearing rodded and unrodded *effective* betas (2-group cases) is of similar magnitude but of opposite sign to that obtained with smearing physical betas (compare Figure 4-1 and Figure 4-6). The net effect is that the smearing of effective betas lifts the power peak (compare cases 3b and 3d) which is advantageous for reducing the difference between 2-group and 6-group. The smearing of kinetics data in the 6-group case presses the power peak down and thus also has the effect of bringing 2-group (beta effective) and 6-group results closer to each other.

This section briefly described the PARCS modifications that are required to establish a 3-D nodal transient methodology that may be employed in multi-group studies. Mini-core transient benchmark description is provided and numerical results are presented to verify that the various modifications function properly and as expected.

It is discovered that PARCS does not have a model for side-dependent discontinuity factors in the event that the standard cross-section model is used. It handles side-dependent discontinuity only if the specialized cross-section models for certain pre-defined transient benchmark problems are run. Since the standard cross-section model is the one that is to be used in real world cases, this deficiency is mended by appropriate code changes. It must be noted that this capability is essential for BWR applications.

Numerical studies are performed to analyze the significance of certain approximations that could be, and often are, applied to the treatment of nodal kinetics data. In particular, it is shown that the simple use of unrodded kinetics data, as is often the case in 3-D nodal transient simulators, is inappropriate and that blending of rodded and unrodded kinetics data in partially rodded nodes may significantly affect the power evolution during a reactivity insertion transient. It is also shown that the flux cusping correction to the nodal data of partially rodded nodes has an important impact on the power peak and the power evolution in such a transient and that neglect of this correction in transient analyses is certainly improper. In fact, it is shown that the difference between two-group and multi-group transient results may be reduced significantly if a proper axial homogenization procedure is applied to all nodal data.

It is further confirmed that the use of parameterized delayed neutron importance factors in two-group calculations is needed to bring two-group and multi-group kinetics calculations closer to each other.

4.5 SUMMARY

The code modifications to attain proper computational platform that allow consistent data transfer between the lattice physics code and the 3-D nodal diffusion code is performed, and delayed neutron parameterization technique developed in the previous chapter is implemented into the neutron kinetics code in this chapter.

Firstly, TransLAT is modified to edit node-average multi-group delayed and prompt neutron emission spectra. TransLAT is modified to compute node-average delayed neutron precursor family dependent importance factors directly (instead of leaving this to an external operation) from the ratio. These modifications allow having all required nodal input data for multi-group kinetics calculations.

Secondly, several PARCS modifications are needed to be done to have consistent multi-group BWR kinetics calculations. These code changes are given below.

- A control rod cusping model is implemented for the multi-group NEM.
- A model for side-dependent discontinuity factors (BWR type ADFs) in the native cross-section format is implemented.
- Control rod blending of kinetics parameters are implemented into the PARCS.
- The code was modified to construct the total importance factor per node according to the parameterization technique.

Finally, the code modifications and implementations are tested in mini-core transient benchmark. Numerical results are presented to verify that the various modifications function properly and as expected.

As far as the remaining differences between two-group and multi-group kinetics calculations are concerned, the selection of the reference multi-group structure, the lack of thermal-hydraulics feedback, and the neglect of axial discontinuity factors (that should be produced by an axial homogenization procedure, if fully developed) are considered as possible causes. For these reasons, the study in the next chapter is mainly performed for the selection of the reference multi-group structure and the investigation for the effectiveness of the parameterization technique in the case of local thermal-hydraulic variations are accounted in the coupled transient calculations.

Chapter 5

MULTI-GROUP KINETICS CALCULATIONS

A new technique that yields consistent generation and modeling of neutron kinetics data in two neutron energy group BWR applications has developed in the Chapter 3. This technique has shown that the delayed neutron data can be generated in consistent way with the current cross section generation methods by utilizing a parameterization methodology for delayed neutron importance factors. Furthermore, the Chapter 4 has provided a computational platform which makes investigation of the accuracy and efficiency of the parameterization method possible. Such an investigation is presented in this chapter.

The first section of this chapter discusses the multi-group kinetics calculations from the perspective of this thesis. Section 2 provides an appropriate multi-group structures selection method that presumably maximizes the capturing capability of neutron emission spectrum effects. Thus, a reference multi-group structure is attained.

In the third section, the delayed neutron importance factor parameterization method is analyzed by employing 3-D coupled TRACE/PARCS transient calculations on which thermal-hydraulic feedbacks play important role. This analysis signifies the importance of the delayed neutron parameterization technique in 3-D coupled BWR transient applications.

5.1 INTRODUCTION TO MULTI-GROUP CALCULATIONS

The growing interest in applying coupled three-dimensional thermal-hydraulics/neutronics transient calculations to improve the safety and economics characteristics of LWR fuel and reactor system designs require consistent generation of nodal nuclear data (library of parameterized nodal equivalent parameters) for both steady-state and transient calculations. In addition to the standard two-group nodal cross-sections and flux discontinuity factors the 2-D lattice physics codes that are utilized to generate such libraries provide neutron kinetics and delayed neutron data for each relevant nodal material composition. This normally includes delayed neutron yield fractions (betas) and decay constants (lambdas) per delayed neutron precursor family, delayed neutron importance factor(s), and inverse neutron speeds.

As it was noted before, another issue that has to be considered in two-group transient calculations is the fact that the difference between prompt and delayed neutron emission spectra cannot be directly accounted for. This effect, which can be clearly seen in a multi-group formulation, is important and as a consequence two-group transient calculation results may be significantly affected. This situation can be improved for two-group calculations if corrected (effective) values of delayed neutron yield fractions are used. As discussed in Chapter 3, it is precisely for this reason that delayed neutron importance factors for each material composition are produced (either directly or as part of a post-processing activity) by lattice physics codes.

The use of the importance factors in two-group kinetics calculations represents at best only a crude approximation designed to compensate for the deficiencies of the

linearly (flux) collapsed two-group time-dependent diffusion equations. A fundamentally better approach would be to solve the nodal kinetics equations in a sufficient number of energy groups to explicitly capture neutron emission spectrum effects. In order to evaluate the accuracy of the two-group approach (utilizing importance factors) and the potential improvement that might be gained by adopting a multi-group approach in 3-D transient calculations, applicable codes and data preparation procedures must be available. In particular, appropriate kinetics data must be extracted from lattice code results and transmitted to a nodal simulator that has a multi-group capability. The nodal kinetics data must furthermore be employed (in the simulator) in a consistent manner with the state representation model for the data.

It has been found that many of the existing industrial lattice codes are customized to generate two-group nodal parameters and that delayed neutron emission spectra are not produced at all, with the consequence that it becomes difficult to perform multi-group nodal static and kinetics calculations with consistent nuclear data. The problem is solved by modifying such lattice codes to produce the required multi-group prompt and delayed neutron emission spectra. The modifications that were implemented in the TransLAT 2-D lattice code in order to produce necessary multi-group nodal data were described in Section 4.1. Likewise, if a specific state representation for the kinetics data must be employed, such as that proposed in the Chapter 3 for the delayed neutron importance factors, then the relevant nodal simulator code must be appropriately modified. These code modifications and method implementations are given in the Section 4.2 and tested in the Section 4.4. These improvements provide a robust computational tool for the

investigation of the accuracy and effectiveness of the delayed neutron parameterization technique.

5.2 SELECTION OF MULTI-GROUP STRUCTURES

With the modifications described in the previous chapter, TransLAT and PARCS provide an appropriate multi-group computational platform for an extensive investigation into the adequacy of the standard two-group kinetics approach (using effective delayed neutron fractions). The first step of such an investigation will be to determine an appropriate multi-group structure and this in itself requires a careful selection procedure that takes cognizance of relevant physical processes. Because the principal objective of such group structure investigation is to evaluate the significance of modeling both the prompt and the delayed neutron fission spectra adequately, the focus will be on selecting proper group boundaries in the above-thermal range (in particular above the thermal region, 0.625 eV in this case). Since the modeling of neutron leakage and neutron moderation may be quite sensitive to the energy divisions in this range, it is not simply a matter of inserting a single group boundary that separates prompt and delayed neutron emission spectra. Moreover, it is not sufficient to select group structures based on simple unit assembly calculations alone, even if such calculations should be the first step in any such selection process. For this reason, realistic reactor configurations in the form of mini cores as the one presented in the previous section, can be considered.

In this section, nodal data having been prepared by standard unit assembly TransLAT calculations in each of the candidate group structures is utilized in steady-state

and mini-core transient calculations. The description of the mini-core transient benchmark is provided in the Section 4.3. It is shown that by inter-comparison of the results of such calculations a judicious refinement of the group structure towards an acceptable reference group structure may be possible. If a reference group structure can be identified, the next step is to compare the results of two-group mini-core transient calculations with the "reference" results as given in this section. Also, with a reference group structure in hand one may attempt to select a reduced group structure for more routine multi-group kinetics applications.

The group structure selection procedure requires a very careful and meticulous study in order not to bias the results. Based on the experience from the numerous efforts performed in the course of this thesis work, it is found that the following two-step procedure must be followed before performing numerical tests on the various multi-group structures.

Step 1: Problem Definition

The problem of interest needs to be determined clearly at the beginning of the multi-group study. The energy groups must be chosen to produce the desired accuracy for the range of problems of interest. The energy range of the problem in this study is the fast neutron energy region (above 0.625eV) because the principal objective of this study is to investigate the accuracy and the efficiency of the parameterization of the delayed neutron importance technique proposed in the Chapter 3. As it is given in the Eq. 3.17, importance factor is a function of the fast energy group parameters (i.e. fast leakage, fast removal, and fast fission). Therefore, this region requires the evaluation of the modeling

both the prompt and the delayed neutron fission spectra adequately by employing properly selected group structures in the multi-group calculations.

Step 2: Physical Phenomena

The selection of the energy group structures must be based on physical considerations before the numerical tests are performed. For the aim of this study, the physical facts can be given as in the following.

- The energy range between 4.00 eV to 0.625 eV should also be considered as a separate group since there is significant upscattering from below 0.625eV into this range occurs.
- Also the energy range between 9.118 keV and 4.00 eV should be at least considered as a separate group to obtain correct flux level for the calculation of resonance absorption.
- Fast region over the resonance (10.0 MeV to 9.118 keV) should be divided into sufficient number of groups to obtain enough detail in the fast energy region to account for leakage and fast fission accurately. This would also properly capture the effects of delayed and prompt spectra explicitly.
- As it can be seen from the Table 5-1, there is no delay neutron contribution above 1.353 MeV. Therefore, this level can be considered as an upper cut-off in order to narrow down the region of interest which will be used in further numerical tests. This region of interest is given as shaded rows at the Table 5-1. It should be noted that the total delayed neutron spectra outside of the shaded region (between groups 29 and 62) is 8.10E-04. This delayed neutron

contribution is neglected here because inserting additional groups into the resonance region would bias the conclusions of this study.

- The energy group boundary, 19.31 keV, is selected as cut-off for the lower portion of the prompt spectra. The total prompt neutron spectrum is 1.05E-03 between group 26 and 97 (see Table 5-1).
- Previously, it was shown in the Section 3.2 that the simplified k-ratio method is an effective method (with 0.06% error of estimating delayed neutron importance factor) if energy level 0.821 MeV is chosen as a cut-off energy. For this reason, a special attention is paid to the energy level, 0.821 MeV in multi-group selection procedure. Thus, importance of this energy level is illuminated not only for simplified k-ratio method but also in the multi-group selection procedure. Numerous different group structures are tested, and it is found that the cut-off boundary 0.821 MeV is definitely needed in multi-group selection procedure in order to be able to capture delayed and prompt spectra effects explicitly. If the Table 5-1 is analyzed, it can be seen that delayed and prompt spectra about 1 MeV have the same value. This can also be seen in Figure 4-5 where the total delayed spectra plot and prompt spectra plot cross each other. Figure 4-5 and Table 5-1 show that the energy range between 10 MeV and 0.821 MeV captures the fast fission phenomena. Also, this range is the range in which most fast neutron leakage takes place and is important for core-reflector interaction.

Table 5-1: 97-Group Prompt and Total Delayed Neutron Fission Spectra

Group	Upper Boundary (eV)	Prompt Neutron Spectra	Total Delay Neutron Spectra	Group	Upper Boundary (eV)	Prompt Neutron Spectra	Total Delay Neutron Spectra
1	1.000E+07	7.20E-03	0.00E+00	**34**	2.613E+03	1.63E-05	2.48E-05
2	7.788E+06	1.85E-02	0.00E+00	**35**	2.035E+03	1.12E-05	1.51E-05
3	6.065E+06	4.12E-02	0.00E+00	**36**	1.585E+03	7.74E-06	9.14E-06
4	4.724E+06	7.02E-02	0.00E+00	**37**	1.234E+03	5.30E-06	5.54E-06
5	3.679E+06	9.85E-02	0.00E+00	**38**	9.611E+02	3.64E-06	3.36E-06
6	2.865E+06	1.18E-01	0.00E+00	**39**	7.485E+02	2.50E-06	2.04E-06
7	2.231E+06	1.22E-01	0.00E+00	**40**	5.830E+02	1.72E-06	1.24E-06
8	1.738E+06	1.13E-01	0.00E+00	**41**	4.540E+02	1.18E-06	7.50E-07
9	1.353E+06	9.73E-02	2.77E-02	**42**	3.536E+02	8.13E-07	4.55E-07
10	1.054E+06	8.00E-02	7.48E-02	**43**	2.754E+02	5.59E-07	2.76E-07
11	8.209E+05	6.33E-02	1.01E-01	**44**	2.145E+02	3.85E-07	1.67E-07
12	6.393E+05	4.84E-02	1.34E-01	**45**	1.670E+02	2.63E-07	1.02E-07
13	4.979E+05	3.59E-02	1.29E-01	**46**	1.301E+02	1.82E-07	6.16E-08
14	3.877E+05	2.59E-02	1.17E-01	**47**	1.013E+02	1.25E-07	3.73E-08
15	3.020E+05	1.84E-02	9.97E-02	**48**	7.889E+01	8.57E-08	2.26E-08
16	2.352E+05	1.30E-02	8.38E-02	**49**	6.144E+01	5.89E-08	1.37E-08
17	1.832E+05	9.13E-03	7.33E-02	**50**	4.785E+01	4.05E-08	8.33E-09
18	1.426E+05	6.31E-03	5.24E-02	**51**	3.727E+01	2.79E-08	5.05E-09
19	1.111E+05	4.40E-03	3.90E-02	**52**	2.260E+01	1.91E-08	3.07E-09
20	8.652E+04	3.04E-03	2.68E-02	**53**	2.902E+01	1.31E-08	1.86E-09
21	6.738E+04	2.10E-03	1.65E-02	**54**	1.760E+01	5.42E-10	1.13E-09
22	5.248E+04	1.45E-03	1.00E-02	**55**	1.371E+01	3.67E-10	6.84E-10
23	4.087E+04	1.00E-03	6.08E-03	**56**	1.068E+01	2.11E-10	4.15E-10
24	3.183E+04	6.89E-04	3.69E-03	**57**	8.315E+00	1.31E-10	2.52E-10
25	2.479E+04	4.74E-04	2.24E-03	**58**	6.476E+00	9.03E-11	1.53E-10
26	1.931E+04	3.28E-04	1.36E-03	**59**	5.044E+00	6.22E-11	9.26E-11
27	1.503E+04	2.24E-04	8.23E-04	**60**	3.928E+00	3.58E-11	5.61E-11
28	1.171E+04	1.55E-04	4.99E-04	**61**	3.059E+00	7.86E-12	3.41E-11
29	9.119E+03	1.06E-04	3.03E-04	**62**	2.382E+00	1.71E-12	2.07E-11
30	7.102E+03	7.31E-05	1.84E-04	**63**	1.855E+00	0.00E+00	0.00E+00
31	5.531E+03	5.03E-05	1.11E-04	**64**	1.726E+00	0.00E+00	0.00E+00
32	4.307E+03	3.45E-05	6.75E-05	**65**	1.595E+00	0.00E+00	0.00E+00
33	3.355E+03	2.38E-05	4.09E-05	**66-97**	1.457 – 0.0	0.00E+00	0.00E+00

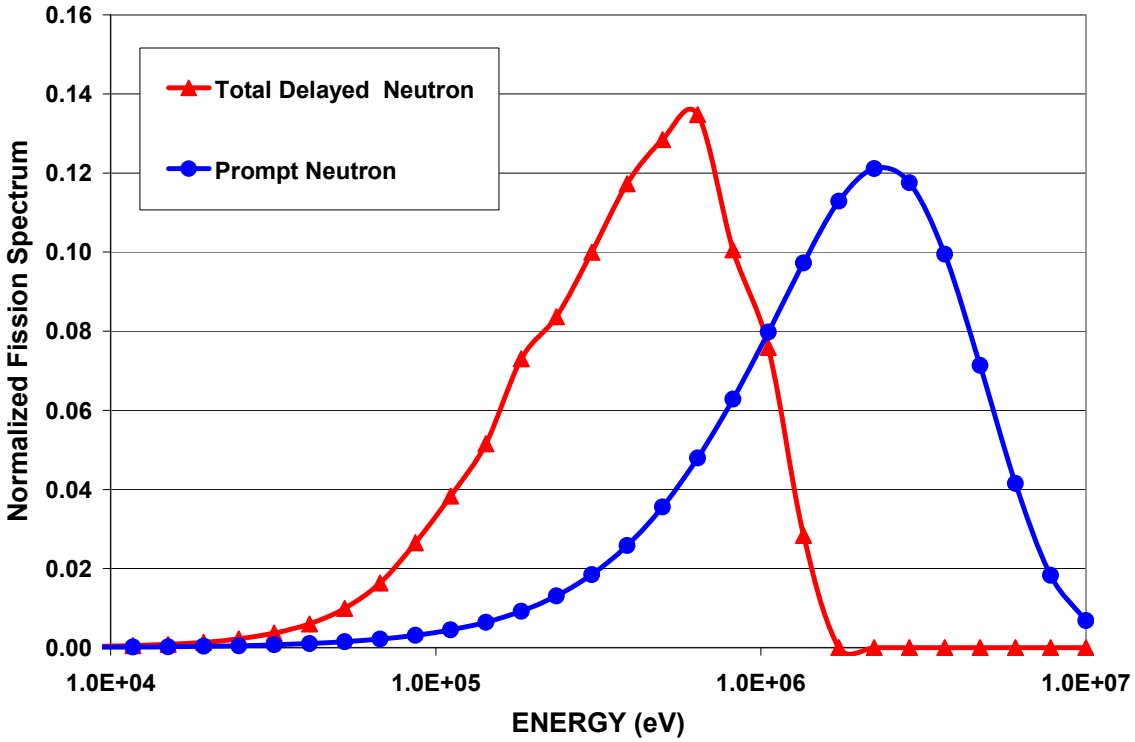

Figure 5-1: 97-Group Prompt and Total Delayed Neutron Fission Spectra

Table 5-2: Preliminary 7-Group Structure for the Multigroup Study

Group	Upper Boundary (eV)	Lower Boundary (eV)
1	1.000E+07	1.353E+06
2	1.353E+06	8.209E+05
3	8.209E+05	1.931E+05
4	1.931E+05	9.119E+03
5	9.119E+03	3.928E+00
6	3.928E+00	6.249E-01
7	6.249E-01	0.000E+00

A 7-group preliminary energy group structure is attained after the procedure given in the above steps is followed. This preliminary 7-group structure given at the Table 5-2 is a starting group sturucture for the multi-group numerical tests. These boundaries must be preserved for the seven and higher group calculations for the consistency point of view. Hence, numerical tests are focused on inserting new boundaries into the region of this problem of interest (shaded rows, group 2, 3 and 4 at the table below).

In order to determine the reference group structure, the best approach would be to divide group 2 to 4 at the Table 5-2 into as much energy group number as possible. If Table 5-1 (or the table in the Appendix) is analyzed, it can be seen that this range can be expanded to 20 different groups. As a result, 24-group structure is attained for the reference mini-core transient calculations.

Throughout this study, numerous nodal data is generated by utilizing lattice code TransLAT, and later these data are transferred to the nodal diffusion code PARCS. In order to make this job feasible, a linkage code is developed by employing the latest FORTRAN standards.

This linkage code mainly performs the following two major tasks:

1. It edits delayed neutron importance factors for each burnup step and for each energy group structure by utilizing the data given in the TransLAT outputs. It creates an importance factor output from which unrodded and rodded output TransLAT files. Basically, this output helps to analyze simplified k-ratio method for legacy and improved cut-off neutron energy boundaries. By

employing simplified k-ratio method onto few group reaction rates, it is also possible to seek a criterion for the selection of few group energy structures which take into account delayed neutron effects.

2. This program also intends to be a linkage code between TransLAT and PARCS.

- It prepares cross section and kinetics data for the native format (multi-group) of PARCS inputs.
- It is possible to transfer data from TransLAT to PARCS for each multi-group edit set and for each burnup step if it is necessary.
- Upscattering correction is also performed in this program.
- This program is designed to prepare input for the PARCS version that takes into account the control rod blending of the kinetics parameters as well as the parameterization technique.

Finally, numerical tests are performed for multi-group study by employing various energy group structures. Summary of these group structures are given in the Table 5-3 and Table 5-4. The mini-core transient benchmark described in the Section 4.3 is utilized to investigate the effects of these energy group structures in real reactor environment. The stand-alone PARCS mini-core transient power results are given in Figure 4-4, Figure 5-3, and Figure 5-4.

Table 5-3: Energy Group Structures Used in Mini-Core Transient Benchmark

2 Group	Upper Boundary (eV)	3 Group	Upper Boundary (eV)	3 Group	Upper Boundary (eV)	6 Group	Upper Boundary (eV)	24 Group	Upper Boundary (eV)
1	1.000E+07	**1**	1.000E+07	**1**	1.000E+07	**1**	1.000E+07	**1**	1.000E+07
		2	1.353E+06			**2**	1.353E+06	**2**	1.353E+06
								3	1.054E+06
				2	8.209E+05	**3**	8.209E+05	**4**	8.209E+05
								5	6.393E+05
								6	4.979E+05
								7	3.877E+05
								8	3.020E+05
								9	2.352E+05
								10	1.832E+05
								11	1.426E+05
								12	1.111E+05
								13	8.652E+04
								14	6.738E+04
								15	5.248E+04
								16	4.087E+04
								17	3.183E+04
								18	2.479E+04
								19	1.931E+04
								20	1.503E+04
								21	1.171E+04
						4	9.119E+03	**22**	9.119E+03
						5	3.928E+00	**23**	3.928E+00
2	6.249E-01	**3**	6.249E-01	**3**	6.249E-01	**6**	6.249E-01	**24**	6.249E-01

Table 5-4: Energy Group Structures Used in Mini-Core Transient Benchmark

7 Group	Upper Boundary (eV)	18 Group	Upper Boundary (eV)	20 Group	Upper Boundary (eV)	22 Group	Upper Boundary (eV)	24 Group	Upper Boundary (eV)
1	1.000E+07	**1**	1.000E+07	**1**	1.000E+07	**1**	1.000E+07	**1**	1.000E+07
2	1.353E+06	**2**	1.353E+06	**2**	1.353E+06	**2**	1.353E+06	**2**	1.353E+06
		3	1.054E+06	**3**	1.054E+06	**3**	1.054E+06	**3**	1.054E+06
3	8.209E+05	**4**	8.209E+05	**4**	8.209E+05	**4**	8.209E+05	**4**	8.209E+05
						5	6.393E+05	**5**	6.393E+05
		5	4.979E+05	**5**	4.979E+05	**6**	4.979E+05	**6**	4.979E+05
		6	3.877E+05	**6**	3.877E+05	**7**	3.877E+05	**7**	3.877E+05
				7	3.020E+05	**8**	3.020E+05	**8**	3.020E+05
		7	2.352E+05	**8**	2.352E+05	**9**	2.352E+05	**9**	2.352E+05
				9	1.832E+05	**10**	1.832E+05	**10**	1.832E+05
		8	1.426E+05	**10**	1.426E+05	**11**	1.426E+05	**11**	1.426E+05
		9	1.111E+05	**11**	1.111E+05	**12**	1.111E+05	**12**	1.111E+05
								13	8.652E+04
		10	6.738E+04	**12**	6.738E+04	**13**	6.738E+04	**14**	6.738E+04
		11	5.248E+04	**13**	5.248E+04	**14**	5.248E+04	**15**	5.248E+04
		12	4.087E+04	**14**	4.087E+04	**15**	4.087E+04	**16**	4.087E+04
								17	3.183E+04
		13	2.479E+04	**15**	2.479E+04	**16**	2.479E+04	**18**	2.479E+04
4	1.931E+04	**14**	1.931E+04	**16**	1.931E+04	**17**	1.931E+04	**19**	1.931E+04
		15	1.503E+04	**17**	1.503E+04	**18**	1.503E+04	**20**	1.503E+04
						19	1.171E+04	**21**	1.171E+04
5	9.119E+03	**16**	9.119E+03	**18**	9.119E+03	**20**	9.119E+03	**22**	9.119E+03
6	3.928E+00	**17**	3.928E+00	**19**	3.928E+00	**21**	3.928E+00	**23**	3.928E+00
7	6.249E-01	**18**	6.249E-01	**20**	6.249E-01	**22**	6.249E-01	**24**	6.249E-01

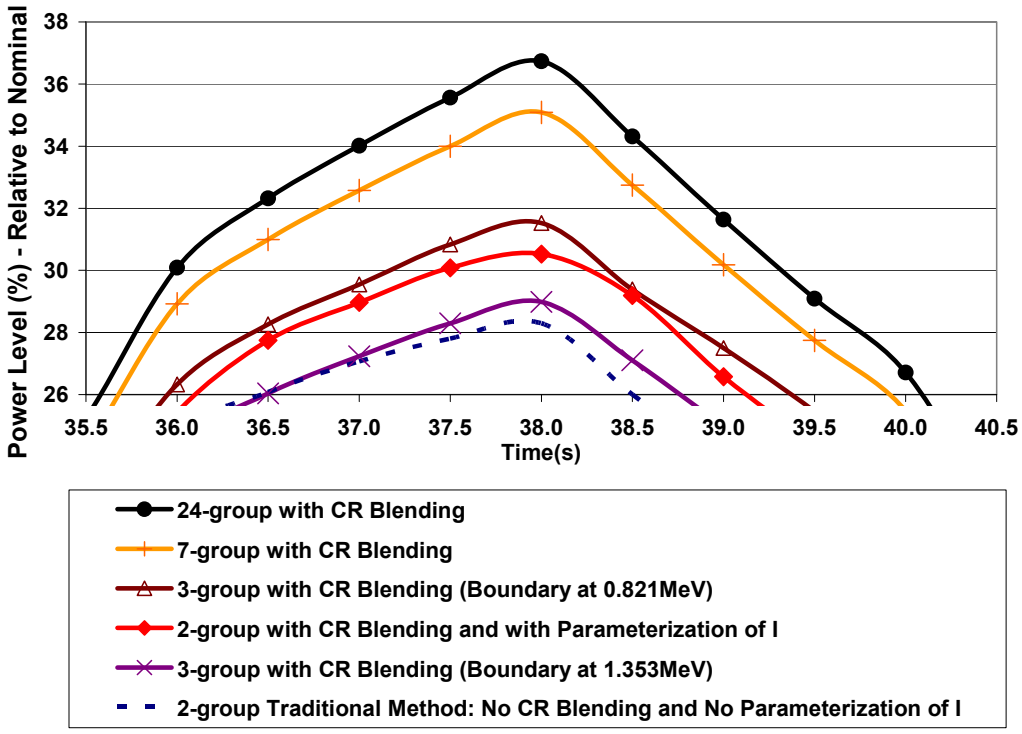

Figure 5-2: Mini-Core Transient Power for Various Energy Group Structures

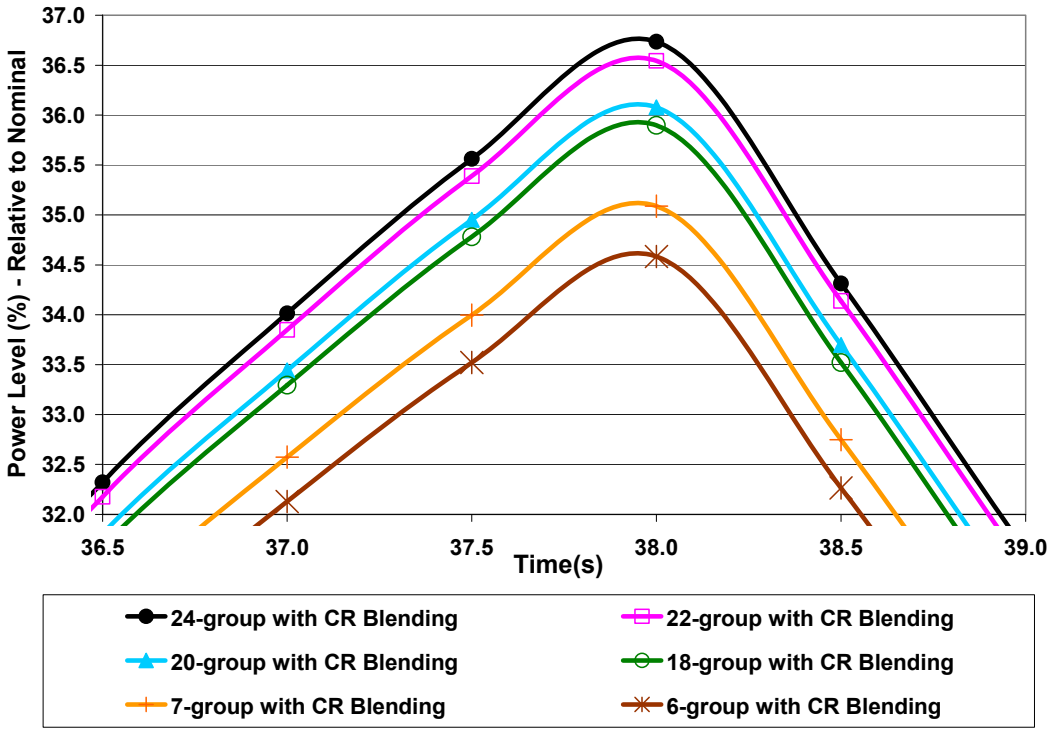

Figure 5-3: Mini-Core Transient Power for Various Energy Group Structures

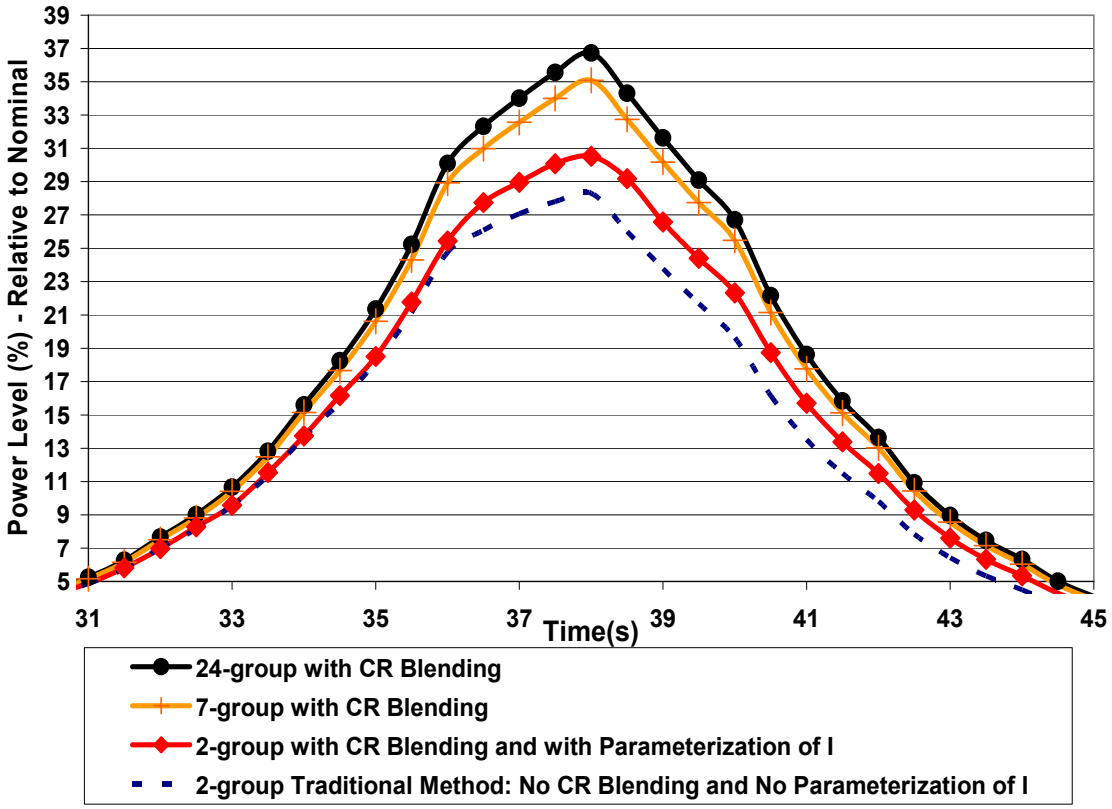

Figure 5-4: Power Comparison for 2, 7 and 24-Group Structures (zoom out)

Stand-alone PARCS mini-core transient benchmark calculations are performed for the energy group structures given in the Table 5-3 and Table 5-4. The transient power evolutions of these group structures are given in Figure 4-4, Figure 5-3 and Figure 5-4. In these figures, 2-group calculations with traditional method utilize one set of unrodded beta effectives (in this case adjoint weighted) during the whole transient. This application is quite standard in the current nodal diffusion calculations. The multi-group calculations are performed for the case of the blending of the rodded and unrodded kinetics data with respect to control rod status in the nodes. These cases are referred as “CR Blending” in the figures. The technique developed Section 3.4 is also presented in these figures with a

legend control rod (CR) blending together with parameterization of the importance factor (I).

As illustrated in Figure 4-4 the power peak value (which coincides at 38 s of the transient) of 2-group traditional method is approximately 8% (over the nominal value) lower than the reference 24-group solution. Figure 4-4 and Figure 5-4 show that parameterization technique improves power results approximately 2% in compared to the traditional method; however, its power peak value is approximately 4% lower than 7-group and 6% lower than the reference 24-group results. This difference here is quite normal since the real influence of the parameterization technique is expected in coupled calculations. This issue is investigated in the next section.

Two different 3-group structure results are given in Figure 4-4 to present the importance of the energy boundary 0.821 MeV (the so-called improved cut-off boundary in the Section 3.3) in multi-group calculations. In the case of the first set, a cut-off value 1.353 MeV is used while the improved boundary 0.821 MeV is applied in the second set. It is understood that this change on the energy boundary improve the power peak value about 2%.

As shown in Figure 5-3, the agreement on the power results are getting better with the increasing number of groups. This is an indication of the fact that carefully selected higher groups have capability to represent the delayed neutron emission spectrum explicitly.

In conclusion to this section, a reference 24-group structure is attained and various group structures are tested in the mini-core transient benchmark problem by employing stand-alone PARCS analyses. The deviation of the 2-group parameterization

results from the reference solution motivates this study to take one step forward to the coupled thermal-hydraulics and neutronics calculations in which reactivity feedback mechanisms presumably have significant impact on the delayed neutron parameterization technique, especially in BWR simulations. Hence, the following section focuses on the feedback effects on the mini-core transient benchmark studies performed so far.

5.3 3-D THERMAL-HYDRAULICS AND NEUTRONICS COUPLED CALCULATIONS

Prediction of a nuclear power plant's behavior under both normal and abnormal conditions has an important effect on its safety and economic operation. Incorporation of full 3-D models of the reactor core into system transient codes allows for a "best-estimate" calculation of interactions between the core behavior and plant dynamics. Recent progress in computer technology has made the development of such coupled system thermal-hydraulic and neutron kinetics code systems feasible.

The local power generation in the reactor core is directly related to the neutron flux, which itself is a function of the reactivity. In BWRs, the reactivity depends strongly on the thermal-hydraulic feedback mechanisms; such as moderator void fraction, and fuel temperature. These mechanisms, no doubt, constitute a challenge to coupled thermal-hydraulics and neutronics codes in simulating the space/time flux (power) variations throughout the reactor core. During the last decade, capabilities of the coupled codes for BWR analysis, in particular TRACE/PARCS are extensively validated in this manner.

Therefore, coupled TRACE/PARCS code is utilized to simulate mini-core transient benchmark analyses performed in this section.

The PARCS code modifications described in the Section 4.2 are consistently implemented into the latest coupled TRACE/PARCS version before starting coupled mini-core transient benchmark analyses. TRACE input model is developed to simulate core thermal-hydraulics behavior properly.

The following procedure is followed during the coupled TRACE/PARCS mini-core transient benchmark analyses.

1- Initialization of the thermal-hydraulics conditions by performing stand-alone steady-state TRACE calculations.

2- Initialization of the neutronics conditions by performing standalone steady-state PARCS calculations, as it is done in the previous section.

3- Initialization of thermal-hydraulics and neutronics conditions by performing coupled steady-state TRACE/PARCS calculations. These calculations must be started from the converged and initialized states of the above items 1 and 2.

4- Transient simulation by performing coupled TRACE/PARCS calculations. These calculations must also be started from the converged initial steady state of the item 3.

Figure 5-5 presents power evolutions of the coupled (CO) and stand-alone (SA) mini-core transient benchmark. The traditional 2-group method, 2-group parameterization technique proposed by this thesis, and 24-group reference results are given in Figure 5-5.

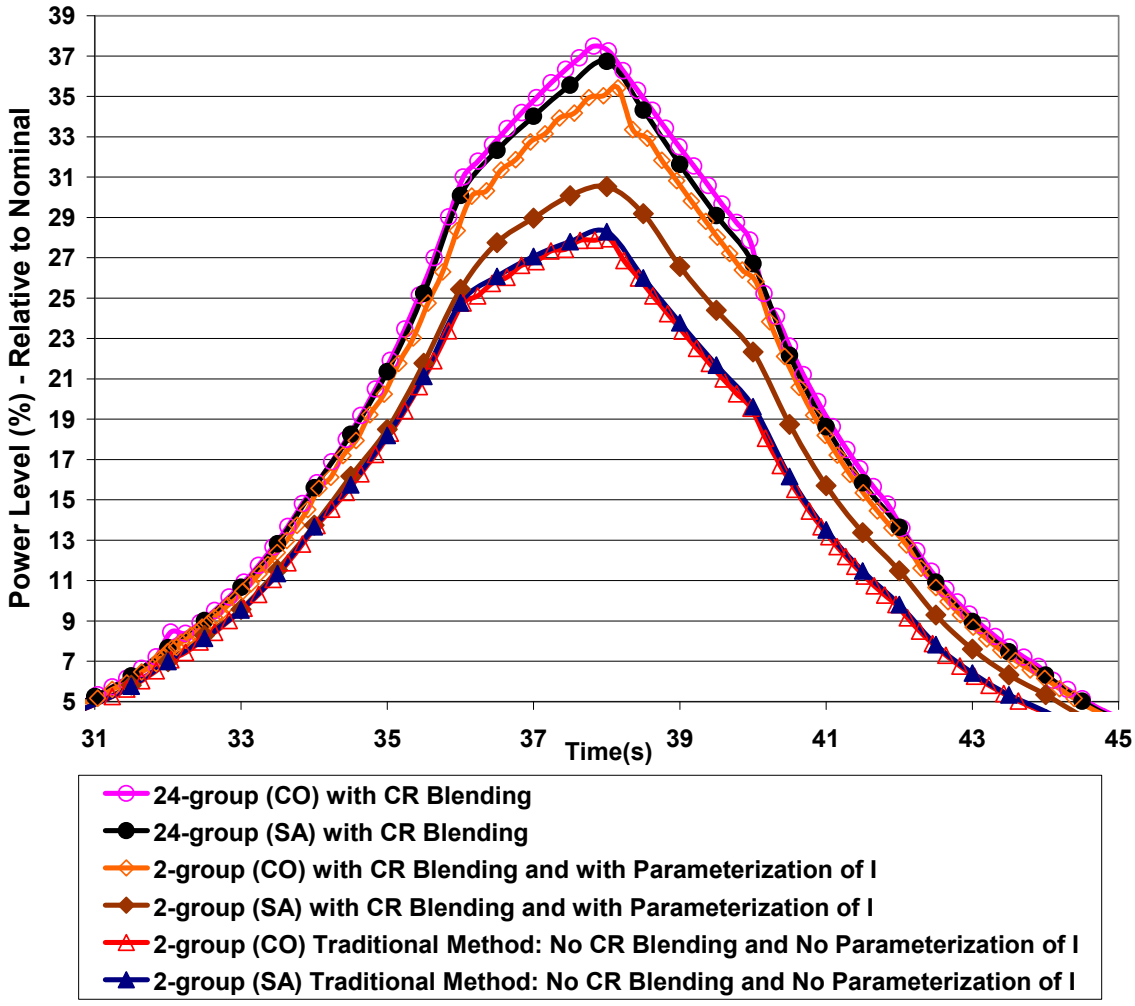

Figure 5-5: Power Comparison of Mini-Core Transient Benchmark – Stand-alone (SA) PARCS vs. Coupled (CO) TRACE/PARCS Calculations

As it can be seen Figure 5-5, a significant improvement is attained when 2-group parameterization technique is utilized in the case of the coupled calculations. The 2-group coupled result with parameterization of the importance factor case is approximately 4% higher than the standalone one. Furthermore, the difference of the power peak value of this case from the reference 24-group coupled solution is less than 2%. This improvement

illuminates the importance of the parameterization technique developed for the delayed neutron importance factor in this research work.

A special attention is also paid to the control rod blending of the kinetics parameters. Figure 4-1 presents 2-group coupled and stand-alone results with and without control rod blending cases. For both coupled and stand-alone calculations, peak power value of without control rod blending cases are approximately 1% (relative to nominal value) lower than the cases with control rod blending of kinetics parameters. This is also consistent with the conclusion drawn in Section 4.4.

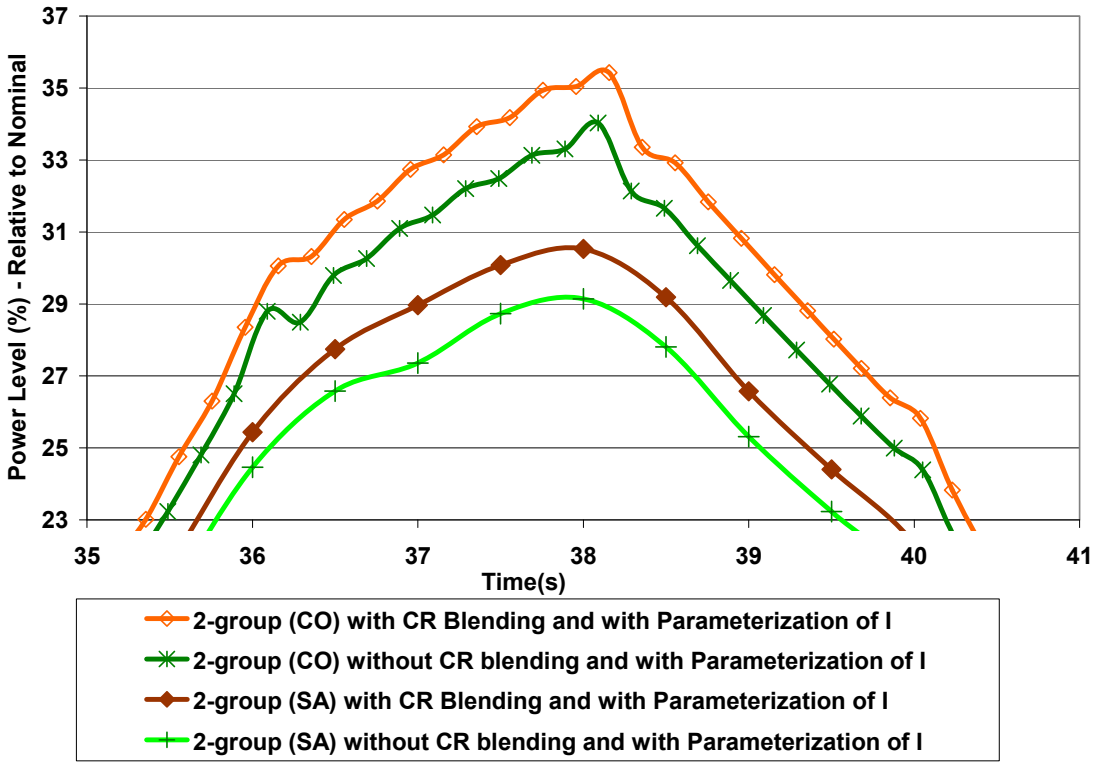

Figure 5-6: Sensitivity on the Control Rod (CR) Blending of the Kinetics Parameters

If 2-group traditional coupled and stand-alone results are compared as shown in Figure 5-5, it can be found that there is no significant differences between the coupled

and stand-alone results. This is also true for the 24-group results. The reason for this phenomenon can be explained by the reactivity plots given in Figure 5-7. It has been found that control rod reactivity is highly dominant in this transient. In other words, void and Doppler reacivities have no significant impact on the transient results. This is beneficial in this study because it allows examining the effectiveness of parameterization technique by its own.

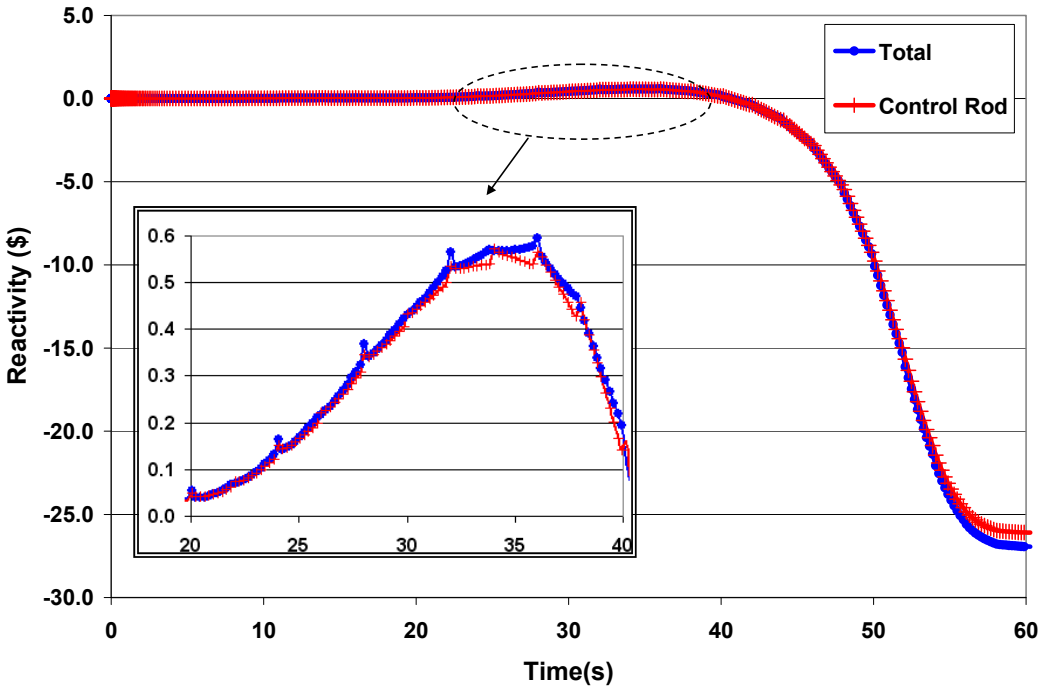

Figure 5-7: TRACE/PARCS Mini-Core Transient - Total and Control Rod Reactivity for 24-group Structure

The core average void fraction (in Figure 5-8), average void fraction at core exit (in Figure 4-6), maximum fuel temperature (in Figure 5-10), and average fuel temperature (in Figure 5-11) coupled results are given in the following figures. In these figures, results from 2-group traditional method and 2-group parameterization technique are compared with the 24-group reference solution.

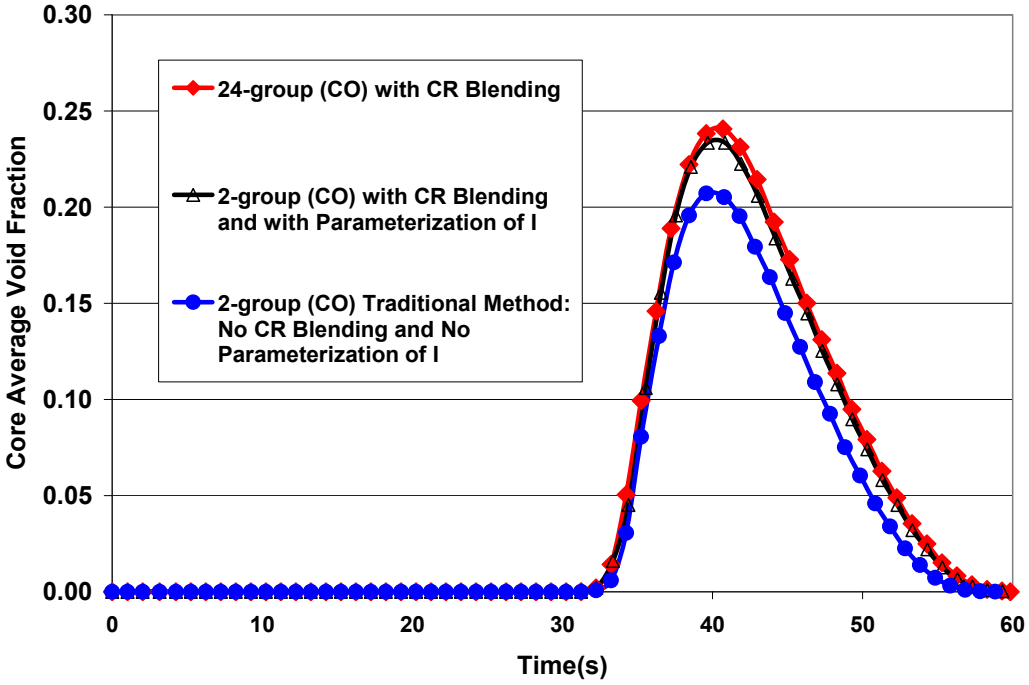

Figure 5-8: TRACE/PARCS Mini-Core Transient - Core Average Void Fraction

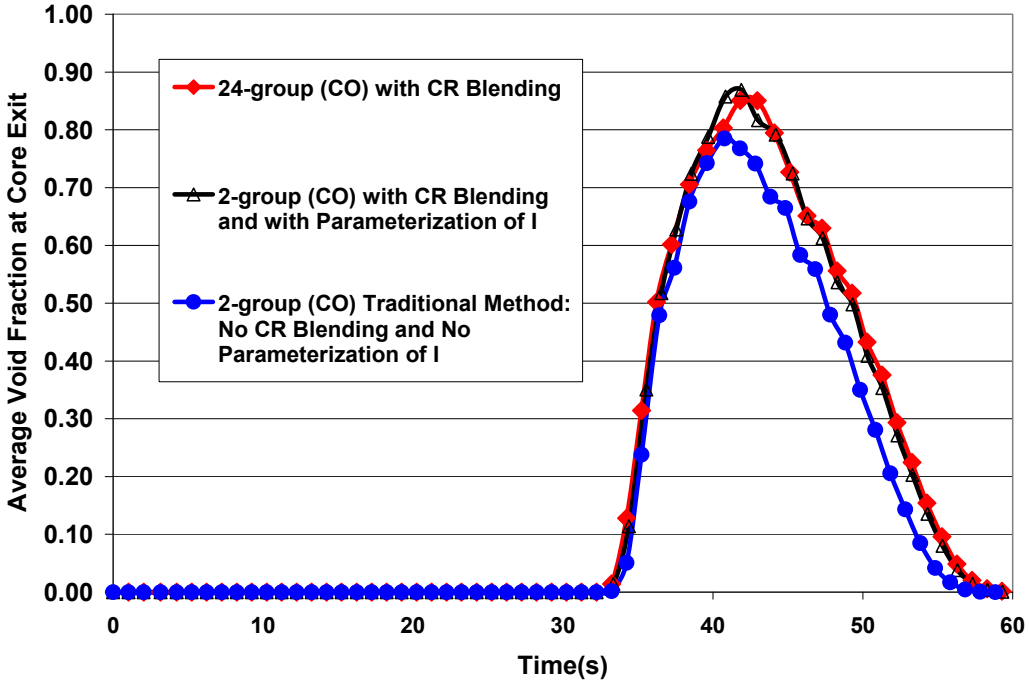

Figure 5-9: TRACE/PARCS Mini-Core Transient - Average Void Fraction at Core Exit

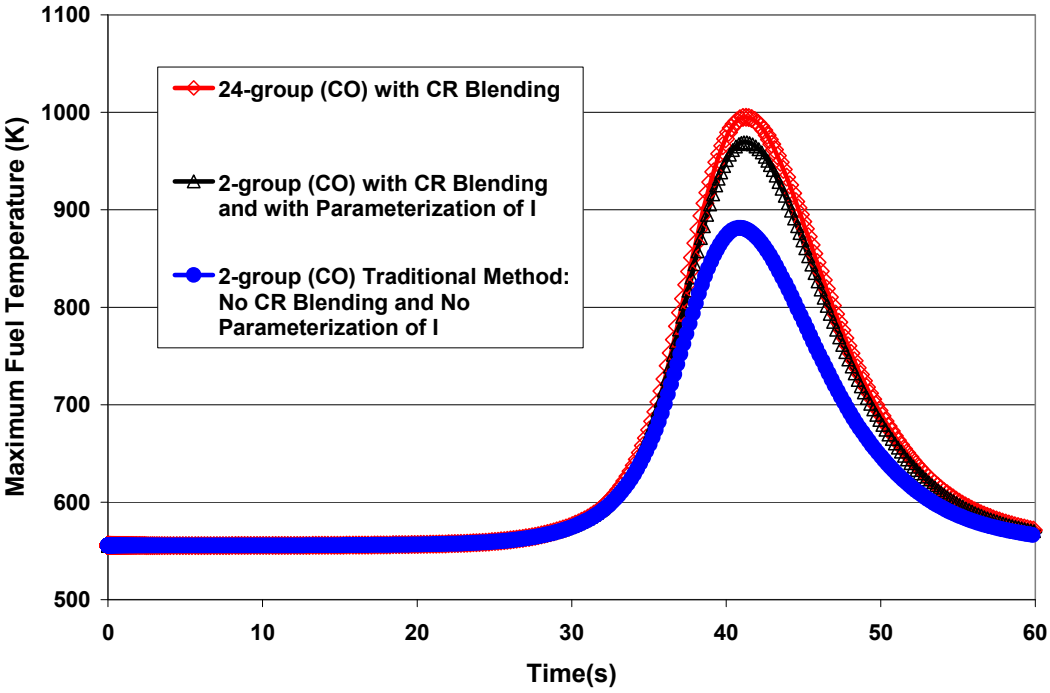

Figure 5-10: TRACE/PARCS Mini-Core Transient - Maximum Fuel Temperature

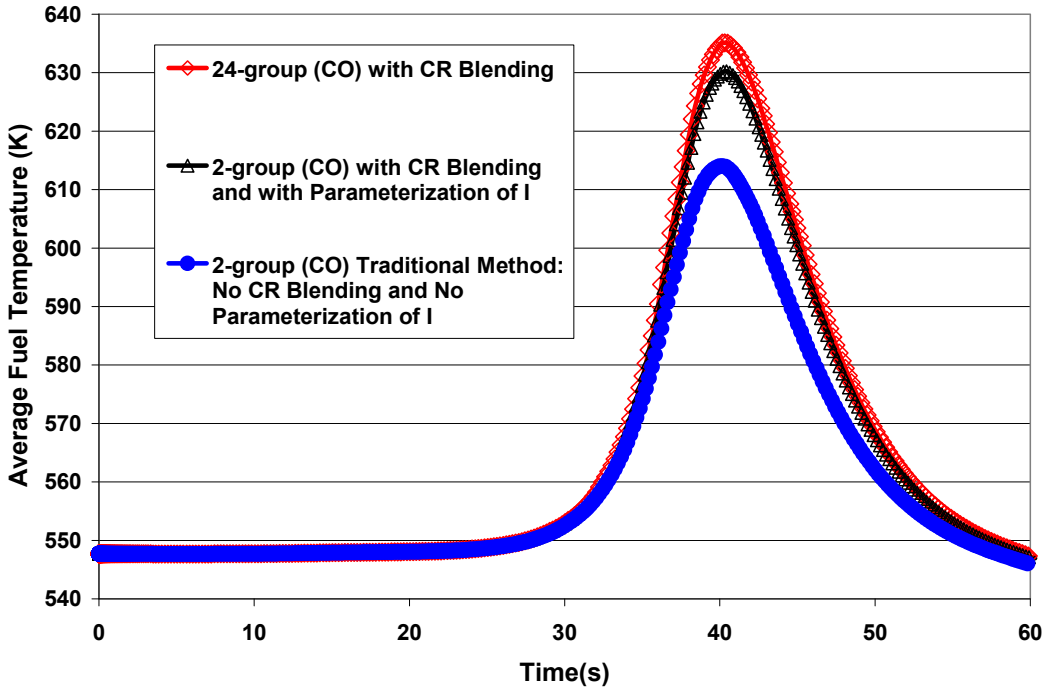

Figure 5-11: TRACE/PARCS Mini-Core Transient - Average Fuel Temperature

As a real of fact, the improvement on the coupled results of the parameterized importance factor is expected. In Section 3.4, it has been shown that the state conditions in the node, in particular moderator void fraction, have strong impact on the delayed neutron importance factor. This impact can be seen at the right hand side of the Figure 3-28. In addition to this, the studies given in the Section 3.2.3 show that a variation of 1% on the delayed neutron importance factor causes a 2-3% change in the power peak value while a 5% variation causes a 10-20% change in the power peak value (see Figure 3-4). Consequently, the changes in the core conditions especially void fraction in the nodes change the importance factor dramatically in the parameterization technique. As given in the above figures, the state conditions in the node are captured by the parameterization technique and this yields the improvement on the coupled power results. This improvement can not be seen in the stand-alone results of the parameterization technique since the state conditions are frozen in these calculations.

In conclusion, effectiveness of the delayed neutron parameterization technique in the case of coupled calculations is investigated in this section. It is found that the use of the parameterized delayed neutron importance factors in two-group calculations is feasible and it produces good agreement with the reference multi-group kinetics calculations in the 3-D thermal-hydraulics/neutronics coupled BWR simulations.

5.4 SUMMARY

In this chapter, firstly reference multi-group energy structure is attained and then, this structure is utilized in 3-D coupled thermal-hydraulics and neutronics calculations.

Thus, the accuracy and effectiveness of the delayed neutron parameterization technique is tested by utilizing mini-core transient benchmark problem.

Throughout this study, numerous nodal data is generated by utilizing lattice code TransLAT, and later these data are transferred to the nodal diffusion code PARCS. In order to make this job feasible, a linkage code is developed by employing the latest FORTRAN standards.

The accuracy of the delayed neutron parameterization technique is tested with the appropriate reference multi-group structure. It is also found that the group structure selection procedure requires a very careful and meticulous work in order not to bias the results.

Finally, the effectiveness of the delayed neutron parameterization technique is investigated by performing coupled mini-core transient calculations. It is found that the utilization of the parameterized delayed neutron importance factors in two-group calculations is feasible and it produces very good agreement with the reference multi-group kinetics calculations in 3-D thermal-hydraulics/neutronics coupled BWR simulations.

Chapter 6

SUMMARY AND CONCLUSIONS

This chapter summarizes the main findings of this study and the conclusions drawn from the work performed throughout this thesis. Some recommendations for the studies beyond this thesis are also given in this chapter.

The objective of this work was to improve the 3-D neutron kinetics modelling in coupled BWR transient calculations by developing, implementing and validating methods for consistent generation of neutron kinetics and delayed neutron data for such coupled thermal-hydraulics/neutronics simulations. The main outcome of this study was a unique and practical methodology developed for 3-D BWR thermal-hydraulics and neutronics coupled nodal diffusion applications. It was named as parameterization of the delayed neutron importance factor technique (or simply "parameterization technique"). In addition to this, a number of developments and contributions have been made to the current neutron kinetics methodologies.

At the beginning of this research, a comprehensive literature review was performed to clarify current status of the kinetics parameters, in particular delayed neutrons, in nuclear data level as well as in the 3-D kinetics applications level. As the result of this literature survey, the studies in the nuclear data files were found mature; however, a need for a more detailed and consistent neutron kinetics approach has been identified for BWR applications. Two important deficiencies were found in the current techniques from the perspective of BWR design and code development. One deficiency

was the assumption that the kinetics parameters to be dependent only on burnup (isotopic content). This assumption does not take into account the local instantaneous variations in the reactor core nodes. The other deficiency was the correction techniques (beta effective methods) which supposedly handle the fission emission spectra difference between prompt and delayed neutrons in two group applications. It was found that the adequacy and sufficiency of these corrections has never been tested for BWR applications. These obstacles in the current methods motivated the studies performed in this thesis.

In addition to the literature review on kinetics parameters, another review was performed to investigate the capabilities of the nuclear computer codes, which were utilized as tools to validate the developments given in this thesis. TransLAT for lattice calculations, PARCS for standalone kinetics calculations, and TRACE/PARCS for coupled thermal-hydraulics/neutronics analysis were selected for this research and the justification of this selection was provided. The preliminary sensitivity studies provided some basis for the purpose of understanding the effects of delayed neutron data in reactor kinetics applications.

In this study, lattice physics code analyses were extensively utilized to establish a basis for consistent generation and modeling of neutron kinetics data. The deficiencies of the delayed neutron fraction methods utilized in the current applications were analyzed carefully, and improved methods were proposed. Enhancing the accuracy of simplified k-ratio method was one of these improvements. It has been shown that with a proper choice of the delayed neutron source range with an energy cut-off 0.77 MeV (0.821 MeV is the closest boundary in TransLAT), the simplified *k*-ratio method can be very effective in estimating the delayed neutron importance factor. This enhancement validated by

utilizing 3-D core simulator shows the importance of this improvement for the lattice codes which has no capability to calculate adjoint weighted delayed neutron fractions.

A meticulous analysis was performed to investigate the state parameter effects on the delayed neutron *importance factor*. The studies from lattice physics calculations indicated that the state conditions have strong effect on the delayed neutron importance factor for the BWR applications. It was also shown that state dependence of the delayed neutron importance factor derived from BWR assembly lattice calculations can be represented by two lumped state parameters. This analysis was also consistent with the current cross section generation techniques.

The state parameter study yielded that the state dependence of delayed neutron importance factors can be represented in terms of two lumped parameters: *nodal fast fission to fast removal* ratio, and the *nodal fast leakage to fast removal* ratio. Thus, a brand new technique named parameterization of the delayed neutron importance factor was developed.

In order to justify the accuracy and the efficiency of the parameterization technique a test problem and a reference solution were necessary. A fundamentally better approach to have reference solution was to solve the nodal kinetics equations in a sufficient number of energy groups to explicitly capture neutron emission spectrum effects. However, it was found that current multi-group nodal transient codes as well as lattice codes to generate the appropriate multi-group nodal data for these simulators were immature for such multi-group calculations. For this purpose, particular coding modifications were performed to the TransLAT lattice physics code and the PARCS nodal kinetics code, to enhance their capabilities for multi-group kinetics calculations.

Firstly, TransLAT was modified to edit node-average multi-group delayed and prompt neutron emission spectra. TransLAT was also modified to compute node-average delayed neutron precursor family dependent importance factors directly (instead of leaving this to an external operation) from the ratio. Then, several PARCS modifications were needed to be done to have consistent multi-group BWR kinetics calculations. A control rod cusping model was implemented into the PARCS for the multi-group NEM. PARCS code modifications also made possible to handle for side-dependent discontinuity factors (BWR type ADFs) in the event that the standard cross-section model is used. Previously, PARCS was handling side-dependent discontinuity only if the specialized cross-section models for certain pre-defined transient benchmark problems are run. Since the standard cross-section model is the one that is to be used in real world cases, this deficiency was mended by appropriate code changes. This capability was essential for BWR applications.

In addition to these modifications, two major method implementations were performed for PARCS. One was the control rod blending of kinetics parameters, and the other was implementation of the delayed neutron parameterization technique.

The code modifications and implementations were tested in the mini-core transient benchmark. The results verified that the various modifications function properly and as expected. Numerical studies were shown that the simple use of unrodded kinetics data, as is often the case in 3-D nodal transient simulators, is inappropriate and that blending of rodded and unrodded kinetics data in partially rodded nodes may significantly affect the power evolution during a reactivity insertion transient. It was also shown that the flux cusping correction to the nodal data of partially rodded nodes has an

important impact on the power peak and the power evolution in such transient and that neglect of this correction in transient analyses is certainly improper. In fact, it was shown that the difference between two-group and multi-group transient results may be reduced significantly if a proper axial homogenization procedure is applied to all nodal data.

With the code modifications and developments, TransLAT and PARCS have provided an appropriate multi-group computational platform.

In order to investigate the accuracy and the efficiency of the delayed neutron parameterization technique, a systematic approached was developed to determine reference multi-group structures. A linkage code was created to provide consistent data transfer between the lattice physics code and the 3-D nodal diffusion code. This tool made numerous of nodal data transfer possible for various multi-group structures.

A reference 24-group energy structure was attained and various group structures were tested in the mini-core transient benchmark problem by performing stand-alone PARCS calculations. It was found that the group structure selection procedure requires a very careful and meticulous study.

Finally, the accuracy and the effectiveness of the delayed neutron parameterization technique were investigated by performing coupled thermal-hydraulics and neutronics mini-core transient calculations. It was found that the utilization of the parameterized delayed neutron importance factors in two-group calculations is feasible and it produces very good agreement with the reference multi-group kinetics calculations in 3-D thermal-hydraulics/neutronics coupled BWR simulations.

Although the work presented in this thesis forms a unified and complete study on the delayed neutron parameterization method, it addresses several issues to be considered in the future work.

As far as the remaining differences between two-group and reference multi-group kinetics calculations are concerned, the neglect of axial discontinuity factors (that should be produced by an axial homogenization procedure, if fully developed) can be considered as a possible cause. Therefore, completion of the axial homogenization procedure in PARCS multi-group kernel should be done in the future. Application of the delayed neutron parameterization technique should also be considered in the full core environment by employing various types of transient calculations.

In conclusion, the methods and developments proposed in this study provide a strong foundation for the future of 3-D coupled BWR kinetics applications.

References

1. M. Edenius and B. Forssen, "CASMO-3, A Fuel Assembly Burnup Program, Users Manual", STUDSVIK/NFA-89/3.

2. 'HELIOS Methods, Version 1.9', 1 December 2005, Studsvik ScandPower.

3. D.B. Jones, and K.E. Watkins, "TransLAT 3-D Lattice Physics Software", TransFX Computer Software Manuals, TWE-TFX-001-M-002, June (2001).

4. R.J.J. Stamm'ler and M.J. Abbate, *Methods of Steady-State Reactor Physics in Nuclear Design*, Academic Press, 1983.

5. S. Langenbuch, W.Maurer, and W. Werner, *Nucl. Sci. Eng.*, **63**, 437 (1977)

6. J. Solis, et al, "OECD/NRC BWR TT Benchmark. Volume 1: Final Specifications", NEA/NSC/DOC(2001)1.

7. B. Akdeniz, "Analysis for Exercise 1 of OECD/NRC Boiling Water Reactor Turbine Trip Benchmark", Master of Science Thesis, the Pennsylvania State University, May 2004

8. B. Akdeniz, K. Ivanov, and A. Olson, "OECD/NRC BWR TT Benchmark. Volume II: Summary Results of Exercise 1", NEA/NSC/DOC(2004)21. ISBN 92-64-01064-5

9. B. Akdeniz, K. Ivanov, and A. Olson, "OECD/NRC BWR TT Benchmark. Volume III: Summary Results of Exercise 2", NEA/NSC/DOC(2006)23. ISBN 92-64-02331-3

10. A. D'Angelo, "An International Cooperation to Improve Delayed Neutron Data", *Progress of Nuclear Energy,* Vol. 41, pp. 1-3, 2002.

11. A. D'Angelo, "*Overview of the Delayed Neutron Data Actinides and Results Monitored By the NEA/WPEC Subgroup 6"*, Progress in Nuclear Energy, Vol. 41, No. 1-4, pp.5-38, 2002

12. S. Okajima, et al, "*Summary of International Benchmark Experiments for Effective Delayed Neutron Fraction", Progress in Nuclear Energy*, Vol. 41, No. 1-4, pp. 285-301, 2002.

13. E. Fort, et al, *"Recommended Values of the Delayed Neutron Yield for U-235, U-238 and Pu-239", Progress in Nuclear Energy*, Vol. 41, No. 1-4, pp. 317-359, 2002.

14. G.D. Spriggs, J.M. Campbell, and V.M. Piksaikin, *"An 8-group Delayed Neutron Model Based on a Consistent Set of Half-lives"*, Progress in Nuclear Energy, Vol. 41, No. 1-4, pp. 223-251, 2002

15. A. D'Angelo, and J. Rowlands, "Conclusions Concerning the Delayed Neutron Data for Major Actinides", *JEF/DOC-920*; and *Progress in Nuclear Energy*, Vol. 41, No. 1-4, pp. 392-412, 2002.

16. W.B. Wilson and T.R. England, "*Delayed Neutron Study Using ENDF/B-VI Basic Nuclear Data"*, Progress in Nuclear Energy, Vol. 41, No. 1-4, pp. 77-107, 2002

17. G.D. Spriggs and J.M. Campbell, *"A summary of Measured Delayed Neutron Group Parameters"*, Progress in Nuclear Energy, Vol. 41, No. 1-4, pp. 145-201, 2002

18. V.M. Piksaikin, et al, *"Energy Dependence of Relative Abundances and Periods of Delayed Neutrons From Neutron-Induced Fission of ^{235}U, ^{238}U and ^{239}Pu In 6-group And 8-group Model Representation"*, Progress in Nuclear Energy, Vol. 41, No. 1-4, pp. 203-222, 2002

19. J.M. Campbell, and G.D. Spriggs, *"8-group Delayed Neutron Spectral Data for Hansen-Roach Energy Group Structure"*, Progress in Nuclear Energy, Vol. 41, No. 1-4, pp. 253-283, 2002

20 K. Smith, "Beta-effective Calculation in CASMO-4", StudsvikScandpower, Inc, report

21. C. Lee, T. Downar, and D. Jones, "Implementation of the Effective Delayed Neutron Fraction with Adjoint Spectrum Weighting into CPM-3", TANSAO 80 (1999).

22. G. Springs, R. Busch, and J. Campbell, "Calculation of the Delayed Neutron Effectiveness Factor Using Ratio of K-eigenvalues", Annals of Nuclear Energy 28. 477-487 (2001)

23. J. Krell, "*Remarks to the calculation of β_{eff}*", 7th AER Symposium on VVER Reactor Physics and Reactor Safety, September 23-27 1997, Hornitz, Germany

24. G.D. Spriggs, J.M. Campbell, R.D. Bush, "Determination of Godiva's Effective Delayed Neutron Fraction Using Newly Calculated Delayed Neutron Spectra", Reactor Physics:General, Section 2

25. A. Ahlin, M. Edenius, and O.P. Tverbakk, *"Definitions of Miscellaneous Quantities Calculated in AEBUXY",* TPM-RF-71-215, ATOMENERGI AB, Sweden (1971).

26. J. Svarny, "Calculation of Point Kinetics Parameters in the MOBY-DICK System", Nuclear Science and Engineering, 128, 76-87, 1998

27. P. Siltanen, E. Kaloinen, F. Wasastjerna, "*Simulation of Reactor Scram Experiments in the LOVIISA and MOCHOVCE VVER Reactors",* XI Meeting on Reactor Physics Calculations in the Nordic Countries, Espoo/Helsinki-Tallinn, April 9-10, 2003

28. J. Svarny, "Application of Different Delayed Neutron Data Sets to the Analysis of Rod Drop Experiments on VVER Cores", Progress in Nuclear Energy, Vol. 41, No. 1-4, pp. 303-315, 2002

29. T. Downar, et. al., "PARCS v2.6 U.S. NRC Core Neutronics Simulator Theory Manual",https://engineering.purdue.edu/PARCS/Code/Manual/Theory/PDF/PARCS_TheoryManual.pdf (2004)

30. F. Maggini, "Contributions to Study Instability in BWR: Application to Peach Bottom-2 NPP", Thesis of Bachelor, The University of Pisa, May 2004

31. F. Odar, C. Murray et al., "TRACE V4.0 User's Manual", May 2003.

32. J. W. Spore, et al., "TRAC-M/FORTRAN 90 (Version 3.0) Theory Manual", July 2003.

33. R. M. Miller, and T. J. Downar, "Completion Report for the Coupled TRAC-M/PARCS Code", August 1999.

34. D. Lee, T. Downar, A. Ulses, B. Akdeniz, and K. Ivanov, "Analysis of the OECD/NRC BWR TT Benchmark with Coupled Neutronics and Thermal-Hydraulics Code TRAC-M/PARCS", Nuclear Science and Engineering, 148, 2004.

35. H. Ideka, and T. Takeda, "Development and Verification of an Efficient Spatial Neutron Kinetics Method for Reactivity-Initiated Event Analyses", *Nuclear Science and Technology*, **38**, 492 (2001).

36. M. Ideka, T. Iwamato, and B. R. Moore, "Development of Kinetics Model for BWR Core Simulator AETNA", *Nuclear Science and Technology*, **40**, 201 (2003)

37. Wm. J. Garland, *"Reactor Physics: Point Kinetics",* Class Notes of Department of Engineering Physics, McMaster University, Hamilton, Ontario, Canada, June 2002

38. B. Akdeniz, E. Müller, D. Panayotov, and K. Ivanov, ”State Representation of the Delayed Neutron Importance Factor for Two-Group Nodal Transient Calculations”, *Trans. Am. Nucl. Soc*., **91** (2004).

39. Erwin Müller, “Nodal Kinetics Data Representation”, Westinghouse Report BTU 04-033, November 2004, Westinghouse Electric Sweden.

40. B. Akdeniz, E. Müller, D. Panayotov, and K. Ivanov, ”Consistent Neutron Kinetics Data Generation for Nodal Transient Calculations”, PHYSOR-2006, September 10-14, Vancouver, BC, Canada

Appendix

97-Group Neutron Energy Structure in Lattice Calculations

Micro-Group Number	Energy Group (eV)	Micro-Group Number	Energy Group (eV)
1	1.000E+7 - 7.788E+6	26	1.931E+4 - 1.503E+4
2	7.788E+6 - 6.065E+6	27	1.503E+4 - 1.171E+4
3	6.065E+6 - 4.724E+6	28	1.171E+4 - 9.119E+3
4	4.724E+6 - 3.679E+6	29	9.119E+3 - 7.102E+3
5	3.679E+6 - 2.865E+6	30	7.102E+3 - 5.531E+3
6	2.865E+6 - 2.231E+6	31	5.531E+3 - 4.307E+3
7	2.231E+6 - 1.738E+6	32	4.307E+3 - 3.355E+3
8	1.738E+6 - 1.353E+6	33	3.355E+3 - 2.613E+3
9	1.353E+6 - 1.054E+6	34	2.613E+3 - 2.035E+3
10	1.054E+6 - 8.209E+5	35	2.035E+3 - 1.585E+3
11	8.209E+5 - 6.393E+5	36	1.585E+3 - 1.234E+3
12	6.393E+5 - 4.979E+5	37	1.234E+3 - 9.611E+2
13	4.979E+5 - 3.877E+5	38	9.611E+2 - 7.485E+2
14	3.877E+5 - 3.020E+5	39	7.485E+2 - 5.830E+2
15	3.020E+5 - 2.352E+5	40	5.830E+2 - 4.540E+2
16	2.352E+5 - 1.832E+5	41	4.540E+2 - 3.536E+2
17	1.832E+5 - 1.426E+5	42	3.536E+2 - 2.754E+2
18	1.426E+5 - 1.111E+5	43	2.754E+2 - 2.145E+2
19	1.111E+5 - 8.652E+4	44	2.145E+2 - 1.670E+2
20	8.652E+4 - 6.738E+4	45	1.670E+2 - 1.301E+2
21	6.738E+4 - 5.248E+4	46	1.301E+2 - 1.013E+2
22	5.248E+4 - 4.087E+4	47	1.013E+2 - 7.889E+1
23	4.087E+4 - 3.183E+4	48	7.889E+1 - 6.144E+1
24	3.183E+4 - 2.479E+4	49	6.144E+1 - 4.785E+1
25	2.479E+4 - 1.931E+4	50	4.785E+1 - 3.727E+1

Table is continued on the next page.

Micro-Group Number	Energy Group (eV)	Micro-Group Number	Energy Group (eV)
51	3.727E+1 - 2.902E+1	76	7.821E-1 - 6.249E-1
52	2.260E+1 - 1.760E+1	77	6.249E-1 - 5.033E-1
53	2.902E+1 - 2.260E+1	78	5.033E-1 - 4.170E-1
54	1.760E+1 - 1.371E+1	79	4.170E-1 - 3.577E-1
55	1.371E+1 - 1.068E+1	80	3.577E-1 - 3.206E-1
56	1.068E+1 - 8.315E+0	81	3.206E-1 - 3.011E-1
57	8.315E+0 - 6.476E+0	82	3.011E-1 - 2.908E-1
58	6.476E+0 - 5.044E+0	83	2.908E-1 - 2.705E-1
59	5.044E+0 - 3.928E+0	84	2.705E-1 - 2.510E-1
60	3.928E+0 - 3.059E+0	85	2.510E-1 - 2.277E-1
61	3.059E+0 - 2.382E+0	86	2.277E-1 - 1.844E-1
62	2.382E+0 - 1.855E+0	87	1.844E-1 - 1.457E-1
63	1.855E+0 - 1.726E+0	88	1.457E-1 - 1.116E-1
64	1.726E+0 - 1.595E+0	89	1.116E-1 - 8.197E-2
65	1.595E+0 - 1.457E+0	90	8.197E-2 - 5.693E-2
66	1.457E+0 - 1.308E+0	91	5.693E-2 - 4.276E-2
67	1.308E+0 - 1.166E+0	92	4.276E-2 - 3.061E-2
68	1.166E+0 - 1.099E+0	93	3.061E-2 - 2.049E-2
69	1.099E+0 - 1.072E+0	94	2.049E-2 - 1.240E-2
70	1.072E+0 - 1.062E+0	95	1.240E-2 - 6.325E-3
71	1.062E+0 - 1.053E+0	96	6.325E-3 - 2.277E-3
72	1.053E+0 - 1.043E+0	97	2.277E-3 - 2.530E-4
73	1.043E+0 - 1.014E+0		
74	1.014E+0 - 9.507E-1		
75	9.507E-1 - 7.821E-1		

VITA

Bedirhan Akdeniz

Bedirhan Akdeniz graduated in 1999 with a B.S. degree in Nuclear Engineering from Hacettepe University in Ankara, Turkey. He stayed one year at the same department as a graduate assistant. He contributed to the courses of nuclear engineering, nuclear design and heat transfer as a teaching assistant. After he fulfilled M.S. course requirements, he started to work on hyperbolic two-phase flow models under supervision of Assoc. Prof. C. Niyazi Sökmen. He began his graduate studies at the Pennsylvania State University in January 2002. Prof. Kostadin Ivanov, on behalf of Nuclear Engineering Program, awarded him with graduate assistantships since then. He received his M.S. degree in Nuclear Engineering in May 2004 with a thesis titled "Analysis for Exercise 1 of OECD/NRC BWR Turbine Trip Benchmark". He worked in several projects as analyst, researcher, and supervisor during the last five years. He was the lead analyst/researcher in the NEA/OECD and NRC BWR Turbine Trip Benchmark. He extensively worked on validation of coupled 3-D core neutron kinetics and system thermal-hydraulics codes. For the last couple of years, he has been supervising the BWR stability project at Reactor Dynamics and Fuel Management Group. During his graduate study, he attended the internship program of Westinghouse Electric Co., Sweden three times. He is a member of Nuclear Science and Engineering Honor Society (*Alpha-Nu-Sigma*), and a member of Engineering Honor Society (*Tau-Beta-Pi*). His recent research work in the area of improved neutron kinetics for coupled 3-D BWR analysis was summarized in his Ph.D. thesis.